INVESTIGATING THE ROLES OF CELL ADHESION MOLECULES IN SYNAPSE FORMATION AND FUNCTION

by

Shawn D. Burton

B.S. in Bioengineering, University of Pittsburgh, 2008

B.S. in Microbiology, University of Pittsburgh, 2008

Submitted to the Graduate Faculty of

Swanson School of Engineering in partial fulfillment

of the requirements for the degree of

Master of Science in Bioengineering

University of Pittsburgh

2011

UNIVERSITY OF PITTSBURGH

SWANSON SCHOOL OF ENGINEERING

This thesis was presented

by

Shawn D. Burton

It was defended on

March 30, 2011

and approved by

Stephen D. Meriney, PhD, Associate Professor, Department of Neuroscience, Center

for Neuroscience, Center for the Neural Basis of Cognition, University of Pittsburgh

Jon W. Johnson, PhD, Professor, Department of Neuroscience, Center for

Neuroscience, Center for the Neural Basis of Cognition, University of Pittsburgh

X. Tracy Cui, PhD, Associate Professor, Department of Bioengineering, McGowan

Institute for Regenerative Medicine, Center for the Neural Basis of Cognition,

University of Pittsburgh

Thesis Advisor: Henry C. Zeringue, PhD, Assistant Professor, Department of

Bioengineering, Center for the Neural Basis of Cognition, University of Pittsburgh

INVESTIGATING THE ROLES OF CELL ADHESION MOLECULES IN SYNAPSE

FORMATION AND FUNCTION

Shawn D. Burton, M.S.

University of Pittsburgh, 2011

Recent findings have revealed a crucial contribution of the adhesion molecule neuroligin-1 to the precise organization and regulation of intercellular synaptic connections within the central nervous system, and disruption of neuroligin-1 signaling *in vivo* fosters cognitive abnormalities. Despite considerable recent progress, several uncertainties remain regarding the exact synaptic function of neuroligin-1. Principle among these uncertainties is whether neuroligin-1 primarily promotes initiation of *de novo* synaptic connections or maturation of functional, pre-existent connections. To begin to address this, experiments must be devised that are capable of dissociating activity-dependent and -independent effects of neuroligin-1 signaling on pre- and postsynaptic compartments. An additional uncertainty is how and when synapses containing neuroligin-1 are specified as either excitatory or inhibitory. Elucidating these synapse specification cascades will prove crucial in defining the contribution of neuroligin-1 to overall network balances of excitation and inhibition that guide proper cognitive development. A final uncertainty is how alternate adhesion complexes may coordinate with neuroligin-1 to initiate or maintain synaptic connections. Differentiating redundant from complementary functions among adhesion systems will help reconcile unresolved discrepancies between *in vitro* and *in vivo* experiments and ultimately provide a clearer understanding of synapse formation and function *in vivo.*

Herein I detail significant new findings clarifying each of these uncertainties. Utilizing a specific transfection protocol, I first demonstrate that neuroligin-1 is capable of robustly inducing presynaptic differentiation independent of proper postsynaptic development and synaptic activity. Second, employing both multi-molecular perturbations and a delimited biological model of the synapse, I show that the

postsynaptic scaffolding molecule PSD95 specifically acts downstream of neuroligin-1-mediated synapse initiation. Third, the model synapse is again employed to differentiate between separate synaptic functions of neuroligin-1 and alternate adhesion molecule SynCAM1. Building from these distinct synaptic functions, I provide preliminary evidence that SynCAM1 matures inactive neuroligin-1-initiated synapses. Fourth, I present the first direct evidence that neuroligin-1 contributes to dendritic morphogenesis in mammalian neurons, consistent with recent findings within the *Xenopus* system. Collectively, these results evince a robust capacity of neuroligin-1 in initial stages of synaptogenesis and contribute to a new theory of neuroligin-1 function in both activity-dependent synapse initiation and activity-dependent synapse maturation.

TABLE OF CONTENTS

vi

LIST OF FIGURES

NOMENCLATURE

Alexa Fluor (AF)

α-amino-3-hydroxy-5-methyl-4-isoxazolepropionic acid receptor (AMPAR)

Analysis of variance (ANOVA)

Autism spectrum disorders (ASD)

Cornu ammonis 1 (CA1)

Ca^{2+}/calmodulin-dependent protein kinase II (CaMKII)

Cyan fluorescent protein (CFP)

Day *in vitro* (DIV)

Deoxyribonucleic acid (DNA)

Drosophila NL ortholog (dNL)

Drosophila NRX ortholog (dNRX)

Discosoma red fluorescent protein (DsRed2)

Embryonic (E)

Excitatory junction potential (EJP)

Excitatory postsynaptic current (EPSC)

γ-aminobutyric acid (GABA)

GABAergic receptor ($GABA_AR$)

γ-D-glutamylglycine (γ-DGG)

Green fluorescent protein (GFP/EGFP)

Influenza hemagglutinin (HA)

Horseradish peroxidase (HRP)

Immunoglobulin-like (Ig)

Inhibitory postsynaptic current (IPSC)

Knockdown (KD)

Lateral amygdalar nucleus (LA)

LentiLox3.7 (LL3.7)

Leucine-rich repeat transmembrane protein (LRRTM)

Long-term potentiation (LTP)

Spontaneous miniature EPSC (mEPSC)

Spontaneous miniature IPSC (mIPSC)

Neuroligin (NL)

N-methyl-D-aspartate receptor (NMDAR)

Neuromuscular junction (NMJ)

NMDAR transport packet (NRTP)

Neurexin (NRX)

Overexpression (OE)

Postnatal (P)

Phosphate-buffered saline (PBS)

Polymerase chain reaction (PCR)

Poly-D-lysine (PDL)

PSD95/Discs large/zona occludens-1 (PDZ)

Postsynaptic density-95 (PSD95)

Root mean squared (RMS)

Ribonucleic acid (RNA)

RNA-interference (RNAi)

Standard error of the mean (SEM)

Src-homology region 3 (SH3)

Synaptic cell adhesion molecule (SynCAM/SC)

Tetrodotoxin (TTX)

Voltage-dependent calcium channel (VDCC)

Vesicular GABA transporter (vGAT)

Vesicular glutamate transporter (vGluT)

ACKNOWLEDGEMENTS

1.0   INTRODUCTION

1.1   DISCOVERY OF NEUROLIGINS AND NEUREXINS AND BASIC MOLECULAR PROPERTIES

The neurexin (NRX) gene family was discovered as a receptor for α-latrotoxin, a potent neurotoxin within black widow spider venom that causes extensive neurotransmitter release and synaptic activity (Ushkaryov et al., 1992; Petrenko et al., 1993; Davletov et al., 1995). Three NRX genes, each expressed by one of two promoters, yield alternatively spliced brain-specific type 1 transmembrane synaptic proteins with distinct long (α-NRXs) or short (β-NRXs) N-terminal extracellular domains and identical intracellular C-termini (Ushkaryov et al., 1992; Ushkaryov et al., 1993; Ushkaryov et al., 1994). NRXs can bind synaptotagmin, the prototypical calcium-sensor for neurotransmitter release, and can also bind CASK and Mint 1, which complex with voltage-dependent calcium channels (VDCCs) and active zone scaffolding, thereby yielding close proximity of NRXs to synaptic vesicle release machinery (Hata et al., 1993; Hata et al., 1996; Biederer and Südhof, 2000). The combination of alternate promoters and multiple splice sites and inserts contributes to potentially thousands of different NRXs differentially expressed both temporally and spatially throughout the brain, possibly as a synapse-specific code (Ullrich et al., 1995; Kang et al., 2008).

Neuroligin-1 (NL1) is a brain-specific type 1 transmembrane protein discovered as a synaptic binding partner of NRX1β in rodents (Ichtchenko et al., 1995; Song et al., 1999). NL1 has an extracellular N-terminus homologous to acetylcholinesterase but does not exhibit esterase activity (Ichtchenko et al., 1995). NL2 and NL3 are also brain-specific synaptic proteins with esterase homology (Ichtchenko et al., 1996; Varoqueaux et al., 2004; Budreck and Scheiffele, 2007). NL4 diverges considerably from NL1-NL3 and is expressed in several organs, including brain (Bolliger et al., 2001; Bolliger et al.,

2008; Jamain et al., 2008). All NLs share a common principle alternative splice site within the extracellular esterase-like domain (site A), while rodent NL1 is further spliced at a secondary extracellular site (site B). Splicing at these sites combines to yield multiple classes of differentially expressed NL1 isoforms: NL1(-), containing no inserts; NL1(A); NL1(B); and NL1(AB) or "NL1", which contains inserts at both A and B splice sites (Ichtchenko et al., 1995; Ichtchenko et al., 1996; Scheiffele et al., 2000; Bolliger et al., 2001; Chih et al., 2006; Bolliger et al., 2008). Of these isoforms, NL1 and NL1(B), collectively referred to as NL1(+B), are expressed most abundantly (Chih et al., 2006), while NL2, NL3, and NL1 isoforms lacking an insert in splice site B are capable of binding α-NRXs (Boucard et al., 2005).

The intracellular C-termini of NLs possess a conserved postsynaptic density-95 (PSD95)/Discs large/zona occludens-1 (PDZ) domain that can bind the third PDZ domain of the excitatory postsynaptic scaffolding molecule PSD95 (Irie et al., 1997). PSD95 is a cardinal component of the glutamatergic postsynaptic density (Cho et al., 1992; Hunt et al., 1996), orchestrating molecular clustering through three PDZ domains, a Src-homology region 3 (SH3) domain, and an inactive guanylate kinase domain (Kim and Sheng, 2004). The first two PDZ domains of PSD95 bind glutamatergic N-methyl-D-aspartate receptors (NMDAR), the glutamatergic α-amino-3-hydroxy-5-methyl-4-isoxazolepropionic acid receptor (AMPAR) trafficking protein stargazin, and Shaker-type voltage-gated potassium channels (Kornau et al., 1995; Kim et al., 1995; Chen et al., 2000; Schnell et al., 2002), providing a link between NLs, excitatory synaptic activity, and membrane excitability. NLs are also capable of intracellular interactions with gephyrin (Poulopoulos et al., 2009), a scaffolding molecule critical to inhibitory synapse development and γ-aminobutyric acid (GABA) receptor (GABA$_A$R) recruitment (Moss and Smart, 2001). Transcription and translation of NRX, NL, PSD95, and NMDAR are coordinately up-regulated after birth, with peak expressions achieved at 2-3 weeks of age (Irie et al., 1997; Song et al., 1999; Varoqueaux et al., 2004; Varoqueaux et al., 2006; Budreck and Scheiffele, 2007; Kim et al., 2008; Jamain et al. 2008), corresponding with the period of peak synaptogenesis in rodents (Harris et al., 1992; Micheva and Beaulieu, 1996; Fiala et al., 1998).

NLs are specifically targeted to somatodendritic synaptic loci via a short intracellular sequence distinct from the PDZ domain and independent of PSD95 binding or transsynaptic linkage (Dresbach et al., 2004; Rosales et al., 2005). Immunoelectron microscopy of NL1 confirmed an exclusive postsynaptic localization and further demonstrated preferential expression of NL1 at asymmetric, excitatory synapses, in strong agreement with immunofluorescent colocalization of NL1 with excitatory AMPAR and not inhibitory $GABA_AR$ in dissociated cortical and cerebellar Purkinje cells (Song et al., 1999). Complementing the localization of NL1 to excitatory postsynapses, immunoelectron microscopy of NL2 revealed preferential localization to postsynapses of symmetric, inhibitory synapses along dendritic shafts, congruent with immuno-fluorescent colocalization of NL2 with inhibitory postsynaptic molecules $GABA_AR$ and gephyrin and inhibitory presynaptic molecules vesicular GABA transporter vGAT and GABA synthesizing enzyme GAD65 (Varoqueaux et al., 2004; Graf et al., 2004; Chih et al., 2005; Levinson et al., 2005; Patrizi et al., 2008; Poulopoulos et al., 2009). Careful analysis further revealed minor populations of endogenous NL1 and NL2 localized to inhibitory and excitatory synapses, respectively, in dissociated hippocampal neurons (Levinson et al., 2005; Levinson et al., 2010). Moreover, endogenous NL2 colocalizes predominantly with inhibitory scaffolding molecule gephyrin *in vivo*, but also demonstrates measurable colocalization with PSD95 (Hines et al., 2008). NL3 demonstrates strong synaptic localization in dissociated hippocampal neurons, exhibiting significant clustering at half of all colocalized PSD95/vGluT1 puncta and gephyrin/vGAT puncta (Budreck and Scheiffele, 2007; Levinson et al., 2010). Consistent with both excitatory and inhibitory NL3 localizations, NL2 co-immunoprecipitates NL3 but not NL1, while NL3 co-immunoprecipitates both NL2 and NL1, suggesting multiple NLs can contribute to single postsynaptic complexes, though these results remain to be confirmed at the ultrastructural level (Budreck and Scheiffele, 2007). Little is currently known about the endogenous localization and functions of NL4.

Presynaptic localization of NRXs has been largely inferred from ultrastructural identification of binding partner NLs as exclusively postsynaptic (Song et al., 1999; Varoqueaux et al., 2004), immunofluorescent colocalization of NRXs with presynaptic proteins and axonal growth cones (Ushkaryov et al., 1992; Dean et al., 2003; Graf et al.,

2004), presynaptic interactions and functions (Hata et al., 1993; Hata et al., 1996; Biederer and Südhof, 2000; Missler et al., 2003), and a role in α-latrotoxin neurotransmitter release (Sugita et al., 1999). Immunoelectron microscopy using a pan-NRX antibody confirmed a presynaptic localization of NRXs at both symmetric and asymmetric synapses, but strikingly revealed an equally strong postsynaptic distribution (Taniguchi et al., 2007), corroborating the curious isolation of NRXs in postsynaptic density fractions and reduction in NMDAR currents of knockout mice lacking all three α-NRXs (Peng et al., 2004; Kattenstroth et al., 2004). Further work is necessary to differentiate the pre- and postsynaptic distributions of specific α- and β-NRX isoforms.

1.2   SYNAPTIC INVOLVEMENT OF NEUROLIGINS AND NEUREXINS IN VITRO

Scheiffele and colleagues presented the first evidence for a synaptic function of NL-NRX signaling by showing that NLs expressed in nonneuronal cells induced full presynaptic differentiation in contacting axons of cocultured neurons (Scheiffele et al., 2000). Remarkably, NL1, NL2, or their extracellular domains presented from primary astrocytes, HEK293 or COS7 cell lines, or lipid-coated beads robustly recruited presynaptic markers synapsin I and synaptophysin (Scheiffele et al., 2000; Dean et al., 2003). Importantly, alternative neuronal adhesion and synaptic molecules N-cadherin, ephrinB1, TAG-1, L1, agrin, and NLswap (a mutant NL1 construct containing the esterase domain of acetylcholinesterase) failed to recruit significant levels of synapsin, thus verifying NLs as specific synaptogenic molecules (Scheiffele et al., 2000). These results were further corroborated at the morphological level using immunoelectron microscopy. Axons contacting NL1-expressing HEK293 cells displayed pronounced elaboration, with electron dense material between closely-apposed cell membranes and synaptic vesicle aggregations (Scheiffele et al., 2000). Axons contacting GFP-expressing HEK293 cells displayed none of these morphological properties (Scheiffele et al., 2000). Application of an antibody targeting the lumenal domain of synaptic vesicle protein synaptotagmin further revealed functional, depolarization-dependent synaptic vesicle exocytosis and recycling at NL1-mediated sites of presynaptic differentiation,

with quantal release of glutamate confirmed using heterologous coexpression of NMDAR with NL1 (Scheiffele et al., 2000; Fu et al., 2003; Sara et al., 2005). Immunostaining for specific excitatory (vGluT1) and inhibitory (GAD65) presynaptic markers further revealed that heterologous NL1 and NL2 recruited both distinct excitatory and inhibitory presynaptic terminals in contacting hippocampal axons (Graf et al., 2004), suggesting additional postsynaptic components are necessary to preferentially localize NL1 to excitatory and NL2 to inhibitory sites.

Soluble NRX1β, which disrupts intercellular NL-NRX interactions, abolished synapsin recruitment by heterologous NLs and similarly lowered synapsin puncta densities in neuronal cultures (Scheiffele et al., 2000). Further, soluble NRX1β reduced basal frequencies of spontaneous miniature excitatory (mEPSC) and inhibitory (mIPSC) postsynaptic currents in dissociated hippocampal neurons, consistent with a decrease in the density of functional excitatory and inhibitory synapses (Levinson et al., 2005). Moreover, low-level expression of fluorescently-tagged NRX1β in hippocampal cultures demonstrated NRX1β clustering at both vGluT1- and GAD65-postive terminals (Graf et al., 2004). This evidence collectively argues that NRX1β is the presynaptic mediator of NL transsynaptic signaling at both excitatory and inhibitory synapses, but cannot discount alternative NL or NRX binding partners. Thus, to verify a synaptic function of NRX1β, Craig and colleagues reversed the mixed-culture assay and demonstrated that heterologous NRX1β was sufficient to recruit both excitatory (PSD95, NMDAR) and inhibitory (gephyrin, GABA$_A$R) postsynaptic components in contacting dendrites of cocultured neurons (Graf et al., 2004). Again, N-cadherin, L1, and domains of agrin failed in equivalent experiments (Graf et al., 2004). Of great interest, both fluorescently-tagged and endogenous NL1-NL3 were recruited to these sites of PSD95 and gephyrin recruitment, suggesting that transsynaptic NRX1β signaling is at least in part mediated by NLs (Graf et al., 2004; Graf et al., 2006; Budreck and Scheiffele, 2007). Mirroring this finding, heterologous expression of NLs in COS7 cells recruited endogenous NRXs at sites of neuron-COS7 contact (Chubykin et al., 2005). Lastly, targeted mutation of NL1 to abolish NRX-binding precluded NL1-induced presynaptic differentiation in the mixed-culture assay (Ko et al., 2009a). Thus, NL-NRX signaling is bidirectional and capable of driving both excitatory and inhibitory synapse formation.

Structure-function analysis of the NL-NRX interaction using mutagenesis revealed that, while monomeric NL1 can bind soluble NRX1β, NL1 dimerization domains must be intact for NL1-expressing cells to adhere to NRX1β-expressing cells (Dean et al., 2003). Strikingly, dimerization-deficient NL1 failed to induce presynaptic differentiation in the mixed-culture assay, providing further evidence for NL1-NRX1β transsynaptic signaling at sites of artificial synapse formation (Dean et al., 2003; but see Ko et al., 2009a). Further, clustering of ectopic NRX1β through multimerized antibody application to simulate endogenous NL binding proved sufficient to recruit synapsin (Dean et al., 2003). Complementary experiments clustering NLs to simulate NRX1β binding demonstrated preferential recruitment of PSD95 by clustered NL1 and gephyrin by clustered NL2 (Graf et al., 2004; Levinson et al., 2005; Poulopoulos et al., 2009; Barrow et al., 2009). Together, these results strongly argue that bidirectional transsynaptic NL-NRX signaling is not only capable, but sufficient to nucleate excitatory and inhibitory synapses *in vitro*.

Direct gain- and loss-of-function perturbations of NL signaling in dissociated neurons have further evinced a crucial role for NLs in synapse formation. Overexpression of NL1 in dissociated cerebellar granule cells or hippocampal neurons induced extensive gains in synaptic vesicle and PSD95 puncta densities, vGluT1 puncta sizes and densities, and dendritic spine morphogenesis, reflecting a role in excitatory synapse development (Dean et al., 2003; Chih et al., 2004; Prange et al., 2004; Chih et al., 2005; Sara et al., 2005; Chubykin et al., 2007; Ko et al., 2009a; Stan et al., 2010; Aiga et al., 2011). Complementary increases in AMPAR (Dean et al., 2003) and NMDAR puncta densities (Chih et al., 2005) have additionally been observed, as well as increased spontaneous mEPSC frequencies (Prange et al., 2004; Levinson et al., 2005; Stan et al., 2010). Surprisingly, NL1 also demonstrated a strong effect on inhibitory synapse formation, with NL1 overexpression driving a significant increase in vGAT puncta sizes and densities and mIPSC frequencies (Prange et al., 2004; Chih et al., 2005; Levinson et al., 2005). Expression of dominant negative NL1 mutants and RNA-interference (RNAi) knockdown of endogenous NL1 expression complementarily reduced vGAT, vGluT1, AMPAR, and spine densities (Prange et al., 2004; Chih et al., 2005; Levinson et al., 2005; Nam and Chen, 2005; Aiga et al., 2011). Soluble NRX1β

6

precluded gains in miniature event frequencies induced by NL1 overexpression, while endogenous NRX clustered with both excitatory and inhibitory presynaptic markers at sites of contact between NL1-overexpressing and neighboring neurons, affirming that NRXs mediate acute NL1 gain-of-function effects (Dean et al., 2003; Levinson et al., 2005; Chih et al., 2006). Similar to NL1, overexpression of NL2 and NL3 also increased densities of both excitatory (vGluT1, spine, AMPAR) and inhibitory (vGAT) synaptic markers, with complementary shifts observed with NL2, NL3, or NL1-NL3 knockdown (Chih et al., 2004; Chih et al., 2005; Levinson et al., 2005), supporting a general role of all NLs in synapse formation. Pronounced and select reduction of mIPSC frequencies with triple NL1-NL3 knockdown further suggests a degree of redundancy at functional excitatory synapses (Chih et al., 2005).

Careful examination of developing terminals in immature cultures further revealed differential recruitment of active zone scaffolding and synaptic vesicle clusters by NL1 overexpression (Wittenmayer et al., 2009). Significantly, terminals impinging onto dendrites of young neurons overexpressing NL1 were insensitive to F-actin disruption by Latrunculin A (Wittenmayer et al., 2009), a property normally observed only in mature boutons (Zhang and Benson, 2001; Wittenmayer et al., 2009). In parallel, NL1-induced terminals displayed greater functional maturation. Neurons overexpressing NL1 exhibited measurable NMDAR currents earlier in development and exhibited faster NMDAR block by MK-801, an open-channel antagonist, suggesting increased release probability and/or greater glutamate release (Wittenmayer et al., 2009; Stan et al., 2010). Moreover, both live staining of the synaptotagmin lumenal domain and styryl dye FM4-64 loading demonstrated NL1 overexpression enlarges average synaptic vesicle recycling pools and enables depolarization-dependent vesicle release and recycling earlier in development (Wittenmayer et al., 2009). Intriguingly, the intracellular domain of NL1 was dispensable in recruiting presynaptic terminals but necessary for conferring enhanced release probability, recycling pool sizes, and Latrunculin A-resistance (Wittenmayer et al., 2009). Moreover, chronic application of NMDAR antagonist AP5 similarly blocked development of Latrunculin A-resistance (Wittenmayer et al., 2009). Thus, functional maturation of NL1-induced presynaptic terminals is NMDAR activity-dependent and requires intracellular interaction between NL1 and other postsynaptic

components. Indeed, terminals formed on NL1-expressing HEK293 cells were sensitive to Latrunculin A (Wittenmayer et al., 2009).

Results of NL overexpression are thus consistent with anatomical and mixed-culture experiments in demonstrating that NL-NRX signaling is capable of driving synapse formation. Moreover, knockdown of NLs in dissociated neurons further demonstrates that NL-NRX signaling is necessary for normal synaptogenesis. Lack of specificity in NL1 and NL2 on glutamatergic and GABAergic synapse development, however, suggests that driving NL signaling may not be enough to confer specificity to nascent synaptic contacts. This is emphasized by the ability of heterologous NL1 and NL2 to artificially induce both excitatory and inhibitory presynaptic differentiation in the mixed-culture assay. Moreover, while pronounced presynaptic effects of NL1 overexpression are robustly observed in all studies, postsynaptic gains in AMPAR and NMDAR puncta densities and mEPSC frequencies are not consistently observed with NL1 overexpression (Dean et al., 2003; Prange et al., 2004; Chih et al., 2005; Sara et al., 2005; Ko et al., 2009a). This suggests that an additional postsynaptic factor may be required not only for maturation of presynaptic terminals, but also for synapse specification as excitatory or inhibitory and postsynaptic maturation via recruitment of neurotransmitter receptors.

PSD95 is a leading candidate for excitatory specification and maturation of NL-mediated synapses given its proximal location within excitatory postsynaptic densities and ability to link NLs with NMDAR and stargazin-AMPAR complexes via PDZ interactions. Concordant with a NL-PSD95 signaling pathway, PSD95 overexpression in dissociated hippocampal neurons and organotypic hippocampal slices mimics excitatory NL1-mediated gains, with increased dendritic spine sizes and densities, synaptophysin clustering, AMPAR EPSC amplitudes, and mEPSC frequencies (El-Husseini et al., 2000; Bresler et al., 2001; Schnell et al., 2002; Béïque and Andrade, 2003; Losi et al., 2003; Stein et al., 2003; Prange et al., 2004). Divergent from NL1 gain-of-function and consistent with a role in excitatory synapse maturation, however, PSD95 overexpression consistently increases AMPAR recruitment and mEPSC frequencies and amplitudes (El-Husseini et al., 2000; Schnell et al., 2002; Losi et al., 2003; Stein et al., 2003; Prange et al., 2004). Moreover, increased PSD95 expression decreases

vGAT puncta densities and mIPSC frequencies while knockdown of PSD95 expression increases vGAT puncta densities and reduces excitatory synapse densities, strongly supporting a role in synapse specification (Prange et al., 2004; Gerrow et al., 2006; Levinson et al., 2010). Chronic PSD95 loss-of-function via genetic deletion complements these findings. PSD95 knockout prevents the normal developmental upregulation of mEPSC frequencies and raises NMDAR to AMPAR EPSC ratios (Béïque et al., 2006). These deficits were ultimately traced to a greater prevalence of immature or "silent" synapses harboring functional NMDAR but lacking functional AMPAR currents (Béïque et al., 2006). Interestingly, average spine size and morphology were unaltered in knockout mice (Béïque et al., 2006).

Direct investigation of NL-PSD95 interactions *in vitro* has provided compelling evidence for NL-PSD95 regulation of synapse specification, maturation, and consequent balances of excitation and inhibition. NL1 overexpression alone in dissociated hippocampal neurons potently augmented total and individual excitatory and inhibitory synapse densities (Chih et al., 2004; Prange et al., 2004; Sara et al., 2005; Chubykin et al., 2007). Coordinate overexpression of PSD95 with NL1 in identical preparations strikingly restricted increases in total synapse densities and sequestered nearly all exogenous NL1 to excitatory sites (Prange et al., 2004). These results were robustly corroborated at the physiological level. Overexpression of NL1 alone triggered increased mEPSC and mIPSC frequencies and had no effect on mEPSC amplitudes (Prange et al., 2004; Levinson et al., 2005), while co-overexpression of PSD95 with NL1 selectively increased both mEPSC frequencies and amplitudes (Prange et al., 2004). Consistently, increased NL1 expression did not strongly recruit AMPAR to synaptic sites (Prange et al., 2004; Chih et al., 2005; but see Dean et al., 2003), while upregulation of PSD95 alone or with NL1 potently recruited AMPAR (Prange et al., 2004). Further, the third PDZ domain of PSD95, which binds NLs, proved dispensable in increasing AMPAR EPSC amplitudes (Schnell et al., 2002). These findings strongly support a role for PSD95 in excitatory synapse specification and further suggest that NL1 and AMPAR accumulate at postsynaptic sites via distinct pathways, i.e. synapse initiation and postsynaptic maturation are dissociable events. Indeed, heterologous expression of NRX1β and multimerized antibody clustering of NL1 recruited both PSD95 and NMDAR,

but not AMPAR, in contacting dendrites of cocultured neurons (Graf et al., 2004; Nam and Chen, 2005). Moreover, unaltered spine densities and sizes in PSD95 knockout animals and increased spine densities with NL1 overexpression further suggests that NL1 signaling may drive spine morphogenesis via a PSD95-indepenent, NMDAR-dependent cascade. PSD95 additionally regulates other NLs. Overexpression of PSD95 recruited both exogenous and endogenous NL2 from inhibitory synapses to excitatory synapses, while knockdown of endogenous PSD95 expression correspondingly increased localization of endogenous NL1-NL3 to inhibitory synapses (Graf et al., 2004; Levinson et al., 2005; Gerrow et al., 2006; Levinson et al., 2010).

Deletion of the third PDZ domain of PSD95 precluded gain-of-function increases in puncta sizes of both endogenous NL1 and presynaptic synaptophysin in dissociated hippocampal cultures (Prange et al., 2004). Coexpression of wild-type PSD95 with a truncated NL1 mutant lacking the C-terminal PDZ domain (NLΔC) similarly blocked increases in synaptophysin puncta size (Prange et al., 2004). NL1 is thus required to mediate presynaptic effects of PSD95. Futai et al. profoundly evinced this NL1-PSD95 link in presynaptic modulation in cultured rat hippocampal slices. Both PSD95 and NL1 overexpression were first separately shown to increase AMPAR and NMDAR EPSC amplitudes (Futai et al., 2007), in accord with prior accounts of increased glutamatergic transmission (El-Husseini et al., 2000; Schnell et al., 2002; Béïque and Andrade, 2003; Losi et al., 2003; Stein et al., 2003; Prange et al., 2004; Levinson et al., 2005; Wittenmayer et al., 2009; Ko et al., 2009a; Stan et al., 2010). PSD95 and NL1 both additionally reduced AMPAR and NMDAR paired-pulse ratios (Futai et al., 2007), a metric conveying increased presynaptic release probability (Dobrunz and Stevens, 1997). Moreover, both RNAi knockdown of PSD95 and expression of the dominant negative NLswap construct separately reduced AMPAR and NMDAR EPSCs and increased AMPAR and NMDAR paired pulse ratios (Futai et al., 2007). Results of several independent experiments confirmed a specific presynaptic effect: the rate of NMDAR block by MK-801 was significantly faster upon PSD95 overexpression and significantly slower upon PSD95 knockdown, congruent with increased glutamate release and channel-opening; titration of extracellular Ca^{2+} concentrations further revealed a strong Ca^{2+}-dependence of EPSC gains with PSD95 overexpression,

suggesting greater presynaptic Ca^{2+} sensitivity; and lastly, γ-D-glutamylglycine (γ-DGG), a competitive AMPAR antagonist proved less effective on neurons overexpressing PSD95, consistent with greater cleft concentrations of glutamate to out-compete γ-DGG (Futai et al., 2007). Of great interest, changes in paired pulse ratios were abolished by coupling PSD95 overexpression with NL1 knockdown and converse coupling of NL1 overexpression with PSD95 knockdown (Futai et al., 2007). In direct agreement, genetic knockout of the third PDZ domain of endogenous PSD95 in mice enhanced AMPAR paired pulse ratios (Migaud et al., 1998). Finally, presynaptic expression of a dominant negative NRX1β mutant with truncated intracellular C-terminus in paired recordings drove similar increases in AMPAR paired pulse ratios with concomitant increased failure rates (Futai et al., 2007). NL1 and PSD95 thus also putatively interact with presynaptic NRX1β to regulate presynaptic release probability. Intriguingly, preparations demonstrated no change in ω-conotoxin or ω-agatoxin sensitivities upon PSD95 overexpression (Futai et al., 2007), suggesting NRX1β-NL1-PSD95 interactions alter coupling of release to Ca^{2+} influx rather than adjusting presynaptic VDCC composition, in striking contrast to α-NRX perturbation (see below).

In view of the strong evidence linking NL-PSD95 interactions with synapse specification and pre- and postsynaptic maturation, consideration of NL/PSD95 balances can reconcile disparities between specific localization of endogenous NLs and nonspecific effects observed with NL perturbations and mixed-culture experiments. NL overexpression beyond basal PSD95 levels drove both excitatory and inhibitory synaptogenesis. Similarly, heterologous expression of NLs in the mixed-culture assay recruited both glutamatergic and GABAergic terminals. Moreover, high overexpression of NL2 disrupted endogenous clustering of postsynaptic PSD95, gephyrin, $GABA_AR$, and NMDAR and functionally lowered mEPSC and mIPSC frequencies and amplitude (Graf et al., 2004). A precise balance between PSD95 and NL expression levels is thus necessary to maintain proper balances between excitatory and inhibitory synapse densities. The balance between gephyrin and NL expression levels likely also contributes to governing synapse specification, as knockdown of gephyrin expression was recently shown to increase the proportion of endogenous NL2 localized to excitatory synapses (Levinson et al., 2010).

Results of *in vitro* studies thus strongly argue that NRX-NL-PSD95/gephyrin signaling mediates synapse specification and pre- and postsynaptic maturation, in addition to initial structural synapse initiation. An insightful alternative hypothesis posited by the Südhof group proposes that NLs primarily mediate activity-dependent synapse *validation*, or the maintenance of functional pre-existent synaptic connections (Chubykin et al. 2007). By this hypothesis, the robust gains in synapse densities observed with NL overexpression are a secondary consequence of the validation or maintenance of more intercellular connections transiently formed and lost in constant flux in developing neuronal cultures. More simply put, NLs decrease synapse losses rather than increase synapse gains. Several *in vitro* and *in vivo* findings support this hypothesis. Increased densities of morphologically-identified synapses with NL1 overexpression are often accompanied by increased synaptic vesicle release and enhanced spontaneous miniature event frequencies, arguing that validated synapses are functional (Prange et al., 2004; Levinson et al., 2005; Stan et al., 2010). Similarly, reductions in synapse densities with acute knockdown of NL expression are accompanied by reductions in synaptic activity (Chih et al., 2005). Critically, genetic deletion of NLs in single, double, and triple knockout mice does not precipitate extensive reductions in synapse densities (see below). Thus, a primary role of NLs in activity-dependent synapse validation rather than initiation of *de novo* synapses could partially reconcile several *in vitro* findings with data from *in vivo* knockout experiments. In a test of their hypothesis, Südhof and colleagues first demonstrated that NL1 overexpression in dissociated hippocampal cultures increased excitatory synapse densities and EPSC amplitudes, as found previously, and specifically enhanced the ratio of NMDAR to AMPAR EPSC amplitudes, suggesting a crucial link between NL1 and NMDAR activity (Chubykin et al., 2007). Provocatively, chronic NMDAR blockade with AP5 from the time of transfection abolished all gains mediated by NL1 (Chubykin et al., 2007). Moreover, inhibition of Ca^{2+}/calmodulin-dependent protein kinase II (CaMKII), a key enzyme that acts downstream of NMDAR activity, similarly abolished EPSC amplitude and NMDAR to AMPAR EPSC ratio gains (Chubykin et al., 2007). Complementary to these findings, chronic blockade of total synaptic activity with AP5, AMPAR antagonist CNQX, and

GABA$_A$R antagonist picrotoxin abolished gains in IPSC amplitudes mediated by NL2 overexpression (Chubykin et al., 2007).

While initial investigations thus support a role for NLs in activity-dependent synapse validation, several lines of evidence argue against rejection of a role in synapse initiation. First, the potent bidirectional recruitment of synaptic markers observed in the mixed-culture assay clearly evinces a robust capacity for synapse initiation, and evidence of neurite adhesion to nonneuronal cells prior to NL-NRX signaling has not been presented. Moreover, while an artificial model of synapse formation, the mixed-culture assay reflects many endogenous properties of synapses – foremost, morphological presynaptic development and maturation at the ultrastructural level and specificity to a small subset of synaptic adhesion molecules. Second, multimerized antibody clustering of NLs and NRXs has repeatedly demonstrated recruitment of several synaptic components in the absence of activity or prior transsynaptic linkage, again evincing a robust capacity for synapse initiation. Third, chronic blockade of NMDAR or total synaptic activity also reduced basal synapse densities and postsynaptic current amplitudes in GFP-expressing control neurons (Chubykin et al., 2007), confounding abolishment of NL1-mediated gains with culture-wide synapse formation deficits. Fourth, chronic NMDAR blockade in immature cultures did not abolish active zone recruitment by NL1 overexpression but did prevent presynaptic maturation, as measured by F-actin-dependence/Latrunculin A-resistance (Wittenmayer et al., 2009), qualifying synapse initiation and presynaptic maturation as dissociable events. Fifth, chronic blockade of synaptic activity could disrupt mechanisms downstream of NL signaling and consequently not reflect a direct role of NLs. Finally, demonstration of activity-dependent validation of nascent synapses by NL-NRX signaling does not discount an additional role in activity-independent synapse initiation. Considerable further investigation will thus ultimately be required to clearly dissociate and define the role(s) of NLs in normal synapse formation and function.

1.3   REGULATION OF NEUROLIGIN AND NEUREXIN SIGNALING BY ALTERNATIVE SPLICING

While the vast majority of NL research has focused on the NL1(AB) isoform, substantial evidence exists for regulation of synapse specification as excitatory or inhibitory by alternative splicing of NLs and NRXs. NL1-NL3 were discovered as binding partners of NRX1-3β lacking a splice site four insert (-S4), suggesting S4 inserts can modulate binding affinity to NLs (Ichtchenko et al., 1995; Ichtchenko et al., 1996). Careful biochemical analysis further revealed that NL1(-B) are capable of additionally binding NRX1β(+S4), albeit at lower affinity than to NRX1β(-S4), suggesting alternative splicing at site B of NL1 is dominant over NRX splicing in determining binding affinities (Boucard et al., 2005). Accordingly, NL2 and NL3, which are not physiologically spiced at site B, demonstrate greater affinities for NRX(+S4) isoforms than do NL1(+B). Indeed, measurements of soluble NRX1β bound to NL-expressing COS7 cells revealed NL2 and NL3 bound NRX1β(+S4) nearly equally as well as NRX1β(-S4), while NL1(AB) demonstrated a strong preference for NRX1β(-S4) (Graf et al., 2006). Consistently, heterologous expression of either NRX1β(+S4) or NRX1β(-S4) proved equally potent in recruiting endogenous NL2, NL3, PSD95, and gephyrin in the mixed-culture assay (Graf et al., 2006; Budreck and Scheiffele, 2007). Further, congruent with greater endogenous abundance of NL1(+B) isoforms (Chih et al., 2006), heterologous NRX1β(-S4) recruited significantly more endogenous NL1 than NRX1β(+S4) (Graf et al., 2006). Lastly, nearly ten years after the discovery of NLs as endogenous binding partners of β-NRXs, NL2 and NL1(-B) were also biochemically shown to strongly bind α-NRXs(±S4) (Boucard et al., 2005). Indeed, heterologous expression of each α-NRX significantly and preferentially recruited endogenous NL2, gephyrin, and GABA$_A$R over NL1 and PSD95 in mixed-culture assays (Kang et al., 2008).

To begin dissecting the physiological implications of these findings in neurons, Scheiffele and colleagues employed both low-level exogenous expression (at levels that did not increase synapse densities) and overexpression of specific NL isoforms in dissociated hippocampal cultures. Under low-level expression conditions, NL1(+B) preferentially targeted excitatory synapses while NL1(A) preferentially targeted inhibitory synapses and NL1(-) showed no preference (Chih et al., 2006). Inclusion of the A insert

in NL2 also increased the propensity of NL2 to target inhibitory synapses, congruent with greater endogenous abundance of NL2(A) isoforms (Chih et al., 2006). Moreover, reduction of endogenous NL2(A) levels through morpholino-oligonucleotide application increased the ratio of NL2(-) to NL2(A) and the proportion of NL2 targeted to excitatory synapses, strongly supporting a link between GABAergic targeting of NLs and the A insert (Chih et al., 2006). Overexpression conditions yielded similar trends; inclusion of the B insert in either NL1 or ectopically in NL2 preferentially drove increased densities and sizes of excitatory synapses while NL1(A) and both NL2(A) and NL2(-) drove equal levels of inhibitory and excitatory synapse formation (Chih et al., 2006). Additionally, application of soluble NRX1β(+S4) to dissociated hippocampal cultures preferentially disrupted GABAergic synapse formation (Chih et al., 2006).

Collectively, these results present compelling evidence for regulation of synapse specificity and/or NL/NRX targeting by B, A, and S4 inserts. Several additional effects of splicing remain to be accounted for, however. In an independent evaluation of NL1(AB) versus NL1(-) overexpression in dissociated hippocampal neurons, Boucard et al. found NL1(AB) preferentially increased synapse and spine densities while NL1(-) primarily enhanced synapse and spine sizes (Boucard et al., 2005). Moreover, NL1(-B) isoforms demonstrated significantly faster initial recruitment rates of presynaptic components than NL1(+B) isoforms in the mixed-culture assay, with rapid recruitment dependent on α-NRX signaling (Lee et al., 2010). Further, to examine the effects of postsynaptic NRXs on transsynaptic NL1 signaling, Scheiffele and colleagues compared NL1(AB) overexpression with coordinate NL1(AB) and NRX1β overexpression and found *cis*-interactions between NRX1β and NL1(AB) prevented NL1-mediated synapse gains (Taniguchi et al., 2007). Surprisingly, block of transsynaptic NL1(AB) signaling by postsynaptic NRX1β occurred independent of S4 splicing, while NRX1α(-S4) also proved partially effective (Taniguchi et al., 2007). Surprisingly, postsynaptic NRX1β overexpression also markedly increased membrane levels of exogenous NL1(AB), suggesting postsynaptic NRXs may facilitate membrane delivery of NLs (Taniguchi et al., 2007). Finally, the Südhof group has found that NL1 overexpression in dissociated cultures increases AMPAR EPSC amplitudes irrespective of splicing, while NL1(-B) overexpression actually decreases IPSC amplitudes (Chubykin et al., 2007). Further

research will be necessary to reconcile gains in morphological synapse densities with changes in evoked current responses, though even these conflicting results agree with the general finding that alternative NL/NRX splicing in part regulates the balance of network excitation and inhibition.

1.4   DYNAMICS OF SYNAPTIC NEUROLIGIN RECRUITMENT

Experiments studying the temporal order of CNS synapse formation have provided evidence consistent with a role of NL-NRX signaling in bidirectional synapse initiation. Examination of "heterochronic" cultures of different aged neurons insightfully demonstrated that axons of recently dissociated neurons are competent to form synapses with dendrites of mature neurons, while the reverse does not hold true (Fletcher et al., 1994). This observation extended prior findings that clusters of recycling synaptic vesicles exist at nonsynaptic axonal sites within young, immature neurons (Matteoli et al., 1992). Moreover, multiple active zone components, including bassoon and piccolo, have been observed to travel as preformed clusters (Zhai et al., 2001). These results collectively suggest that presynaptic components are constructed prior to synaptogenesis and are trafficked to or nucleate new synapses at nascent sites of axodendritic contact (Ziv and Garner, 2001; Ziv and Garner, 2004). Combined applications of time-lapse fluorescence microscopy, styryl dye FM4-64 loading, and retrospective immunolabeling have corroborated this theory. Clusters of synaptic vesicles capable of depolarization-dependent exocytosis and recycling were observed to form within 30 min of nascent axodendritic contact, with bassoon occupying all new synaptic terminals, while postsynaptic components were recruited on a slower timescale of ~45 min (Friedman et al., 2000; Bresler et al., 2001). Similarly, stationary synaptophysin clusters at sites of nascent axodendritic contact have been observed to recruit PSD95, either as a mobile cluster or through coalescence from a diffuse dendritic pool (Bresler et al., 2001; Gerrow et al., 2006). Collectively, these results argue that presynaptic differentiation can precede postsynaptic differentiation, and further suggest that principal postsynaptic components are recruited independently.

Indeed, strong evidence exists for independent recruitment of glutamatergic receptors to new synapses. Several electrophysiological and immunocytochemical experiments have identified "silent" synapses harboring functional NMDAR without AMPAR both early in development (Durand et al., 1996; Wu et al., 1996; Isaac et al., 1997; Rumpel et al., 1998; Washbourne et al., 2002) and later (Liao et al., 1999). These studies demonstrate that not only does NMDAR recruitment precede that of AMPAR, but that NMDAR activity is involved in and possibly necessary for "unsilencing" of synapses through AMPAR insertion. Time-lapse microscopy has further shown that NMDAR travel with PDZ-domain scaffolding proteins in highly mobile NMDAR transport packets (NRTPs) along dendritic microtubules of immature, day *in vitro* (DIV) 3-7 neurons prior to synapse formation (Washbourne et al., 2002). AMPAR clusters exhibited lower mean velocities and fewer total mobile clusters than NMDAR, and accordingly only a minority of mobile NMDAR puncta colocalized with AMPAR, suggesting NRTPs primarily do not contain AMPAR (Washbourne et al., 2002). In line with identification of "silent" synapses, highly mobile NRTPs moved to nascent axodendritic contact sites within tens of minutes, followed by mobile AMPAR clusters on a much longer timescale of 1-2 hr (Washbourne et al., 2002).

PSD95 and NMDAR also cluster independently in immature, DIV3-7 neurons, with PSD95 absent from most NRTPs (Rao et al., 1998; Washbourne et al., 2002; Gerrow et al., 2006). A small pool of PSD95 clusters exhibit actin-dependent mobility, while the majority of PSD95 exists in diffuse dendritic pools and clustered together at stationary sites with other PDZ scaffolding components (Washbourne et al., 2002; Gerrow et al., 2006). The difference in cytoskeletal dependence between NRTPs and PSD95 clusters further confirms that mobile packets of each are separately recruited to synapses. Strikingly, stationary clusters of PSD95 at sites of nascent axodendritic contact can also nucleate new synapses through the recruitment of active synaptic vesicle cycling, mirroring the recruitment of PSD95 apposing synaptophysin clusters (Gerrow et al., 2006). Together, these observations lend considerable validity to reports of bidirectional synapse formation in mixed-culture and multimerized antibody clustering experiments. Exceedingly few synapses were observed to arise at sites of new axodendritic contact initially lacking both pre- and postsynaptic components (Gerrow et

al., 2006), suggesting that in most cases, postsynaptic components or sites of active synaptic vesicle cycling serve in transsynaptic recruitment, reminiscent of the mixed-culture assay.

In immature DIV3-7 neurons, NL1 exists in punctate and diffuse pools (Barrow et al., 2009), in strong agreement with prior accounts of weak endogenous and exogenous NL clustering (Prange et al., 2004; Levinson et al., 2005). Punctate NL1 can be further divided based on mobility and colocalization. Time-lapse microscopy revealed detectable levels of NL1 in most stationary, but not mobile, PSD95 clusters, in agreement with observed recruitment of active synaptic vesicle cycling by stationary PSD95 clusters (Gerrow et al., 2006) and accounts of NL1-PSD95 transsynaptic regulation of presynaptic differentiation (Prange et al., 2004; Futai et al., 2007). Thus, a large portion of punctate NL1 is stationary in NL1/PSD95 clusters (Gerrow et al., 2006; Barrow et al., 2009). Only a minority of NL1 exists in mobile clusters, but strikingly, mobile NL1 clusters were observed in the majority of active dendritic filopodia, often at filopodial tips (Barrow et al., 2009).

Employing high framerate (25 s/frame) time-lapse microscopy and low-level exogenous NL1 expression in immature cultures, Barrow et al. observed significant NL1 clustering at sites of nascent axodendritic contact within seconds to minutes of contact, likely from the diffuse pool (Barrow et al., 2009). Of outstanding importance, this observation provided the first tangible evidence that accumulation of NL1 occurs rapidly enough to mediate the first signal in synapse initiation. Consistent with coalescence from the diffuse pool, application of soluble NRX to immature neuronal cultures or direct clustering of epitope-tagged NL1 expressed at low levels both rapidly reduced the diffuse NL1 pool to increase synaptic NL1 clusters (Barrow et al., 2009). PSD95 was similarly recruited from diffuse pools by NL1 clustering, but over much longer timescales than NL1 (Barrow et al., 2009), consistent with prior reports (Bresler et al., 2001; Gerrow et al., 2006).

Notably, strong colocalization and cotransport of mobile NL1 with NRTPs was detected early in dissociated cultures (Barrow et al., 2009). Indeed, endogenous NL1-NL3 but not presynaptic proteins were detected in biochemically isolated NRTPs from P2-3 cortex (Barrow et al., 2009). Further, application of soluble NRX rapidly reduced

the number of mobile NL1/NMDAR clusters, suggesting NRTPs are recruited to nascent axodendritic contact sites via transsynaptic NL-NRX linkage (Barrow et al., 2009). Results suggest, however, that NL1-mediated synapse initiation is independent of NRTP cotransport, as coalescence from diffuse pools within seconds of axodendritic contact occurs without NRTPs and deletion of the C-terminal PDZ domain of NL1 abolishes cotransport with NRTPs but has no effect on NL1 synaptic localization (Dresbach et al., 2004; Barrow et al., 2009).

Time-lapse microscopy data of NL1-mediated synapse initiation is congruent with results of *in vitro* gain- and loss-of-function experiments and in strong agreement with the reported role of NL1-NRX signaling in dendritic filopodial stabilization in *Xenopus* (see below). Recent evidence also suggests that synapse strength may be regulated by activity-dependent cycling of NL1 and NRX (Thyagarajan and Ting, 2010; Schapitz et al., 2010), consistent with an additional role in synapse validation and ongoing function at mature synapses. The dynamics of other NLs and individual NRX isoforms remain to be studied, but intriguingly, NL2 appears mostly extrasynaptic but colocalized with $GABA_AR$ in immature neurons (Varoqueaux et al., 2004), suggesting a parallel cotransport mechanism may contribute to GABAergic synapse initiation.

1.5   POTENTIAL FOR COMBINED NEUROLIGIN AND SYNCAM SYNAPTIC SIGNALING

SynCAM (synaptic cell adhesion molecule) 1 (SC1) was first identified as a synaptic molecule in a bioinformatic screen for transmembrane proteins bearing an extracellular immunoglobulin-like (Ig) domain and intracellular PDZ domain (Biederer et al., 2002). SC1 harbors three N-terminal extracellular Ig domains and one intracellular PDZ domain capable of binding CASK but not PSD95, similar to the intracellular PDZ domain of NRXs (Biederer et al., 2002; Biederer, 2006). SC1 expression is upregulated postnatally in parallel with NLs, NRXs, and the peak period of synaptogenesis in rodents (Harris et al., 1992; Micheva and Beaulieu, 1996; Fiala et al., 1998; Biederer et al., 2002; Fogel et al, 2007). Moreover, SC1 is widely expressed throughout the brain

and exhibits a synaptic localization, shown with both immunohistochemistry and immunoelectron microscopy (Biederer et al., 2002; Fogel et al., 2007). Confirming a synaptic function, overexpression of SC1 in dissociated hippocampal neurons significantly increased the frequency of spontaneous miniature events without affecting event amplitudes, suggesting enhanced SC1 signaling can increase the number of mature synapses (Biederer et al., 2002; Sara et al., 2005; Fogel et al., 2007). Expression of the dominant negative extracellular mutant SCΔIg, in which all three Ig domains were removed, did not affect spontaneous event frequency or amplitude (Biederer et al., 2002; Sara et al., 2005).

Of great interest, SC1 was the second molecule reported after NLs to display significant synaptogenic potential in the mixed-culture assay. Heterologous expression of SC1 in HEK293 cells induced significant clustering of synaptophysin and functional synaptic vesicle exocytosis and recycling in contacting axons of cocultured neurons (Biederer et al., 2002; Sara et al., 2005). Moreover, spontaneous glutamatergic events were recorded in HEK293 cells coexpressing SC1 with AMPAR subunit GluR2, confirming functional glutamate release at artificial SC1-mediated synapses (Biederer et al., 2002; Sara et al., 2005).

Further bioinformatic analysis defined three additional members of the SC family: SC2-SC4 (Biederer, 2006). All SCs are differentially expressed throughout the brain, alternatively spliced, and exhibit developmentally-regulated post-translational modifications (Biederer et al., 2002; Biederer, 2006; Fogel et al, 2007; Thomas et al., 2008; Fogel et al., 2010; Galuska et al., 2010). Unique from NLs and NRXs, SC1-SC3 are capable of strong homophilic adhesion, and also display heterophilic SC1/SC2, SC2/SC4, and SC3/SC4 adhesion pairs *in vivo* (Biederer et al., 2002; Fogel et al., 2007; Thomas et al., 2008), with interaction affinities differentially regulated by post-translational modifications (Fogel et al., 2010). Immunoelectron microscopy utilizing a pan-SC antibody localized SCs to both pre- and postsynaptic compartments, while low-level exogenous expression of epitope-tagged SC1 and SC2 demonstrated colocalization with both excitatory and inhibitory synaptic markers (Biederer et al., 2002; Fogel et al., 2007). SC2 is also capable of recruiting synapsin in the mixed-culture assay (Fogel et al., 2007), while heterologous SC1 expression has additionally been

shown to recruit endogenous SCs in contacting neuronal processes (Fogel et al., 2010). SCs are thus a family of synaptic adhesion molecules that likely contribute to developmental synaptogenesis in mammals.

Biederer and colleagues have recently examined both conditional "Tet-off" transgenic SC1 mice, displaying roughly eight fold increased SC1 expression, as well as traditional SC1 knockout mice (Robbins et al., 2010). Consistent with *in vitro* overexpression, transgenic SC1 overexpression doubled mEPSC frequencies without affecting amplitudes in acute P14 hippocampal slices, while knockout yielded a complementary halving of frequencies (Robbins et al., 2010). *In vivo* SC1 perturbations did not otherwise alter neurotransmission, with equal NMDAR to AMPAR EPSC ratios and paired pulse ratios (Robbins et al., 2010), in agreement with *in vitro* SC1 overexpression in which evoked EPSC amplitudes were unaltered (Chubykin et al., 2007). Surprisingly, the eight fold increase in SC1 expression of conditional transgenic mice yielded only minimal morphological changes, with a ~25% increase in asymmetric synapse and spine densities (Robbins et al., 2010). Moreover, SC1 knockout triggered a small but significant 10% reduction in asymmetric synapse densities in hippocampal sections (Robbins et al., 2010). These minimal changes in synapse densities parallel *in vitro* results, where SC1 overexpression did not alter synapsin densities and SC2 overexpression only moderately increased the number of sites with active synaptic vesicle exocytosis and recycling (Sara et al, 2005; Fogel et al., 2007; Chubykin et al., 2007). Taken together, the strong changes in spontaneous activity and minimal changes in synapse densities observed with *in vitro* and *in vivo* SC perturbations suggest that SCs primarily act to mature a subset of synapses, which may indirectly alter synapse densities through a synapse maintenance pathway. Indeed, tetracycline-inducible blockade of SC1 overexpression from P14 to P28 in transgenic mice returned excitatory synapse and spine densities to basal levels (Robbins et al., 2010), strongly suggesting that increased SC1 expression is required for continued maintenance of increased synapse densities.

While *in vitro* and *in vivo* results are thus largely consistent with an endogenous role of SCs in synapse maturation or activity-dependent synaptic maintenance, they do not account for the recruitment of functional presynaptic terminals by heterologous SCs

in the mixed-culture assay. A direct comparison of the synaptogenic potential of NL1 and SC1 in the mixed-culture assay may resolve this discrepancy, but thus far this experiment has not been performed. Further, a currently untested theory of SC signaling at the synapse posits that SCs may functionally mature nascent NL-initiated synapses (Sara et al., 2005). Considerable work thus remains in clarifying the specific synaptic roles of SCs.

1.6   SYNAPTIC INVOLVEMENT OF NEUROLIGINS AND NEUREXINS IN VIVO

Investigation of NL-NRX roles in synapse formation and function *in vivo* began with genetic deletion of α-NRXs. Initial evaluation of single, double, and triple α-NRX knockout mice surprisingly revealed normal gross brain morphology and synapse ultrastructure despite impaired respiration and viability (Missler et al., 2003). Adult double knockout mice and perinatal triple knockout mice both exhibited ~30-40% reduction in symmetric, inhibitory synapse densities with coordinate decreases in GABA synthesizing enzyme GAD67 and vGAT clustering (Missler et al., 2003; Dudanova et al., 2007). Examination of adult double knockout mice also curiously revealed a measurable reduction in dendritic branch length (Dudanova et al., 2007). In contrast to the moderate morphological phenotype, electrophysiological recordings in both acute brainstem and cultured neocortical slices of triple knockout mice revealed pronounced deficits in evoked inhibitory and excitatory postsynaptic responses (Missler et al., 2003). Careful analysis demonstrating increased failure rates, reduced spontaneous miniature event frequencies, and unaltered miniature event amplitudes and agonist-response traced the α-NRX knockout phenotype to a presynaptic origin. Reduced sensitivity to N-type VDCC antagonist ω-conotoxin, minimal change in Ca^{2+}-independent sucrose-mediated release, and decreased whole-cell N-type VDCC currents further isolated the deficit to N-type VDCCs, consistent with VDCC-dependence of ~50% of spontaneous miniature events in brainstem neurons (Missler et al., 2003; Zhang et al., 2005). Intriguingly, protein levels and membrane expression of N-type VDCCs were unaltered by α-NRX knockout, while whole-cell VDCC currents recorded in dissociated cultures

from α-NRX knockout mice were only reduced after synapse formation (Missler et al., 2003). Thus, knockout of α-NRX revealed a specific deficit in synaptic N-type VDCC function. Partial rescue of spontaneous miniature event frequencies, evoked success rates, and whole-cell VDCC currents by transgenic NRX1α (and not NRX1β) expression in α-NRX knockout mice verified specificity of the deficit to α-NRX function. Consistently greater deficits across nearly all metrics with each additional α-NRX deletion also suggests contribution of each α-NRX to regulation of synaptic N-type VDCC function (Missler et al., 2003; Zhang et al., 2005).

Further analysis of cultured neocortical slices from triple α-NRX knockout mice also surprisingly revealed a deficit in NMDAR-mediated currents not previously discernable in Mg^{2+}-containing recording solutions. In the presence of tetrodotoxin (TTX) and absence of Mg^{2+}, mEPSC peak amplitudes were unaffected by triple α-NRX deletion, consistent with prior data (Missler et al., 2003), but events exhibited decreased slow-rising currents, suggesting reduced contribution of slower NMDAR (Kattenstroth et al., 2004). Consistent with impaired NMDAR function, evoked EPSCs at +40 mV holding potential exhibited markedly reduced amplitudes in triple α-NRX knockout slices when normalized to evoked responses at -70 mV in Mg^{2+}-containing solution (Kattenstroth et al., 2004). This reduced NMDAR to AMPAR EPSC ratio, which discounts potential inter-slice stimulation differences, could not be traced to altered NMDAR expression or phosphorylation levels (Kattenstroth et al., 2004). Strikingly, wild-type neurons cocultured within triple α-NRX knockout slices displayed normal NMDAR currents (Kattenstroth et al., 2004), suggesting that deficits in the NMDAR response is not due to loss of presynaptic α-NRX, but rather may reflect a postsynaptic effect, consistent with pre- and postsynaptic distributions of NRXs (Taniguchi et al., 2007).

Study of single knockout mice, which display greater viability than perinatally lethal triple α-NRX knockouts, enabled both extension of electrophysiological analyses to developed cortical circuits as well as behavioral evaluation of adult mice (see below). Deletion of NRX1α yielded select reduction in mEPSC frequencies in acute hippocampal slices, with no change in amplitude or inhibitory events (Etherton et al., 2009). Measurement of field excitatory postsynaptic potentials across all stimulus amplitudes similarly revealed a reduction in excitatory transmission (Etherton et al.,

2009). Equal NMDAR to AMPAR EPSC ratios between wild type and NRX1α knockout mice suggests that the observed deficits may be presynaptic in origin (Etherton et al., 2009), congruent with the extensive characterization of triple α-NRX knockout mice (Missler et al., 2003), though more detailed analysis is required. Importantly, these collective results confirm that α-NRXs are critical to synaptic transmission and that disruption of even a single α-NRX yields measurable changes in synaptic function.

Similar to triple α-NRX knockout, deletion of NL1-NL3 precipitated irregular respiration and perinatal lethality but surprisingly did not alter gross brain morphology or cytoarchitecture (Varoqueaux et al., 2006). Immunohistochemistry and electron microscopy of respiratory brainstem nuclei also similarly revealed a moderate decrease in GABAergic synapse and receptor densities, with a large deficit in inhibitory transmission including reduced spontaneous postsynaptic current amplitudes and frequency, reduced mIPSC frequencies, and reduced evoked amplitudes with greater failure rates (Varoqueaux et al., 2006). Triple NL knockout also attenuated excitatory transmission in acute brainstem slices, with lower spontaneous and miniature event frequencies than wild type and heterozygous controls, while dissociated cortical neurons from triple NL knockout mice displayed excitatory synapse densities, ultrastructure, and function comparable to wild-type cultures (Varoqueaux et al., 2006). Results thus lean towards preferential deficits in inhibitory neurotransmission with triple NL knockout.

As with NRX investigations, study of single NL knockout mice has enabled direct examination of *in vivo* contributions of NLs to developing and mature cortical circuits. Acute hippocampal and neocortical slices from 2-3 week old NL1 knockout mice displayed select deficits in glutamatergic transmission, with specific reduction in NMDAR to AMPAR EPSC ratios (Chubykin et al., 2007). Similar deficits in NMDAR to AMPAR EPSC ratios with NL1 deletion were also observed in striatal medium spiny neurons in acute slice (Blundell et al., 2010). Contrary to excitatory transmission, inhibitory outputs were unaltered across all extracellular stimulation inputs and IPSC amplitudes in paired recordings were similarly unaltered by NL1 deletion (Chubykin et al. 2007; Gibson et al., 2009). As expected, reduction in NMDAR-mediated currents by NL1 deletion attenuated NMDAR-dependent long term potentiation in area CA1 of acute

24

hippocampal slices using an established theta burst protocol (Blundell et al., 2010). Despite an altered capacity for synaptic plasticity, but consistent with only moderate reductions in inhibitory synapse densities with NL1-NL3 deletion (Varoqueaux et al., 2006), deletion of NL1 alone incurred no changes in excitatory, inhibitory, or total synapse densities in hippocampal sections (Blundell et al., 2010). Careful examination of dissociated hippocampal cultures prepared from NL1 knockout mice did, however, reveal that NL1 deletion prevented the normal developmental decrease in F-actin-dependence and increase in vesicle recycling pool size (Wittenmayer et al., 2009), suggesting NL1 is indispensible for presynaptic maturation. Intriguingly, disruptions of PSD95 and PSD95-NL interactions *in vivo* also resulted in aberrant CA1 long term potentiation (Migaud et al., 1998; Béïque et al., 2006), suggesting that mechanisms of NL-PSD95 synapse specification and maturation observed *in vitro* also occur *in vivo*. Knockout of NL3 did not significantly affect synapse densities in hippocampal or cortical sections, similar to NL1 deletion, and further did not alter either excitatory or inhibitory input-output curves (Tabuchi et al., 2007). NL4 deletion remains to be examined at a cellular and physiological level.

Consistent with greater deficits in inhibitory synaptic development and function in triple NL knockout mice, deletion of NL2 alone precipitates greater synaptic impairments than deletion of any other single NL. NL2 knockout mice exhibited irregular postnatal respiration, similar to triple NL knockout animals, but were otherwise viable and fertile, suggesting the perinatally lethal phenotype of triple knockout arises largely through developmental loss of NL2 (Poulopoulos et al., 2009). Complementary to NL1 knockout and in agreement with an inhibitory localization and function, deletion of NL2 yielded a select deficit in inhibitory transmission (Chubykin et al., 2007; Poulopoulos et al., 2009). Detailed investigation of acute slices from both postnatal respiratory brainstem and adult hippocampus of NL2 knockout mice showed severe reductions in inhibitory spontaneous and miniature event frequencies and amplitudes, evoked amplitudes and success rates, and agonist response, with no such change in glutamatergic transmission (Chubykin et al., 2007; Poulopoulos et al., 2009). Careful examination of hippocampal sections and dissociated cultures demonstrated unaltered presynaptic terminal densities (Blundell et al., 2009; Poulopoulos et al., 2009) but remarkably

revealed a select disruption of perisomatic gephyrin and GABA$_A$R clustering (Poulopoulos et al., 2009). This select deficit in perisomatic inhibitory synapses was further observed physiologically, with a reduction in GABAergic event kinetics congruent with loss of functional electrotonically-proximal inhibitory synapses (Poulopoulos et al., 2009). Deletion of NL2 thus not only confers prominent deficits in inhibitory neurotransmission, but also impairs proper inhibitory synapse formation. In strong accordance with these findings, knockout of collybistin expression both prior to and during synaptogenesis profoundly disrupted GABA$_A$R and gephyrin clustering and GABAergic transmission, but strikingly did not lower inhibitory presynaptic terminal densities, NL2 cluster densities, or colocalization of NL2 with inhibitory presynaptic terminals (Papadopoulos et al., 2007; Papadopoulos et al., 2008; Poulopoulos et al. 2009). Similarly, knockout of GABA$_A$R expression and consequent ionotropic GABAergic transmission did not alter proper synaptic localization of NL2 opposite GABAergic terminals (Patrizi et al., 2008), providing compelling evidence for involvement of NL2 in activity-independent synapse formation. Lastly, NL2 was recently shown to be the only NL capable of activating collybistin-mediated targeting of gephyrin to membranes, strongly implicating NL2 in endogenous GABA$_A$R recruitment (Poulopoulos et al., 2009).

Results from El-Husseini and colleagues examining transgenic NL mice strengthen principal findings from knockout mice. Specifically, NL1 and NL2 were separately introduced into wild-type strains to examine *in vivo* gain-of-function effects. Importantly, transgenic overexpression was minimal, ranging from one to four fold over wild type expression across different transgenic strains, and nearly all cellular, physiological, and behavioral phenotypes displayed dose-dependence with the NL overexpression level, strongly supporting specificity of results and lack of compensatory alterations (Hines et al., 2008; Dahlhaus et al., 2010). Transgenic NL2 mice displayed enhanced vGAT intensities in immunohistochemical sections and ultrastructurally exhibited significantly enhanced symmetric synapse densities, contact lengths, areas, and vesicle pool sizes (Hines et al., 2008). Transgenic NL2 mice also displayed more moderate increases in asymmetric synapse contact length, area, and vesicle pool size, coincident with localization of a minority of NL2 to excitatory synapses, as observed in

26

wild type mice (Hines et al., 2008). These morphological effects were further paired with an increase in mIPSC frequency in acute cortical slices from transgenic NL2 mice (Hines et al., 2008). Ultrastructural analysis of transgenic NL1 mice exhibited complementary and select gains in asymmetric synapse densities, contact lengths, and vesicle pool sizes, with no changes observed in symmetric synapse densities or properties (Dahlhaus et al., 2010). Golgi impregnation further revealed increased spine sizes and densities in transgenic NL1 mice, but no change in dendritic arborization (Dahlhaus et al., 2010). Functionally, transgenic NL1 mice exhibited moderately reduced capacities for long-term potentiation in acute hippocampal slices, likely due to larger baseline EPSC amplitudes (Dahlhaus et al., 2010).

Multiple conclusions may be directly drawn from results of the *in vivo* knockout and transgenic mouse studies. First, NLs and NRXs are critical for proper synaptic transmission, both early in development and in mature circuits. This is clearly manifest in triple knockout perinatal lethality, reduced synaptic VDCC activation in α-NRX knockouts, disrupted glutamatergic transmission and long term potentiation with NL1 knockout and α-NRX knockouts, and severe deficits in inhibitory transmission with NL2 knockout. Second, in accordance with immuno-electron and -fluorescent localizations and *in vitro* analyses, endogenous NL1 and NL2 preferentially regulate excitatory and inhibitory synaptic function, respectively. Third, NLs and NRXs are not the only synaptic molecules capable of initiating synapse formation. Direct interpretation of knockout results to further conclude that NL-NRX signaling is not endogenously involved in normal synapse initiation is problematical, however, and requires full consideration of complex compensatory shifts in whole-brain protein expression, potential for coordination of multiple synaptic adhesion complexes, and homeostatic shifts in circuit formation (see Discussion).

These same factors prevent direct interpretation of the role NL signaling plays in maintenance of mature, active synapses. Moreover, significant differences between synapses of mature wild type and constitutive knockout animals could also reflect combined developmental alterations in both synapse formation and function. Thus, to avoid these confounds and directly examine NL contributions to mature synapses *in vivo*, Kim et al. elegantly employed local infusion of lentivirus into the lateral amygdalar

27

nucleus (LA) of adult rats to query the functional consequences of acute, focal, and partial RNAi-mediated knockdown of NL1 expression in behaviorally-relevant mature circuits over repeated trials (Kim et al., 2008). A ~50% reduction in NL1 expression in LA reduced NMDAR to AMPAR EPSC ratios without altering mEPSC frequency, amplitude, or asynchronous quantal amplitudes in thalamo-amygdala connections, collectively confirming that NL1 is necessary for maintenance of amygdalar NMDAR currents (Kim et al., 2008), in close agreement with prior results in NL1 knockout hippocampus (Chubykin et al., 2007; Blundell et al., 2010). Both knockdown of NL1 and titrated application of NMDAR antagonist AP5 to achieve similar current reductions abolished long-term potentiation (LTP) along thalamo-amygdala connections (Kim et al., 2008), uncovering an even greater involvement of NL1 in NMDAR-dependent LTP than previous accounts in NL1 knockout mice (Blundell et al., 2010).

Recent *in vivo* investigations in non-mammalian model systems have provided compelling support for a conserved role of NL-NRX signaling in synapse development. *Drosophila* express a single NRX ortholog (dNRX) that shares all major protein domains with mammalian α-NRX but is not functionally regulated by alternative splicing (Zeng et al., 2007; Li et al., 2007). dNRX is neuron-specific and widely expressed throughout the central and peripheral nervous systems, with significant expression first detected near the completion of axonal pathfinding (Zeng et al., 2007; Li et al., 2007). Subcellularly, dNRX is strongly clustered at central synapses and neuromuscular junctions (NMJs) (Zeng et al., 2007; Li et al., 2007). dNRX null mutants exhibited reduced viability, similar to α-NRX knockout mice, and impaired locomotion (Zeng et al., 2007: Li et al., 2007). Immunofluorescent and ultrastructural analysis revealed that dNRX mutation approximately halved the density of central synapses (Zeng et al., 2007) and similarly halved the density of presynaptic boutons at NMJs, despite no deficits in axonal pathfinding (Li et al., 2007; Banovic et al., 2010). In complementary experiments, doubling the endogenous dNRX expression increased NMJ bouton density by 30% (Li et al., 2007). Residual synapses at NMJs of dNRX null mutant flies exhibited aberrant morphological development, with clear signs of presynaptic invagination and cleft expansion and potentially compensatory active zone lengthening and increased glutamate receptor clustering (Li et al., 2007). Morphological abnormalities were

moreover coupled with reduced excitatory junction potential (EJP) amplitudes but increased frequency and amplitude of spontaneous miniature EJPs, yielding decreased EJP quantal content (Li et al., 2007). Similar to α-NRX knockout mice, dNRX null mutant flies demonstrated reduced calcium sensitivity but normal calcium channel distribution, suggesting dNRX is necessary for proper coupling of vesicle fusion to calcium entry (Li et al., 2007).

Banovic et al. recently identified a *Drosophila* NL1 ortholog (dNL1) in a mutagenesis screen searching for reduced NMJ size (Banovic et al., 2010). Similar to dNRX, dNL1 shares all major protein domains with mammalian NLs and is found abundantly at postsynaptic densities of NMJs (Banovic et al., 2010). Careful temporal analysis of NMJs in dNL1 null mutant or knockout larvae revealed a specific impairment in addition of new boutons, rather than impaired maintenance of established boutons (Banovic et al., 2010). Moreover, loss of dNL1 signaling incurred pronounced postsynaptic deficits, including membrane detachment and postsynaptic invagination complementing dNRX mutant phenotypes (Banovic et al., 2010). Prevalent identification of ultrastructurally normal presynaptic terminals apposed to aberrant postsynaptic structures further suggests that dNL1 signaling is critical in initial stages of proper synapse formation (Banovic et al., 2010). dNL1 mutants also exhibited reduced glutamatergic receptor clustering and Ca^{2+}-independent EJP reductions, further suggesting a role of dNL1 in proper postsynaptic maturation and functional transmission (Banovic et al., 2010).

Employing two-photon time-lapse microscopy of alive, unanaesthetized *Xenopus* tadpoles, Haas and colleagues have provided compelling evidence for a role of NL-NRX signaling in morphogenesis of dendritic arbors (Chen et al., 2010). Interruption of NL1-NRX signaling at both the network level, by soluble NRX infusion, and the single cell level, using single cell electroporation to express NLswap or morpholino-oligonucleotides targeting endogenous NL1, markedly reduced dendritic filopodial densities by increasing rates of filopodial elimination, with corresponding increases in filopodial motility reflecting decreased stabilization (Chen et al., 2010). These morphological deficits were also strongly coupled with reduced excitatory synapse densities and mEPSC frequencies (Chen et al., 2010). Gain-of-function experiments

overexpressing NL1 demonstrated complementary increases in filopodial density and stability, yielding a unique spatially-restricted yet complex dendritic arborization pattern not previously observed in mammalian overexpression studies (Chen et al., 2010). Of significant interest, mechanisms of NL1-mediated filopodial maintenance (i.e. lifetime) and stability (i.e. decreased motility) proved dissociable. Both expression of NLΔC and chronic NMDAR blockade during NL1 overexpression precluded NL1-mediated gains in stabilization but still conferred significantly increased filopodial lifetimes (Chen et al., 2010). These results provocatively suggest that NL1-NRX tethering is capable of maintaining axodendritic contacts in an activity-independent manner, while activity-dependent intracellular NL1 interactions are necessary to stabilize filopodial cytoskeletons.

1.7   COGNITIVE AND BEHAVIORAL IMPLICATIONS OF NEUROLIGIN AND NEUREXIN SIGNALING

Autism spectrum disorders (ASDs) encompass heterogeneous syndromes combining deficits in social interaction, communication impairments, and restricted interests with repetitive behaviors or motor activities, and are often associated with impaired cognitive performance (Abrahams and Geschwind, 2008). ASDs exhibit a strong genetic link and affect males roughly four times more often than females, suggesting potential X-linked inheritance or susceptibility (Abrahams and Geschwind, 2008). ASDs are not associated with neurodegeneration and appear relatively late in development, leading some to hypothesize an etiology involving synapse formation, function, and/or plasticity (Zoghbi, 2003). In 2003, a screen of affected siblings and their families separately isolated a specific point mutation in NL3 (R451C) and a frameshift nonsense mutation in NL4 (D396X) in two sets of siblings diagnosed with ASD (Jamain et al., 2003). Soon after, independent analysis of a third family affected with ASD and X-linked mental retardation re-isolated the NL4 nonsense mutation (Laumonnier et al., 2004). Notably, both human NL3 and NL4 are encoded on the X-chromosome (Bolliger et al., 2001). Moreover, mutations in NRX1 and synaptic scaffolding molecule Shank3 have also

been implicated in ASDs (Südhof, 2008). These links with ASDs, together with extensive *in vitro* and *in vivo* results demonstrating the crucial role of NL-NRX signaling in synapse formation and function, have motivated several recent investigations into behavioral and cognitive impacts of NL and NRX perturbation.

Initial cellular investigations revealed that the NL3 R451C point mutation implicated in ASDs leads to retention of NL3 within the endoplasmic reticulum and consequently poor membrane delivery (Comoletti et al., 2004; Chih et al., 2004). The D396X mutation in NL4 leads to protein truncation and secretion, ultimately yielding similarly poor membrane delivery (Comoletti et al., 2004; Chih et al., 2004). Expression of exogenous NL3 R451C in dissociated hippocampal neurons further demonstrated that the minority of expressed protein that does reach the dendritic membrane is still capable of recruiting presynaptic components in contacting axons (Chih et al. 2004). NL3 R451C reaching the cell membrane of COS7 cells also proved capable of eliciting presynaptic differentiation in the mixed-culture assay, confirming a synaptogenic potential of NL3 R451C (Chubykin et al., 2005). Thus, the main deficit invoked by the R451C substitution, and likely also the D396X frameshift, involves membrane delivery and not synaptic function *per se*.

Surprisingly, however, a genetic knock-in strategy replacing endogenous NL3 with NL3 R451C in mice revealed a specific gain-of-function effect. Knock-in mice proved viable and fertile, with normal gross brain anatomy while exhibiting a 90% reduction in detectable NL3 protein levels, consistent with endoplasmic reticulum retention and subsequent degradation of mutant NL3 (Tabuchi et al., 2007). Immunohistochemical analysis of adult knock-in mice revealed a pronounced increase in vGAT puncta densities, however, commensurate with increased whole-brain protein levels of vGAT and gephyrin in immunoblots (Tabuchi et al., 2007). Ultrastructural analysis of cortex did not reveal altered synapse densities, however, suggesting strengthening of GABAergic connections by NL3 R451C knock-in (Tabuchi et al., 2007). Indeed, acute cortical slices exhibited increased mIPSC frequencies, IPSC amplitudes, and postsynaptic responses to GABA agonist application (Tabuchi et al., 2007). Strikingly, these inhibitory gains were not observed in NL3 knockout mice, confirming a previously unsuspected gain-of-function effect of the R451C substitution in NL3

(Tabuchi et al., 2007). Of note, the NL3 R451C knock-in also decreased whole brain NL1 protein levels, suggesting decreased NL1 signaling likely contributes to the enhanced inhibition observed (Tabuchi et al., 2007).

Implications of NL-NRX signaling in ASD have motivated considerable interest in behavioral phenotypes of the previously described NL and NRX mouse genotypes. Surprisingly, NL3 R451C knock-in mice exhibited only minimal behavioral differences from littermate controls despite the reported GABAergic gain-of-function, with no indication of deficits in social interaction or repetitive behavior relevant to ASD symptoms (Chadman et al., 2008; but see Tabuchi et al., 2007). In contrast, complete knockout of NL3 expression precipitated multiple behavioral changes. NL3 knockout mice demonstrated greater motor activity in open-field and elevated plus maze tests than littermate controls without noticeable differences in anxiety-like behavior, such as time spent in roofed portions of the elevated plus maze or avoidance of the open-field center (Radyushkin et al., 2009). This increased motor activity, together with equal performances on rotorod tests of motor learning and coordination, suggests that NL3 knockout mice exhibit general hyperactivity (Radyushkin et al., 2009). In tests of social behavior, NL3 knockout mice showed no difference in time spent interacting with a novel conspecific versus a novel inanimate object in either single or tripartite chamber tests compared to littermate controls (Radyushkin et al., 2009). NL3 knockout mice did exhibit reduced discrimination between a novel conspecific and a previously encountered conspecific in the tripartite chamber however, which together with poorer performance in the buried food-finding test than controls suggests a general impairment in olfaction (Radyushkin et al., 2009). In a test of communication, NL3 knockout mice produced significantly fewer ultrasonic courting calls than controls when placed next to a female mouse in estrous, though differences in latencies to first call did not reach significance (Radyushkin et al., 2009). Finally, NL3 knockout mice showed decreased freezing in both contextual and cued fear conditioning paradigms despite equal performance in the Morris water maze, arguing for a specific deficit in fear association with unaltered spatial learning and memory (Radyushkin et al., 2009). Interestingly, similar to NL3 R451C knock-in mice, NL3 knockout mice displayed reduced NL1 expression (Tabuchi et al., 2007), confounding direct interpretation of behavioral

changes but nevertheless revealing clear behavioral relevance of perturbed NL1/NL3 signaling.

Genetic deletion of NL4 yielded a more specific behavioral phenotype than loss of NL3. NL4 knockout mice exhibited no change in sensory processing, including olfaction; no change in general motor activity, learning, or coordination; intact freezing behavior during contextual and cued fear conditioning paradigms; and no deficits in spatial learning and memory (Jamain et al., 2008). During tests of social interaction, however, NL4 knockout mice curiously displayed a significant preference for wild-type conspecifics over other NL4 knockout mice, while in the tripartite chamber NL4 knockout mice demonstrated no preference toward a novel conspecific and no preference between novel and previously encountered conspecifics, altogether suggesting altered social interactions in NL4 knockout mice (Jamain et al., 2008). These mice further displayed significant deficits in ultrasonic courting vocalizations, with both longer latencies to the first vocalization and fewer total vocalizations (Jamain et al., 2008). Thus, developmental loss of NL4 provocatively yields specific behavioral deficits in social interaction and communication – hallmarks of ASDs.

Consistent with reduced NMDAR to AMPAR EPSC ratios and consequent deficits in hippocampal LTP, NL1 knockout mice showed impaired spatial learning and memory in the Morris water maze, with no differences found in tests for general motor activity, motor coordination and learning, anxiety-like behavior, sensory processing, or contextual or cued fear conditioning (Blundell et al., 2010). A specific deficit in the Morris water maze coupled with aberrant hippocampal long-term plasticity was also discovered in transgenic mice with roughly doubled NL1 expression (Dahlhaus et al., 2010), strongly arguing that developmental NL1 levels are crucial to proper spatial learning and memory. Notably, repeated measures of adult rats revealed significantly less freezing behavior in the contextual and cued fear conditioning paradigm after acute NL1 knockdown in LA, with no change in general motor activity, anxiety-like behavior, or pain sensitivity (Kim et al., 2008), extending knockout and transgenic findings to suggest that NL1 may be critically involved in multiple behaviors believed to involve NMDAR-dependent synaptic plasticity. Different from NL3 and NL4 knockout strains, NL1 knockout yielded only minimal alterations in social interaction, with only moderate

differences found between knockout and littermate controls in one test of several (Blundell et al., 2010). Intriguingly, NL1 knockout mice were reported to spend extensive time on stereotyped grooming activities, a behavioral alteration presumably linked with reduced NMDAR to AMPAR EPSC ratios and presumably altered plasticity in striatum (Blundell et al., 2010). Similar excessive grooming was also reported for NRX1α knockout mice, with otherwise normal behavior (Etherton et al., 2009).

Disparate from impairments in spatial learning and memory and fear association and stereotyped behavior observed in NL1 knockout mice and the reduced social interactions of NL3 and NL4 knockout mice, developmental loss of NL2 specifically triggered increased anxiety-like behavior in both open-field and dark/light box tests, including less time and fewer entries into the open-field center and lit portion of the dark/light box (Blundell et al., 2009). Strikingly, transgenic mice with roughly doubled NL2 expression displayed similar increases in anxiety-like behavior in open field, dark/light box, and elevated plus maze tests (Hines et al., 2008). Distinct from NL2 knockout mice, however, transgenic NL2 mice also demonstrated altered social interactions, displaying reduced interactions with a novel conspecific compared to control littermates and no preference between a novel and previously encountered conspecific in the tripartite chamber (Hines et al., 2008). Interestingly, transgenic NL2 mice are also the only *in vivo* strain thus far reported to demonstrate spike-wave discharges in EEG recordings, suggesting potential susceptibility to seizure (Hines et al., 2008).

1.8   CONCLUSIONS

In vitro experiments have demonstrated a critical role of NL-NRX signaling in synapse initiation, specification, and pre- and postsynaptic maturation. Recent *in vivo* studies using knockout, acute knockdown, and transgenic approaches have corroborated several of these findings and additionally emphasized crucial roles of NL-NRX in synaptic function and plasticity. Considerable work remains before the roles of NLs and NRXs throughout development and adulthood are completely understood, however.

Principle among current uncertainties and a hotly contested issue in the literature is whether NL-NRX signaling is primarily involved in synapse initiation or activity-dependent synapse validation. To begin to address this, experiments must be devised that are capable of dissociating activity-dependent and -independent effects of NL-NRX signaling on pre- and postsynaptic compartments. A greater understanding of synapse specification will also be necessary, including whether scaffolding molecules restrict initiation of specific synapse types and how scaffolding molecules coordinate with alternative splicing regulation. Understanding how NL-NRX complexes coordinate with other transsynaptic adhesion complexes, such as the recently identified SC family, will prove crucial in reconciling discrepancies between *in vitro* and *in vivo* experiments. Toward this objective, both *in vitro* multi-molecular perturbations and cross breeding of knockout strains will prove invaluable. Further, the field is beginning to uncover a much broader picture of NL-NRX interactions in the scope of shaping overall neural networks. Initial work in *Xenopus* has evinced a critical involvement of NL-NRX signaling in dendritic arborization. Much research lays ahead in expounding this phenomenon in developing mammalian neurons. Finally, *in vivo* behavioral studies thus far conducted have revealed critical involvement of NLs and NRXs in proper behavioral development, and indeed are beginning to elucidate portions of the synaptic ASD etiology. Conditional knockout and transgenic approaches will be vital for future investigations of how NL-NRX signaling contributes in mature networks to regulate these behaviors.

Herein I capitalize on the ability of high NL overexpression to disrupt recruitment of key postsynaptic components to dissociate transsynaptic NL1 signaling from postsynaptic differentiation. This strategy, together with reevaluation of chronic NMDAR blockade experiments, demonstrates that NL1 is capable of robustly inducing presynaptic differentiation independent of synaptic activity. Importantly, this experiment re-derives in hippocampal neurons the activity-independent synapse formation previously only observed in mixed-culture assays and refutes claims that NMDAR activity is necessary for NL1 contributions to synapse densities. Combined NL1/PSD95 perturbation in hippocampal neurons is then used to confirm that endogenous PSD95 is not necessary to mediate initial recruitment of presynaptic terminals, while results from the mixed-culture assay clarify that binding of PSD95 alone does not restrict NL1-

mediated synapse formation, as previously suggested (Prange et al., 2004). Preliminary investigations of combined NL1/SC1 perturbations in dissociated hippocampal cultures suggest that SC1 may functionally activate immature synapses induced by NL1 overexpression, providing tentative evidence for coordinate NL1/SC1 signaling at the same synapse. Lastly, I present initial evidence of an effect of NL1 overexpression on dendritic arborization in mammalian neurons, with high NL1 overexpression driving complex yet spatially-restricted perisomatic dendritic branching.

2.0   EXPERIMENTAL METHODS

2.1   ANTIBODIES AND DNA CONSTRUCTS

The following primary antibodies were used: chicken anti-HA (Millipore AB3254; 1:250), mouse anti-βIII tubulin (kindly provided by Dr. Willi Halfter; 1:20), rabbit anti-synapsin I (Millipore AB1543; 1:500), mouse anti-MAP2 (Sigma Aldrich M9942; 1:200), mouse anti-Tau-1 (Millipore MAB3420; 1:1000), mouse anti-PSD95 (Thermo Scientific MA1-046; 1:200), rabbit anti-FLAG (Affinity Bioreagents PA1-984B; 1:500), and sheep anti-actin (Millipore AB3265; 1:1000). Secondary antibodies used in immunocytochemistry were Alexa Fluor (AF) conjugates (Invitrogen) and used at 1:1000 dilution. These included: AF555:goat anti-mouse, AF647:goat anti-mouse, AF488:goat anti-rabbit, AF555:goat anti-rabbit, and AF555:goat anti-chicken. Secondary antibodies used in immunoblotting were horseradish peroxidase conjugates. These included: HRP:goat anti-rabbit (Invitrogen SJ29096, 1:10000), HRP:rabbit anti-sheep (Millipore 12-342; 1:1000), and HRP:rabbit anti-chicken (Millipore AP162P; 1:10000).

For all NL1 experiments, the NL1(AB) isoform was used. NL1(AB) and NLswap constructs were kindly provided by Dr. Peter Scheiffele and previously described (Scheiffele et al., 2000). Briefly, the influenza hemagglutinin (HA) epitope tag was inserted downstream of the N-terminal signal sequence in the extracellular domain of NL1 and NLswap. Both HA:NL1 and HA:NLswap were expressed from the chicken beta actin promoter of the pCAGGS vector. LentiLox3.7 (LL3.7) and the LL3.74 variant were kindly provided by Dr. Martha Constantine-Paton and used for expression of soluble GFP and DsRed2, respectively, as well as in RNAi experiments to express short hairpin RNA sequences from the U6 promoter. The PSD95 expression construct was kindly provided by Dr. Morgan Sheng and expressed PSD95 from the CMV promoter of the pGW1 vector. The SC1 expression construct was kindly provided by Dr. Thomas Biederer and previously described (Fogel et al., 2007). Briefly, the FLAG epitope tag

was inserted within the extracellular domain, and FLAG:SC1 was expressed using the pCAGGS vector. The SCΔIg expression construct was kindly provided by Dr. Thomas Südhof and was previously described (Biederer et al., 2002). Briefly, the three Ig domains of SC1 were deleted, and SCΔIg was expressed from the CMV promoter of the pCMV5 vector. For lentivirus production, VSVg and Δ8.9 vectors were kindly provided by Dr. Martha Constantine-Paton.

For RNAi knockdown of PSD95, a previously validated short hairpin sequence "shPSD95" (Zeringue and Constantine-Paton, unpublished data) was used. For SC1 knockdown, the short hairpin sequence "shSC1" was designed in accordance with published design criteria (Reynolds et al., 2004). The shSC1 efficacy was tested by coexpression of FLAG:SC1 and shSC1 (at a ratio of 1:3) in HEK293 cells and immunoblotting against the FLAG epitope. For RNAi control experiments, a scrambled version of shPSD95, "shPSD95scr" was used. Short hairpin sequences were as follows:

shPSD95, 5' → 3' sense strand
tGATGAAGACACGCCCCCTCttcaagagaGAGGGGGCGTGTCTTCATCtttttttc
shPSD95, 5' → 3' antisense strand
tcgagaaaaaaGATGAAGACACGCCCCCTCtctcttgaaGAGGGGGCGTGTCTTCATCa

shPSD95scr, 5' → 3' sense strand
tGCCCTACCACCGAGGTCAAttcaagagaTTGACCTCGGTGGTAGGGCtttttttc
shPSD95scr, 5' → 3' antisense strand
tcgagaaaaaaGCCCTACCACCGAGGTCAAtctcttgaaTTGACCTCGGTGGTAGGGCa

shSC1, 5' → 3' sense strand
tCAGAAGGAGGACAGAACAAttcaagagaTTGTTCTGTCCTCCTTCTGtttttttc
shSC1, 5' → 3' antisense strand
tcgagaaaaaaCAGAAGGAGGACAGAACAAtctcttgaaTTGTTCTGTCCTCCTTCTGa

2.2   CELL CULTURE AND TRANSFECTION

For experiments in dissociated neuronal cultures, hippocampal neurons were dissociated from E18-19 C57BL/6 mouse embryos and plated at 30,000 cells/cm^2 on confluent mouse neocortical glial monolayers previously prepared on glass coverslips coated with poly-D-lysine (PDL). Cultures were maintained in neurobasal medium supplemented with 2% B27 (Invitrogen), 1% penicillin-streptomycin, and 0.5 mM L-glutamine in a 37ºC/5% CO_2 incubator. One quarter of the total culture medium was exchanged for fresh medium every 2-3 days. Cultures maintained in 3 µM cytosine arabinofuranoside beginning at DIV2 to prevent glial overgrowth.

Prior to transfection at DIV9-10, glass coverslips containing neuron/glia cultures were transferred to a new 35 mm dish containing 2 ml fresh culture medium without penicillin-streptomycin. Neurons were transfected using Lipofectamine 2000 (Invitrogen) essentially as described by the manufacturer with the following modifications: for each 35 mm dish, 2 µg total DNA was mixed with 1.5 µl Lipofectamine 2000 reagent in 80 µl total volume of Opti-MEM (Invitrogen) and added dropwise. After 1 hr, coverslips containing neuron/glia cultures were removed from the transfection dish and placed in a new 35 mm dish containing 2 ml fresh culture medium and incubated for 5 min. Coverslips were then transferred back to the original culture medium and maintained for 3-4 days until processing for immunocytochemistry or electrophysiology. For NMDAR activity blockade, 100 µM D-AP5 was added to cultures at the time of transfection and renewed every 1-2 days.

Human embryonic kidney 293 (HEK293) cells were maintained in DMEM supplemented with 10% fetal bovine serum, 1% penicillin-streptomycin, 1% sodium pyruvate, and 1% nonessential amino acids. For transfection, nearly confluent HEK293 cultures were dispersed with trypsin and seeded at a density of 9x10^5 cells/ml onto dishes coated with PDL and transfected 3-8 hr later using Lipofectamine 2000 as described by the manufacturer. Transfected HEK293 cultures were processed 1-2 days later for mixed-culture assays or immunocytochemistry.

For mixed-culture assays, cortical or hippocampal neurons were dissociated from E18-19 C57BL/6 mouse embryos and plated at 30,000 cells/cm^2 directly onto glass

coverslips coated with PDL and laminin. Cultures were maintained identical to neuron/glia cultures described above except initial plating medium contained 25 µM glutamate. HEK293 cells were transfected at neuronal DIV8-9 and seeded 1-2 days later at 250 cells/cm^2 onto pure neuronal cultures. Mixed-cultures were maintained for 1-2 days prior to processing for immunocytochemistry.

2.3   IMMUNOBLOTTING

Protein was extracted from HEK293 cultures using ice cold lysis buffer (20 mM Tris, pH 7.5, 150 mM NaCl, 1 mM EDTA, 1% Triton X-100, 0.5% deoxycholate, 0.1% SDS, and complete protease inhibitor cocktail (Roche)). Protein concentrations were quantified using a modified Lowry assay (Bio-Rad Laboratories). Cell lysates were prepared in Laemmli buffer, denatured at 95ºC for 3 min, and equal total masses loaded into 6% gels. After electrophoresis, proteins were transferred to nitrocellulose membranes using a wet transfer method. Membranes were blocked in 5% instant nonfat dry milk then incubated sequentially with primary and secondary antibodies prepared in 2% instant nonfat dry milk solutions. All incubations were carried out for 1-3 hr at room temperature or overnight at 4ºC. Protein signals were detected using HRP-mediated chemiluminescence.

2.4   IMMUNOCYTOCHEMISTRY

Cells were fixed in a 4% paraformaldehyde/4% sucrose, phosphate-buffered saline (PBS) solution at 37ºC for 10 min. For intracellular epitopes, fixed cells were permeabilized with a 0.3% Triton X-100 PBS solution. Nonspecific binding was blocked using a 1-3 hr room temperature or overnight 4ºC incubation in a 5% BSA PBS solution. Cells were sequentially incubated with primary and secondary antibodies diluted in a 1% BSA PBS solution for 1-3 hr each at room temperature. For endogenous PSD95

staining and quenching of soluble GFP signals, cells were alternatively fixed in ice cold methanol.

2.5   IMAGING AND ANALYSIS

Neuron images were collected on an upright Olympus Fluoview 1000 confocal microscope using a 40X or 60X oil-immersion objectives in maximum intensity projections of 0.5 µm-step z-stacks at 1024x1024 or 2048x2048 resolution, as specified. Equivalent settings were used across all images for each experiment. Dendritic puncta densities were quantified in NIH ImageJ using the analyze particles function and a neurite-specific background subtraction procedure (Glynn and McAllister, 2006). Only puncta completely or partially overlapping with thresholded dendritic soluble GFP or MAP2 signals were counted in densities. Mean intensities of immunostained HA:NL1 within a dendritic branch were quantified after neurite-specific background subtraction and measured as the total mean intensity of all pixels within a defined dendritic branch segment, including membrane, cytoplasmic, and spine compartments. Dendrites were defined either by positive MAP2 immunoreactivity or morphologically, based on thick diameters and clear presence of spiny protrusions. Dendritic spines were identified and counted manually, with protrusions longer than ~5 µm or displaying clear branching not included in counts. For two-dimensional Sholl analysis, a thresholded 8-bit maximum intensity projection image was loaded into NIH ImageJ and a point selected within a centered soma. The numbers of neurites intersecting with successively larger circles surrounding the somal point (with radius interval 20 µm) were then counted using a custom plugin freely available from the lab of Dr. Anirvan Ghosh, University of California San Diego.

HEK293 images were collected on upright Olympus Fluoview 500 and 1000 confocal microscopes using a 60X or 100X oil-immersion objective in maximum intensity projections of 1.0 µm- or 0.5 µm-step z-stacks at 1024x1024 or 2048x2048 resolution, as specified. The percentage of HEK293 cell area colocalized with suprathreshold synapsin I was quantified as a metric for induction of presynaptic

differentiation (Biederer and Scheiffele, 2007). Briefly, synapsin I fluorescence was thresholded by identifying 10 background points and subtracting their mean grayscale intensity +2 standard deviations from the entire synapsin I grayscale field. Fluorescence of HEK293 cell cotransfection marker GFP or DsRed2 was then thresholded to define the HEK293 cell outline and used to confine the synapsin I field.

Statistical comparisons of imaging data among groups were made using t-tests for 2 groups and one-way ANOVAs for 3 groups, with posthoc Tukey-test completed upon significant ANOVA results ($p < 0.05$). Column numbers in each figure indicate the number of cells quantified per condition, with error bars denoting SEM. All statistical comparisons were performed using OriginPro 8.0. Figures were prepared using NIH ImageJ, OriginPro 8.0, and Adobe Illustrator CS2.

2.6   ELECTROPHYSIOLOGY

Whole-cell patch-clamp recordings of DIV12-14 hippocampal neurons were made at room temperature using an Axopatch 200A amplifier. The intracellular solution contained (in mM) 135 CsCl, 10 HEPES, 1 EGTA, and 4 Mg-ATP (pH 7.4) and the extracellular solution contained (in mM) 150 NaCl, 4 KCl, 2 $MgCl_2$, 10 glucose, 10 HEPES, and 2 $CaCl_2$, yielding a junction potential of ~5.7mV that was offset prior to recording. Compensation for series resistance was not applied. Neurons were voltage-clamped at -70 mV and spontaneous miniature events were recorded in the presence of 1 µM TTX. Data were low-pass filtered at 2kHz and sampled at 20 kHz. Miniature synaptic events were identified using Clampfit 9 (Molecular Devices) with an amplitude threshold ~4 times greater than the RMS noise level and confirmed visually. Total distributions of miniature event amplitudes were statistically compared using the Kolmogorov-Smirnov test, while event frequencies were compared using one-way ANOVA, with posthoc Tukey-test completed upon significant ANOVA results ($p < 0.05$). A 1 kHz posthoc filter was applied to representative traces presented in figures for greater visual clarity.

2.7 LENTIVIRUS PRODUCTION AND CONCENTRATION

For lentivirus production, HEK293 (type FT, Invitrogen) grown to 90% confluence in 10 cm dishes were transfected using Lipofectamine 2000 (Invitrogen), generally as above. Per each 10 cm culture, 2.7 µg VSVg, 4.0 µg Δ8.9, and 5.3 µg of the transfer vector were cotransfected using 36 µl Lipofectamine 2000. Media containing viral particles was collected, 24, 48, and 60 hr post-transfection and stored at 4ºC until concentration. For concentration, total collected media was filtered through 0.45 µm PVDF filters and centrifuged at 3000 rpm to remove cellular debris. Filtered supernatant was then centrifuged at 25,000 rpm for 90 min at 4ºC, and pelleted viral particles were resuspended in cold PBS and stored at -80ºC. Viral titers were then determined using HEK293 cells.

3.0   RESULTS

3.1   ACTIVITY-DEPENDENT AND -INDEPENDENT NEUROLIGIN-1 SIGNALING IN DISSOCIATED HIPPOCAMPAL NEURONS

3.1.1   Characterization of neuroligin-1 overexpression in dissociated hippocampal neurons

To begin investigating the roles of NL1 in synapse formation and function, protocols for preparation, culture, and transfection of primary hippocampal neurons from E18-19 C57BL/6 mice were first optimized. For all experiments, neurons were cultured at a moderately sparse final density of 30,000cells/cm^2. Inclusion of neocortical glial feeder layers led to more robust cultures, with viability maintained up to at least three weeks. All neuron transfections were thus performed in neuron-glia cocultures. Overexpression of HA-tagged NL1 was achieved through liposome-mediated transfection of 2µg total DNA per 35mm culture dish (500 ng of the HA:NL1 expression vector, 1µg of GFP-expressing LL3.7, and 500 ng of LL3.7ΔGFP or a second expression construct for multi-molecular perturbations). Addition of LL3.7ΔGFP, a variant of LL3.7 with the GFP coding sequence replaced by a custom multi-cloning site, was used to achieve comparable transfection ratios and efficiencies across all experiments without biasing fluorescent signals between perturbations. Neurons were transfected at DIV9-10 and analyzed 3-4days later.

Under the described conditions, successful transfections yielded several dozen neurons per culture displaying strong fluorescence throughout all processes within a day of transfection. Transfected neurons exhibited no signs of compromised viability throughout the duration of each experiment. To evaluate cotransfection and coexpression efficiency, neurons were cotransfected with LL3.7, pGW1-PSD95, and pCAGGS-HA:NLswap, and immunostained for PSD95 and the HA epitope. Preliminary

experiments established that PSD95 overexpression was clearly discernable above basal punctate PSD95 staining (data not shown). Of 15 neurons imaged, all showed significant GFP and NLswap expression and PSD95 overexpression (Figure 1), confirming >95% cotransfection and coexpression efficiency.
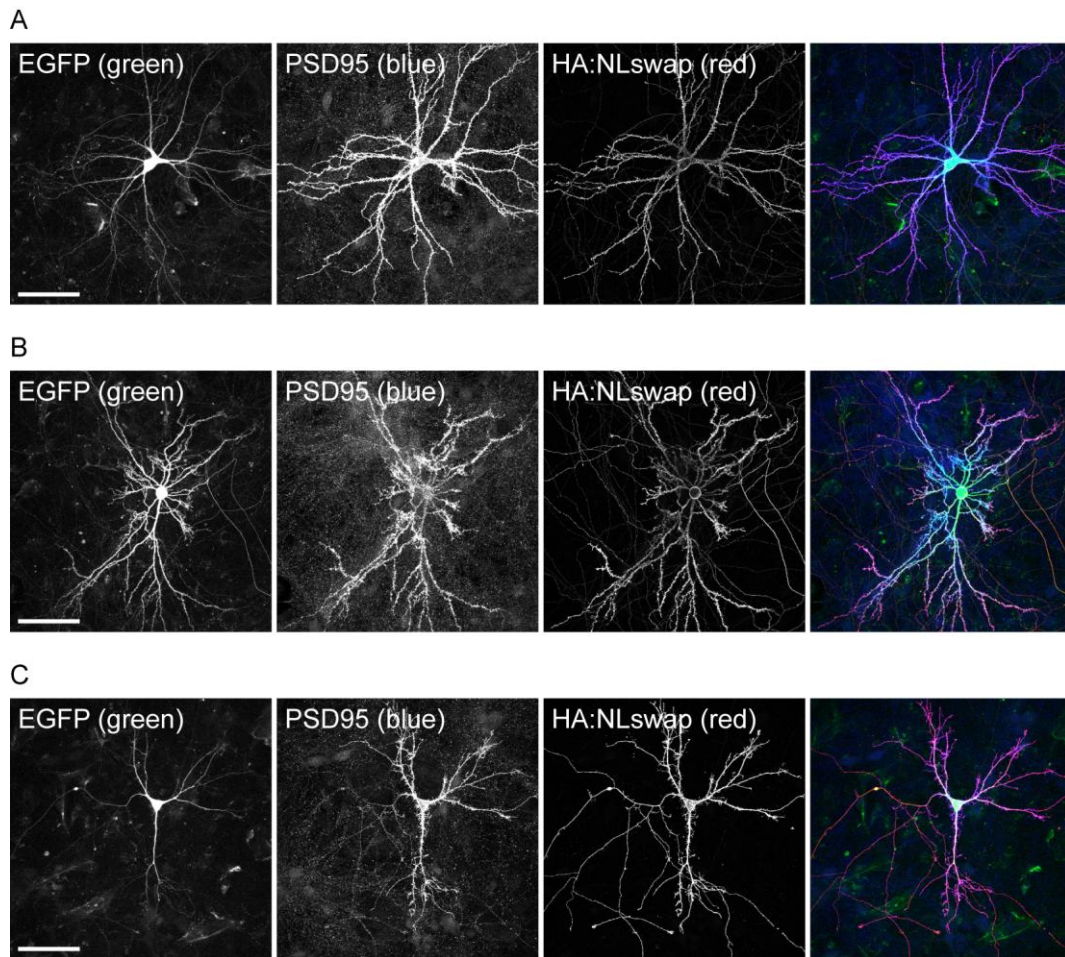
Figure 1: Evaluation of triple transfection and coexpression efficiencies

Dissociated hippocampal neurons were cotransfected with LL3.7, pCAGGS-HA:NLswap, and pGW1-PSD95 at DIV9 and processed at DIV12 for HA:NLswap and PSD95 immunostaining. Imaging of GFP, NLswap, and PSD95 revealed strong coexpression in all 15 neurons imaged; note the excessive PSD95 signal in transfected neurons compared to the endogenous punctate signal in surrounding neurites. Three representative neurons are shown. Rightmost figures show merge of individual channels displayed on left. Scale bars: 33µm. Objective: 40X. Digital zoom: 1X. Resolution: 1024x1024. Confocal step size: 0.5µm.

Employing the described transfection protocol, exogenous NL1 was strongly expressed throughout all dendritic processes (Figure 2). HA:NL1 exhibited strong membrane localization and was often found clustered in spine heads (Figure 2, regions of interest), consistent with prior reports of weak endogenous and exogenous NL1 clustering (Prange et al., 2004; Levinson et al., 2005; Barrow et al., 2009). In addition, HA:NL1 was observed diffusely throughout all cytoplasmic dendritic compartments and further mislocalized to axonal processes (Figure 2, arrows). Image acquisition parameters were identical across all images and chosen to elicit maximum intensities just below saturation to achieve the greatest detection range. Axonal HA:NL1 intensities were well above background levels and consistently observed in transfected neurons (but not in neighboring neurons), suggesting positive axonal staining was specific. NL1 has not been endogenously observed in axons (Dresbach et al., 2004; Rosales et al., 2005; Song et al., 1999), nor reported in prior overexpression studies, suggesting that the transfection parameters used achieved high levels of overexpression not previously considered.
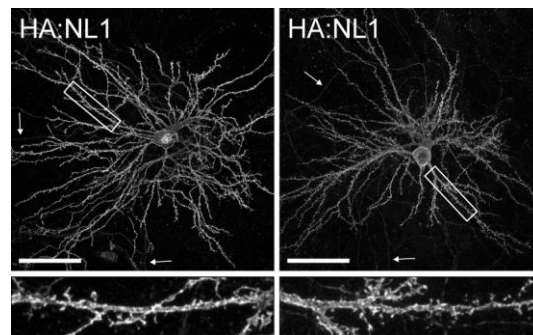
Figure 2: High overexpression of NL1 in dissociated hippocampal neurons

Dissociated hippocampal neurons were transfected with 500 ng of a plasmid expressing HA:NL1 at DIV9-10 and processed at DIV12-14 for exogenous HA:NL1 immunostaining. In both representative neurons shown, exogenous HA:NL1 can be seen to concentrate in dendritic membranes and spines, with additional diffuse localization throughout the dendritic shaft. Note that at this overexpression level, HA:NL1 also mislocalizes to axons (arrows), which are clearly distinguished by their aspiny and thin morphology in this preparation. Boxed regions of interest (50µm long) are enlarged in insets. Scale bars: 50µm. Objective: 60X. Digital zoom: 1X. Resolution: 2048x2048. Confocal step size: 0.5µm.

3.1.2   High neuroligin-1 overexpression triggers synapse formation and morphological changes

While not physiological, the NL1 expression levels achieved using the described overexpression protocol present a unique opportunity to dissociate transsynaptic NL1 signaling from postsynaptic differentiation. Craig and colleagues have previously shown that high overexpression of NL2 disrupts clustering of postsynaptic PSD95, gephyrin, NMDAR, and GABA$_A$R, suggesting that proper NL2 levels are necessary for endogenous clustering of several postsynaptic components (Graf et al., 2004). It remains unknown, however, whether similar strong disruption of postsynaptic clustering affects NL1-mediated recruitment of presynaptic terminals. Importantly, related experiments expressing intracellular NL1 mutants do achieve comparable dissociation between transsynaptic signaling and postsynaptic differentiation; for instance, NL1ΔC expression still increased synaptic NMDAR puncta densities (Chih et al., 2005).

Thus, as a first step to evaluate the effects of high NL1 overexpression on presynaptic terminal recruitment, the distribution of presynaptic marker synapsin was examined 3-4 days post-transfection. Additionally, a construct expressing soluble GFP or DsRed2 was included in all transfections to mark transfected neurons and enable complete visualization of neurites and dendritic spines. Under these conditions, high NL1 overexpression triggered robust synapsin clustering (Figure 3), with all dendritic processes clearly outlined in suprathreshold synapsin puncta (Figure 3A). In comparison, expression of GFP alone did not result in any noticeable change in synapsin densities compared to neighboring untransfected neurons (Figure 3B). The NLswap construct, in which the esterase domain of acetylcholinesterase is exchanged for the homologous extracellular domain in NL1, was included as a second control to confirm specificity of results to transsynaptic NL1 signaling, which requires the intact extracellular NL1 domain (Scheiffele et al., 2000; Dean et al., 2003). Quantification of suprathreshold synapsin puncta densities along isolated dendritic branches revealed a highly significant, three to four fold gain in synapse densities with high NL1 overexpression compared to GFP and NLswap controls (Figure 3G). Dendritic spines of NL1-overexpressing neurons often exhibited multiple colocalized synapsin clusters. Moreover, dense clustering of synapsin around neurons overexpressing NL1 led to

overlap between clusters, suggesting reported values underestimate actual synapsin densities. Indeed, quantification of identical preparations after methanol fixation instead of paraformaldehyde fixation revealed slightly higher densities (Figure 5). Average puncta sizes were thus not quantified to prevent bias from overlapping clusters. Examination of synapsin cluster densities alone, however, was sufficient to evince pronounced transsynaptic signaling by NL1 under high overexpression conditions.

High overexpression of NL1 also conferred a significant morphological effect, driving robust increases in dendritic spine densities (Figure 3A, C, E regions of interest). Dendrites of NL1-overexpressing neurons displayed both typical, mushroom-shaped spines and irregular, thin filopodia-like spines. Quantification of total spines densities revealed a significant increase in NL1-overexpressing neurons compared to both GFP- and NLswap-expressing neurons (Figure 3H). These results are surprising, given the high level of NL1-overexpression, and suggest that a portion of excitatory synapses are still capable of some degree of maturation corresponding to spine maintenance despite the dispersion of many postsynaptic components with high NL overexpression (Graf et al., 2004).
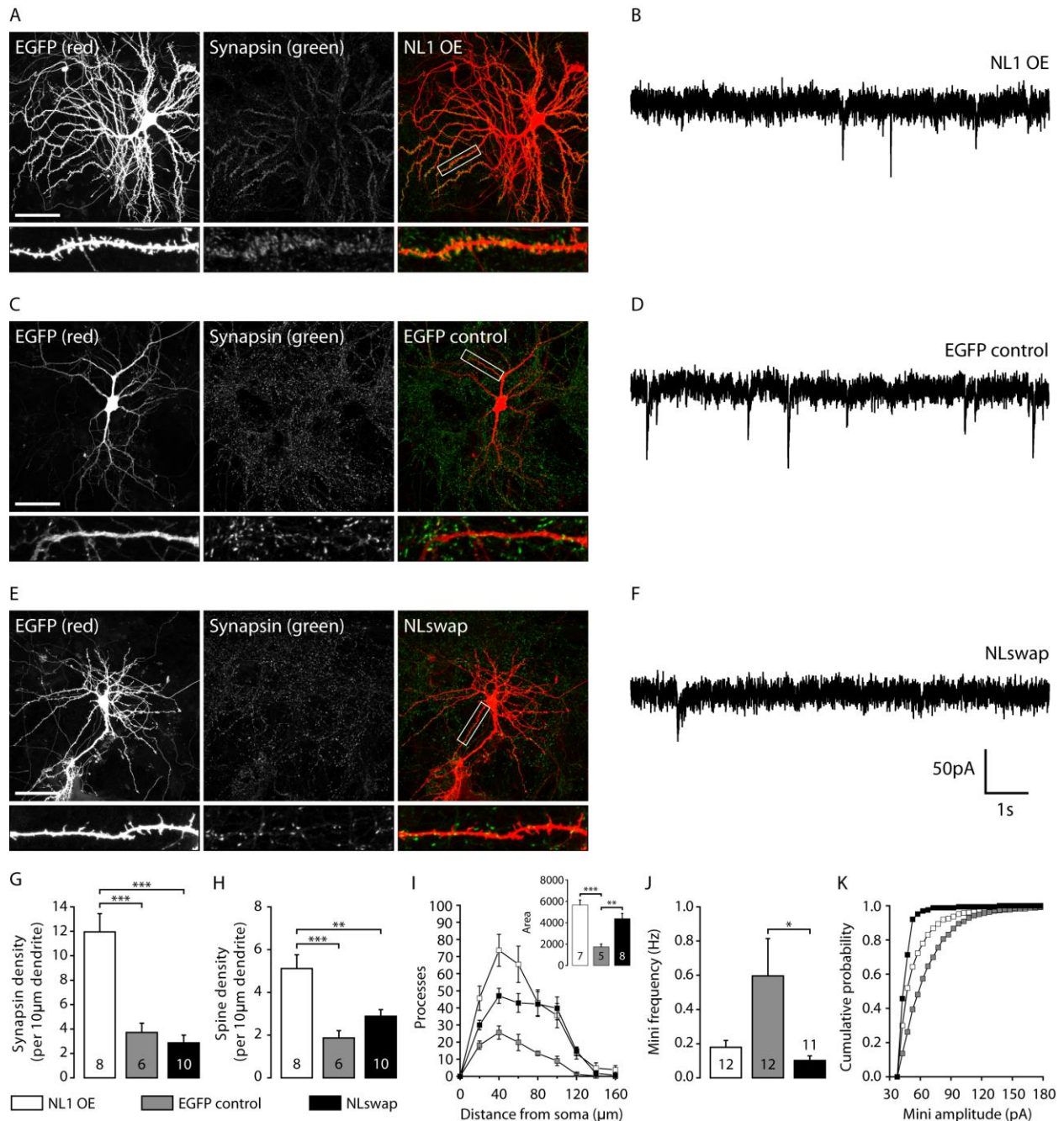
Figure 3: High overexpression of NL1 drives presynaptic differentiation, spine formation, and process outgrowth while reducing spontaneous miniature event frequency

Dissociated hippocampal neurons were transfected with plasmids expressing (A,B) HA:NL1 and GFP, (C,D) GFP, or (E,F) HA:NLswap and GFP at DIV9-10 and processed at DIV12-14 for (A,C,E) synapsin immunostaining or (B,D,F) electrophysiology. NL1 overexpression (OE) triggered a marked increase in (G) synapsin puncta density and (H) spine morphogenesis compared to GFP and NLswap conditions. (I) Sholl analysis revealed a significant increase in dendritic arbor complexity with NL1 overexpression or NLswap expression compared to GFP controls (inset: area under Sholl curves). (J) High NL1

49

overexpression or NLswap expression demonstrated similar reductions in spontaneous miniature event frequency compared to GFP controls, while (K) NLswap expression shifted the cumulative distribution of spontaneous miniature events to lower amplitudes compared to GFP and NL1 overexpression conditions ($p < 0.001$, Kolmogorov-Smirnov test). High NL1 overexpression also appeared to reduce miniature event amplitudes from the GFP condition, but this effect did not reach statistical significance ($p > 0.05$, Kolmogorov-Smirnov test). Rightmost figures in A, C, and E show merge of individual channels displayed on left. Boxed regions of interest (50µm long) defined in merged images are enlarged in insets. Scale bars: 50µm. Objective: 60X. Digital zoom: 1X. Resolution: 2048x2048. Confocal step size: 0.5µm. ***$p < 0.001$, **$p < 0.01$, *$p < 0.05$, ANOVA, Tukey post-hoc test.

Gross analysis of total neuron morphology further revealed complex dendritic arborization in neurons overexpressing NL1 versus simpler arbors of GFP-expressing neurons (compare Figure 3A and C). Surprisingly, NLswap expression also appeared to trigger more complex total arbors than GFP-expressing controls (compare Figure 3E and C). To quantify this effect, a basic two-dimensional Sholl analysis was performed and the integrated area of each resulting distribution was used for statistical comparison of overall arbor complexities. Both NL1 overexpression and NLswap expression significantly increased total arbor complexities from GFP control levels (Figure 3I). Intriguingly, a subset of NL1-overexpressing neurons further displayed a unique pattern of intense perisomatic dendritic branching (Figure 4). This spatially-restricted yet complex arborization was never observed in neurons expressing GFP or NLswap, suggesting both transsynaptic NL1 signaling and the intracellular postsynaptic interactions remaining under high overexpression conditions contribute to dendritic arborization, consistent with recent findings in *Xenopus* tadpoles (Chen et al., 2010). Of note, the limited two-dimensional Sholl analysis applied was often unable to clearly resolve and account for this dense perisomatic arborization in maximum intensity projections, resulting in marked underestimation of perisomatic complexity in high NL1 overexpression conditions across multiple experiments.
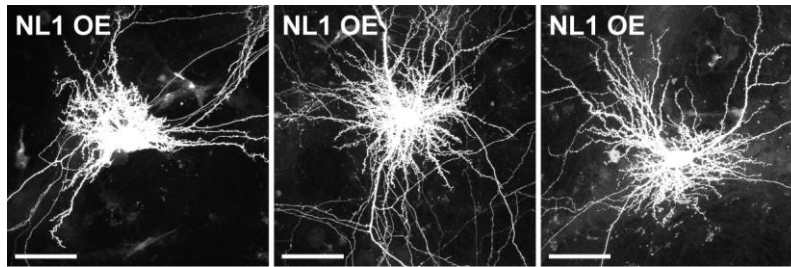
Figure 4: High NL1 overexpression triggers intense perisomatic dendritic branching in a subset of hippocampal neurons

Dissociated hippocampal neurons were transfected with plasmids expressing HA:NL1 and GFP under high overexpression conditions at DIV9-10 and processed at DIV12-14 for immunostaining. Three representative neurons from two separate experiments demonstrate the unique spatially-restricted yet complex dendritic arborization morphology induced in a subset of NL1-overexpressing neurons. Scale bars: 50µm. Objective: 60X. Digital zoom: 1X. Resolution: 2048x2048. Confocal step size: 0.5µm.

3.1.3   New synaptic contacts induced by high neuroligin-1 overexpression are immature

To assess whether the putative synaptic connections induced by high NL1 overexpression are functional, whole-cell patch-clamp electrophysiology was used to record spontaneous miniature synaptic events. Using this technique, an increase in the frequency of events would reflect an increase in the number of functional synaptic contacts, while an increase in the amplitude of events would likely correspond to increased recruitment of neurotransmitter receptors to postsynaptic compartments of functional synaptic contacts. In the presence of 1µM TTX, which blocks action potential-dependent activity, control GFP-expressing neurons averaged approximately one spontaneous miniature event every two seconds (Figure 3D and J), with considerable variability consistent with the random connectivity established in dissociated neuronal cultures. Most spontaneous miniature events displayed fast decay kinetics, with time constants below 10 msec, consistent with a preponderance of excitatory connections and pyramidal neurons in dissociated hippocampal cultures. Strikingly, the robust gains in synapsin cluster densities observed with high NL1 overexpression were not coupled with an increase in spontaneous miniature event frequency (Figure 3B). Rather, NL1-

51

overexpressing neurons displayed frequencies equal to NLswap-expressing neurons, which were roughly five to six fold lower than control cells (Figure 3J). While the decrease in event frequencies observed in NL1-overexpressing neurons did not reach statistical significance due to high variation in control neurons, the strong decreasing trend profoundly contrasts with the robust morphological gains observed. Similar results were additionally obtained in separate trials using dissociated cortical cultures (data not shown). Lack of increased spontaneous miniature event frequency with high NL1-overexpression thus suggests that new synaptic contacts are functionally immature, lacking both AMPAR and GABA$_A$R activity. Moreover, tendency towards decreased frequencies below basal levels suggests that the high level of exogenous NL1 expression was indeed efficacious in disrupting proper postsynaptic differentiation, thereby decoupling transsynaptic NL1 signaling from postsynaptic AMPAR or GABA$_A$R activity. Lastly, NLswap expression significantly shifted the distribution of total miniature event amplitudes to lower values compared to both GFP expression and NL1 overexpression (Figure 3K). High NL1 overexpression also appeared to reduce miniature event amplitudes from basal levels, but this effect did not reach statistical significance. Reductions from basal event amplitudes are consistent with disruption of proper postsynaptic differentiation.

3.1.4   Titration of neuroligin-1 overexpression

To better characterize the degree of NL1 overexpression and consequent effects on synapsin clustering, the amount of the NL1 expression vector being transfected was systematically varied. Importantly, the total mass and general composition of transfected DNA was kept constant by offsetting the amount of pCAGGS-HA:NL1 with LL3.7ΔGFP. This should ensure comparable cotransfection and coexpression efficiencies across all transfections. Three levels of NL1 overexpression were considered: 500 ng NL1 expression vector, 100-200 ng NL1 expression vector, and 20-50 ng NL1 expression vector. In addition to synapsin immunostaining, exogenous NL1 was additionally visualized using an anti-HA antibody to directly examine how NL1 expression levels relate to synapsin clustering. Constraints in available antibodies

prevented simultaneous GFP visualization with HA and synapsin visualization; MAP2 immunostaining was thus employed to define dendritic segments.

Transfection of 500 ng of the NL1 expression vector replicated results presented above. Specifically, exogenous NL1 was again observed clustered in dendritic spine heads and along dendritic membranes, as well as diffusely in dendritic shafts and axonal processes (Figure 5A). Further, synapsin was robustly clustered along all neurites, with methanol fixation providing a slightly higher puncta resolution. Transfection of 100-200 ng of the NL1 expression vector yielded consistently lower HA intensities (Figure 5B), as expected. Further, synapsin puncta densities were significantly lower than observed with 500 ng expression vector (Figure 5D). Similar decreases were observed with the lowest level of overexpression tested. Transfection of 20-50 ng of the NL1 expression vector yielded dim HA fluorescence, with occasional synaptic and nonsynaptic puncta along dendritic shafts (Figure 5C). Additionally, synapsin puncta densities were significantly lower than both 100-200 ng and 500 ng levels, with densities only slightly higher than previously achieved with GFP expression, though numbers are not directly comparable due to different fixation methods.

These results thus demonstrate that increased NL1 expression drives increased synapsin recruitment in a dose-dependent manner, strongly arguing that synapsin clustering is a specific effect of transsynaptic NL1 signaling. Additionally, transfection of 500 ng of the NL1 expression vector drove more pronounced effects than either of the other overexpression levels examined, confirming that this protocol achieves higher levels of overexpression.
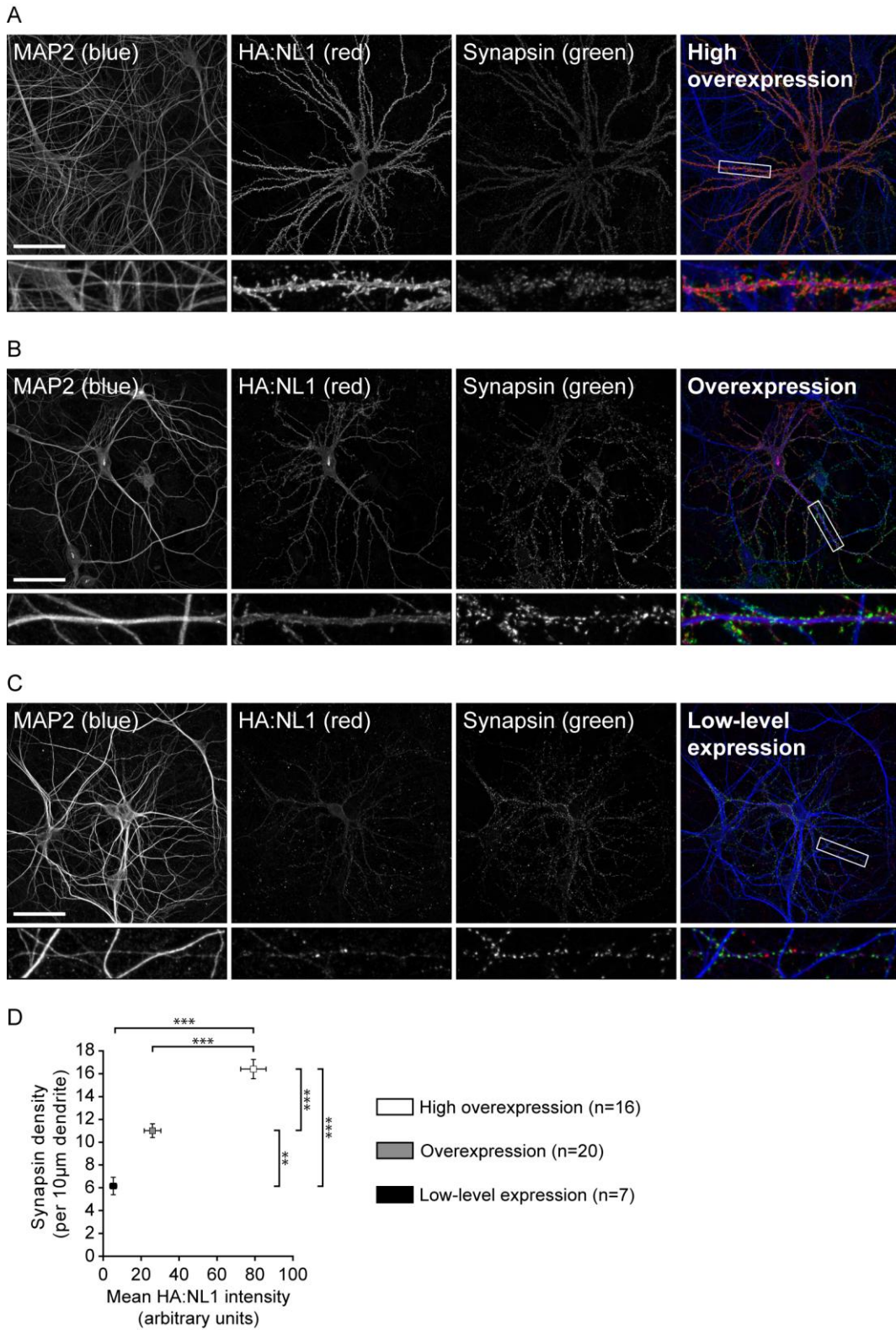
**Figure 5: Titration of exogenous NL1 expression in dissociated hippocampal neurons**

Dissociated hippocampal neurons were transfected with varying levels of a plasmid expressing HA:NL1 at DIV9 and fixed with ice-cold methanol at DIV12 for synapsin, MAP2, and exogenous HA:NL1

immunostaining. The LL3.7ΔGFP plasmid was used in each transfection to bring the total mass of DNA to 2μg to ensure comparable transfection efficiencies. (A) "High overexpression" was achieved using 500 ng of the HA:NL1 expressing plasmid; exogenous NL1 exhibits diffuse staining throughout dendrites, with clusters preferentially localized to spine heads. Exogenous NL1 expression is also clearly visible in MAP2-negative axons, as shown in Figure 1. (B) "Overexpression" was achieved using 100 or 200 ng of the HA:NL1 expressing plasmid; both amounts resulted in nearly identical mean HA:NL1 intensities and synapsin densities, and were thus pooled as a single perturbation level. (C) "Low-level expression" was achieved using 20 or 50 ng of the HA:NL1 expressing plasmid, with both amounts yielding similar results, as above. Transfected neurons exhibited exceedingly low HA:NL1 intensities and were consequently difficult to locate. Exogenous NL1 nevertheless exhibited only weak clustering, with both synaptic and extrasynaptic clusters observed. (D) Increased expression of exogenous NL1 induced consistently increased synapsin puncta densities. Rightmost figures show merge of individual channels displayed on left. Boxed regions of interest (50μm long) defined in merged images are enlarged in insets. Scale bars: 50μm. Objective: 60X. Digital zoom: 1X. Resolution: 2048x2048. Confocal step size: 0.5μm. ***p<0.001, **p<0.01, ANOVA, Tukey post-hoc test.

3.1.5 High neuroligin-1 overexpression induces transsynaptic synapsin clustering independent of NMDAR activity

It has recently been proposed that NL1 signaling increases synapse densities indirectly through validation of pre-existent intercellular linkages in a NMDAR activity-dependent mechanism and not directly via initiation of *de novo* synapses (Chubykin et al., 2007). In a test of this theory, Chubykin et al. demonstrated that chronic application of NMDAR antagonist AP5 from the time of transfection prevented NL1 overexpression from increasing synapsin cluster densities (Chubykin et al., 2007). These results, while supporting a link between NL1 synaptic function and NMDAR activity, do not differentiate between the exclusive role in synapse validation proposed and multiple roles in synapse initiation, maturation, and validation. Moreover, chronic NMDAR blockade lowered basal synapsin cluster densities in GFP-expressing control neurons, thereby confounding overexpression results (Chubykin et al., 2007). Thus, high NL1 overexpression experiments were repeated with and without chronic NMDAR blockade to further test the proposed activity-dependent validation hypothesis.

Surprisingly, chronic AP5 treatment had no noticeable effects on synapsin recruitment by NL1 overexpression (Figure 6C). Suprathreshold synapsin puncta were still observed to strongly outline all neurites independent of AP5 presence (Figure 6A and B). Chronic NMDAR blockade did, however, significantly temper spine morphogenesis (Figure 6D), consistent with a residual population of functional glutamatergic synapses present under high NL1 overexpression conditions. Moreover, while the basic two-dimensional Sholl analysis employed did not reveal statistically significant differences in total dendritic arbor complexities, neurons subjected to chronic NMDAR blockade never displayed the unique intense perisomatic dendritic branching observed in a subset of NL1-overexpressing neurons with intact NMDAR activity. These results clearly demonstrate that synaptic NL1 signaling is not exclusively dependent on NMDAR-activity.
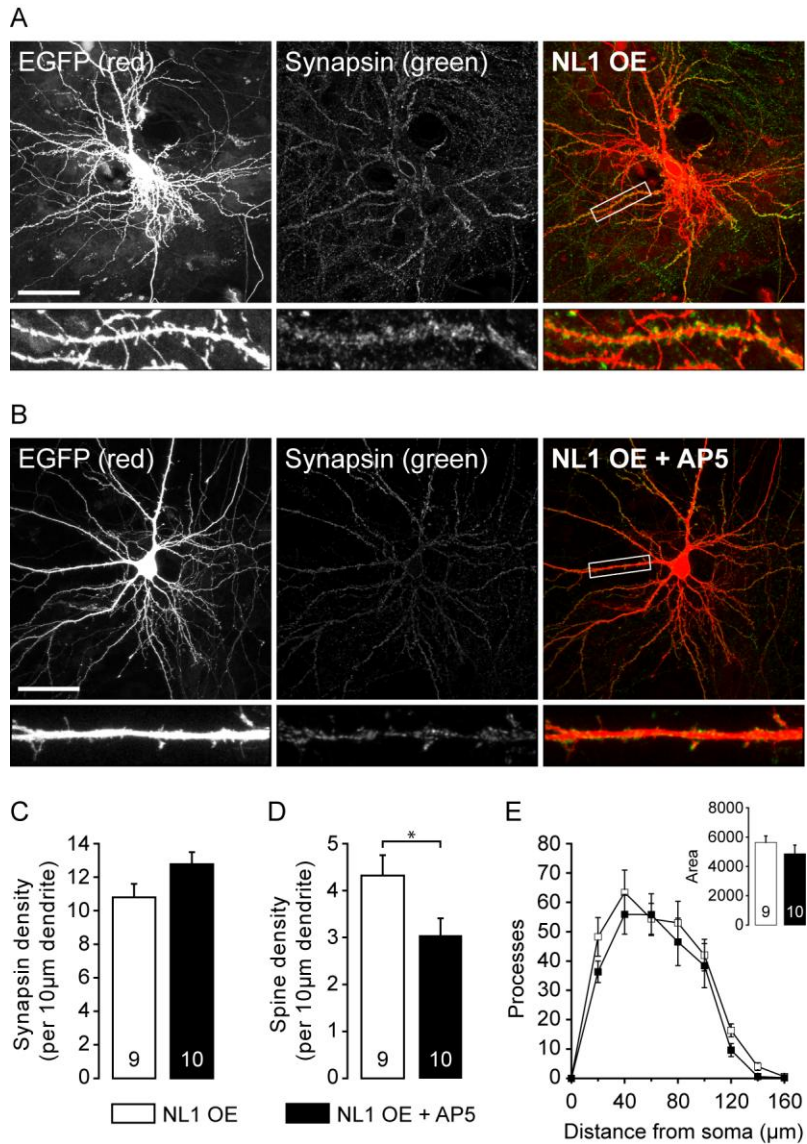
Figure 6: NL1 overexpression in hippocampal neurons drives presynaptic differentiation independent of NMDA receptor activity

Dissociated neurons were transfected with plasmids expressing HA:NL1 and GFP at DIV9-10 and (A) cultured normally or (B) subjected to chronic D-AP5 (100 µM) treatment until fixation at DIV12-13 for synapsin immunostaining. (C) NMDAR blockade had no significant effect on NL1-mediated gains in synapsin puncta densities. (D) Chronic NMDAR blockade tempered NL1-mediated dendritic spine morphogenesis. (E) Sholl analysis revealed no significant difference in dendritic arbor complexity with NMDAR blockade (inset: area under Sholl curves). Rightmost figures show merge of individual channels displayed on left. Boxed regions of interest (50µm long) defined in merged images are enlarged in insets. Scale bars: 50µm. Objective: 60X. Digital zoom: 1X. Resolution: 2048x2048. Confocal step size: 0.5µm. *p<0.05, t-test.

3.2   NEUROLIGIN-1 INITIATES PRESYNAPTIC DIFFERENTIATION INDEPENDENT OF PSD95 INTERACTIONS

3.2.1   PSD95 does not restrict neuroligin-1-mediated synapse initiation in the mixed-culture assay

El-Husseini and colleagues have presented considerable evidence defining a role for scaffolding molecules PSD95 and gephyrin in regulating specificity of NL-mediated synapses as glutamatergic or GABAergic (Prange et al., 2004; Levinson et al., 2005; Levinson et al., 2010). How scaffolding molecule interactions regulate NL-mediated synapse initiation, however, remains unclear. Coordinate overexpression of PSD95 with NL1 in neurons strongly restricts total synapse densities and sequesters nearly all exogenous NL1 to excitatory synapses (Prange et al., 2004), suggesting PSD95 may restrict NL1-mediated synapse formation. In contrast, results from the mixed-culture assay demonstrate that coexpression of PSD95 with NL1 enhances the initial rate of bassoon recruitment compared to HEK293 cells expressing NL1 alone (Lee et al., 2010), suggesting PSD95 may enhance synapse formation through retrograde signaling or NL1 clustering. The effects of PSD95 coexpression on total synapsin recruitment by NL1 in the standard mixed-culture assay have not been examined.

Thus, to directly explore PSD95 regulation of NL1-mediated synapse formation, techniques for the standard mixed-culture assay were first optimized. Initial examination of heterologous expression of NL1 versus NLswap in nonneuronal HEK293 cells demonstrated pronounced recruitment of presynaptic terminals by NL1 alone (Figure 7). Suprathreshold synapsin puncta strongly outlined the entire perimeter of NL1-expressing HEK293 cells and further traced up the height of these cells (Figure 7A). Moreover, immunostaining of neuronal microtubule βIII-tubulin revealed clear interaction of neurites with NL1-expressing HEK293 cells, with neuronal processes robustly surrounding and "climbing" over the cells. Mixed-cultures with HEK293 cells expressing NLswap displayed neither of these effects, however; synapsin was not noticeably clustered around or on NLswap-expressing cells and neurites exhibited no detectable interaction with these cells (Figure 7B). As individual synapsin puncta over NL1-expressing cells were often not clearly discernable, the total suprathreshold synapsin

pixel area was instead quantified and normalized to the total HEK293 cell area. This metric revealed a significant accumulation of synapsin over NL1-expressing HEK293 cells compared to NLswap-expressing cells (Figure 7C), as expected from previous reports (Scheiffele et al., 2000).
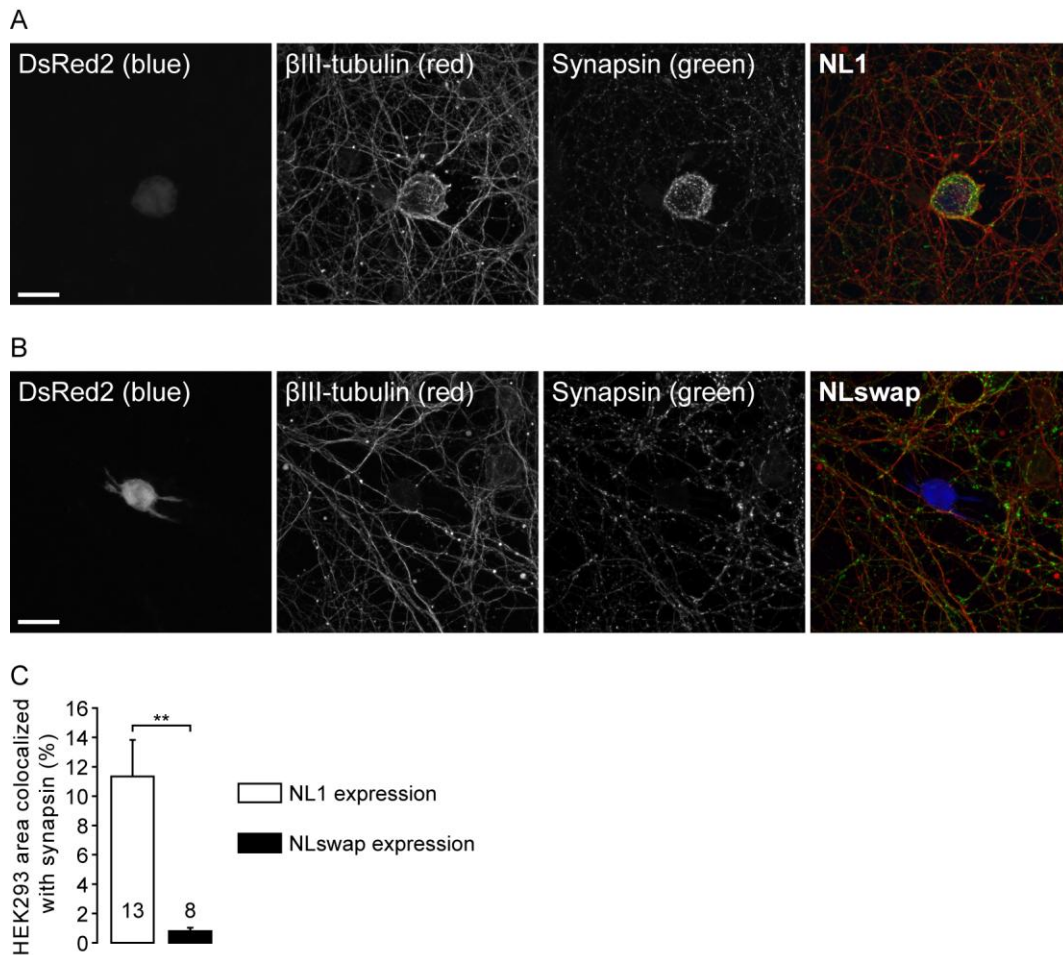
Figure 7: Heterologous expression of NL1 in nonneuronal cells induces presynaptic differentiation in contacting process of cocultured neurons in the mixed-culture assay

HEK293 cells expressing (A) HA:NL1 or (B) HA:NLswap together with transfection marker DsRed2 were cocultured with DIV9 dissociated cortical neurons for two days before fixation and immunostaining for synapsin and βIII-tubulin to mark neuronal processes. (C) Heterologous expression of NL1 recruited significantly greater levels of synapsin than expression of NLswap or DsRed2 alone (data not shown), consistent with marked neurite interaction with NL1-expressing HEK293 (compare βIII-tubulin staining across A and B). Rightmost figures show merge of individual channels displayed on left. Scale bars:

20µm. Objective: 100X. Digital zoom: 1X. Resolution: 2048x2048. Confocal step size: 0.5µm. **p<0.01, t-test.

Having thus established a working protocol for analyzing synapsin recruitment by isolated NL1 expression in the absence of other postsynaptic components, effects of PSD95 interactions were next considered. PSD95 expressed in HEK293 cells exhibited a diffuse peri-membrane distribution in confocal z-stacks (Figure 8A). For comparison, surface expression of transmembrane NL1 in separate HEK293 cells was visualized (Figure 8C). Coexpression of NL1 with PSD95 in HEK293 cells led to a strong redistribution of total cellular PSD95 to the membrane (Figure 8B), consistent with NL1-PSD95 interactions previously observed (Irie et al., 1997). Note also that coexpression of PSD95 with NL1 did not alter membrane delivery of NL1 (Figure 8D). Thus, coexpression of NL1 and PSD95 in HEK293 cells provides a viable approach to investigating the effect of PSD95 binding alone on NL1-mediated synapse initiation.
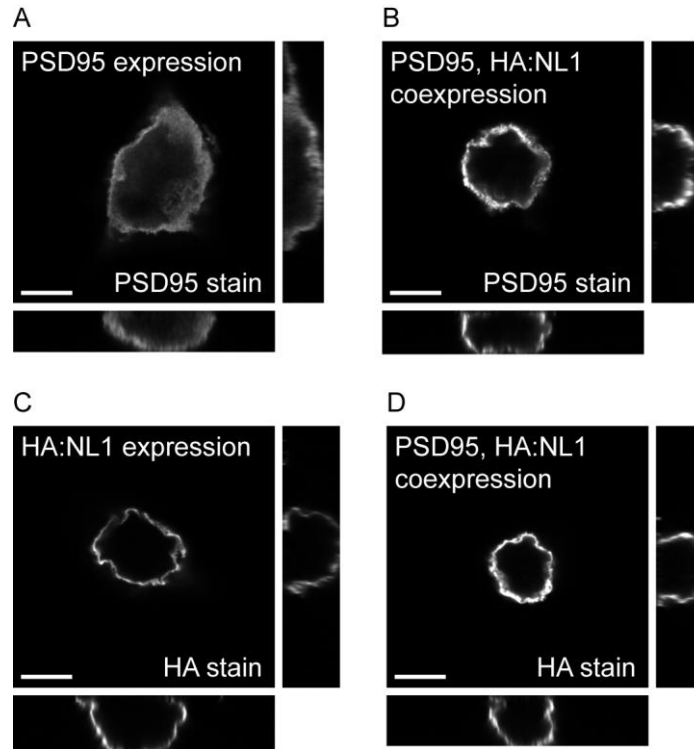
Figure 8: NL1 and PSD95 properly interact when coexpressed in HEK293 cells

HEK293 cells were transfected with PSD95 (A) or HA:NL1 (C) expression vectors or both (B, D) and processed for immunostaining two days later. For PSD95 immunostaining (A, B) cells were permeabilized using 0.3% Triton X-100 prior to blocking and antibody incubations. For HA immunostaining (C, D), cells were not permeabilized, enabling staining of surface HA:NL1. Each main image displays the fluorescent signal halfway through the height of the HEK293 cell, as determined using confocal z-stacks, while vertical and horizontal images display midline side views throughout the entire cell depth. Note coexpression of NL1 with PSD95 confers strong PSD95 membrane localization akin to patterns observed with surface-staining of HA:NL1, suggesting NL1 recruits PSD95 to the membrane as previously reported (Irie et al., 1997). Scale bars: 10μm. Objective: 60X. Digital zoom: 4X. Resolution: 2048x2048. Confocal step size: 0.5μm.

Expression of PSD95 alone in HEK293 cells cocultured with dissociated hippocampal neurons did not lead to noticeable recruitment of presynaptic terminals (Figure 9C), as expected for the cytoplasmic protein and similar to NLswap expression above. Expression of NL1 alone in HEK293 cells again demonstrated robust aggregation of synapsin (Figure 9A), consistent with above results. After two days of

coculture with neurons, HEK293 cells coexpressing NL1 with PSD95 exhibited similar synapsin recruitment as NL1-expressing cells (Figure 9B). Quantification of the cell area colocalized with suprathreshold synapsin confirmed equal artificial synapse formation by NL1- and NL1/PSD95-expressing HEK293 cells (Figure 9D). These results suggest that the increased initial rate of bassoon recruitment observed with PSD95 coexpression ultimately does not lead to greater densities of induced presynaptic terminals. Moreover, interaction of PSD95 with NL1 alone is not sufficient to preclude NL1-mediated induction of presynaptic differentiation.
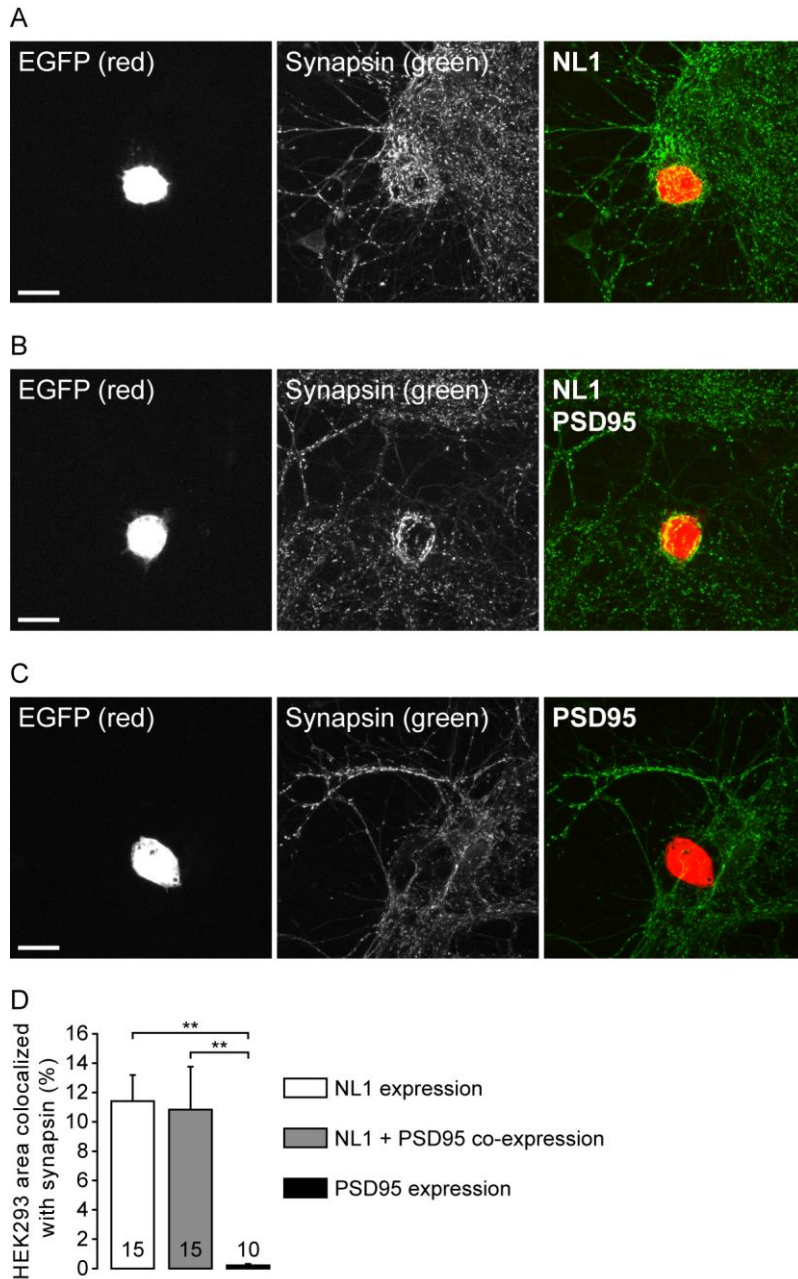
Figure 9: Coexpression and interaction of PSD95 with NL1 does not restrict induction of presynaptic differentiation by NL1 in the mixed-culture assay

Nonneuronal HEK293 cells expressing (A) NL1, (B) NL1 and PSD95, or (C) PSD95 together with transfection marker GFP were cocultured with DIV9-10 dissociated hippocampal neurons for 1-2 days before fixation and immunostaining for synapsin. (D) Heterologous expression of NL1 recruited significantly greater levels of synapsin than expression of PSD95 alone, while coexpression of PSD95 did not affect NL1-mediated synapsin recruitment. Rightmost figures show merge of individual channels displayed on left. Scale bars: 20μm. Objective: 100X. Digital zoom: 1X. Resolution: 1024x1024. Confocal step size: 1μm. $**p<0.01$, ANOVA, Tukey post-hoc test.

3.2.2 Knockdown of endogenous PSD95 expression does not preclude neuroligin-1-mediated gains in synapse densities

Results from the mixed-culture assay suggesting an inability of PSD95 to enhance NL1-mediated synapse formation may be confounded by the robust synaptogenic potential of NL1 incurring a ceiling effect on synapsin recruitment. Moreover, while a useful model of isolated postsynaptic interactions, the mixed-culture assay cannot fully describe the complexity of endogenous synapse formation. Thus, to further explore the effect of PSD95 interactions on NL1-mediated synapse formation, experiments were envisioned to coordinately perturb both NL1 and PSD95 expression levels in dissociated neuronal cultures. Specifically, concomitant overexpression of NL1 with RNAi-mediated knockdown of PSD95 expression should partially isolate NL1 versus complexed NL1/PSD95 signaling. Such perturbations have previously been employed to demonstrate interdependent NL1/PSD95 retrograde regulation of presynaptic release probability, but concurrent effects on synapse densities were not explored (Futai et al., 2007). Further, such experiments would complement previous investigations where mutation of PSD95 or NL1 PDZ domains precluded gains in synaptic vesicle cluster sizes (Prange et al., 2004).

Before combining PSD95 knockdown with NL1 overexpression, it was first necessary to evaluate whether residual PSD95 clusters exist under high NL1 overexpression conditions. Robust gains in dendritic spine densities and a significant effect of chronic NMDAR blockade in the above high NL1 overexpression experiments (Figures 3 and 6, respectively) suggests that a population of functional glutamatergic synapses capable of NMDAR-mediated activity and spine maturation and maintenance exists. PSD95, which can physically link NL1 with NMDAR and has a role in maturation of excitatory synapses, is presumably clustered at these residual synapses. Indeed, staining of endogenous PSD95 in NL1-overexpressing neurons revealed measurable densities of suprathreshold PSD95 puncta, often properly localized to dendritic spine heads (Figure 10A). Coexpression of HA:NL1 with a short hairpin RNA targeting PSD95

for RNAi-mediated knockdown markedly reduced residual PSD95 densities (Figure 10B), with quantification of PSD95 cluster densities revealing a significant three to four fold reduction (Figure 10C).
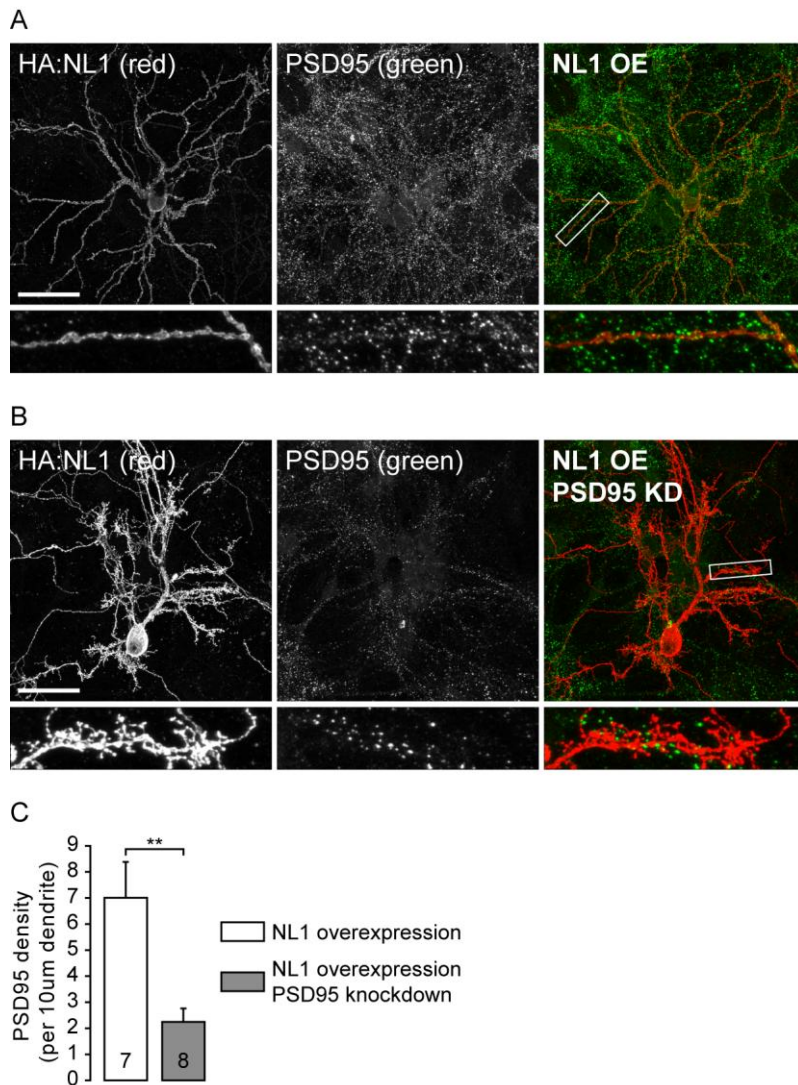
Figure 10: Knockdown of PSD95 in neurons overexpressing NL1

Dissociated hippocampal neurons were transfected with plasmids expressing (A) HA:NL1, (B) HA:NL1 with a short hairpin RNA targeting PSD95 for RNAi knockdown (KD), or (D) HA:NL1 and PSD95 at DIV9-10 and processed at DIV12-14 for HA:NL1 and PSD95 immunostaining. (C) Short hairpin expression significantly lowered densities of suprathreshold PSD95 puncta colocalized with HA:NL1-expressing dendritic segments. Rightmost figures show merge of individual channels displayed on left. Boxed regions

of interest (50µm long) defined in merged images are enlarged in insets. Scale bars: 50µm. Objective: 60X. Digital zoom: 1X. Resolution: 2048x2048. Confocal step size: 0.5µm. **p<0.01, t-test.

As before, high NL1 overexpression induced pronounced recruitment of synapsin puncta and spine morphogenesis along all dendritic branches and complex total dendritic arborization patterns (Figure 11A). In contrast, knockdown of PSD95 expression alone did not noticeably decrease synapsin densities from baseline levels (Figure 11C), consistent with previous findings (Prange et al., 2004). Coordinate high NL1 overexpression with PSD95 knockdown yielded a similar pattern of strong synapsin clustering outlining all neurites as observed with high NL1 overexpression alone (Figure 11B). Indeed, both high NL1 overexpression and the combined NL1/PSD95 perturbation induced statistically equivalent increases in synapsin puncta densities compared to PSD95 knockdown alone (Figure 11D). Coordinate reduction of PSD95 expression did temper the degree of dendritic spine morphogenesis observed with high NL1 overexpression alone, however (Figure 11E), suggesting residual PSD95 levels do contribute at mature glutamatergic synapses. Lastly, differences in total dendritic arbor complexities between the three experimental conditions tested did not reach statistical significance due to high variances (Figure 11F). Results thus show that PSD95 expression is dispensable for the robust synapse formation driven by high NL1 overexpression in neurons. Collectively, results from the mixed-culture assay (Figure 9) and multi-molecular perturbations (Figure 11) suggest that PSD95 is not involved in NL1-mediated synapse initiation.
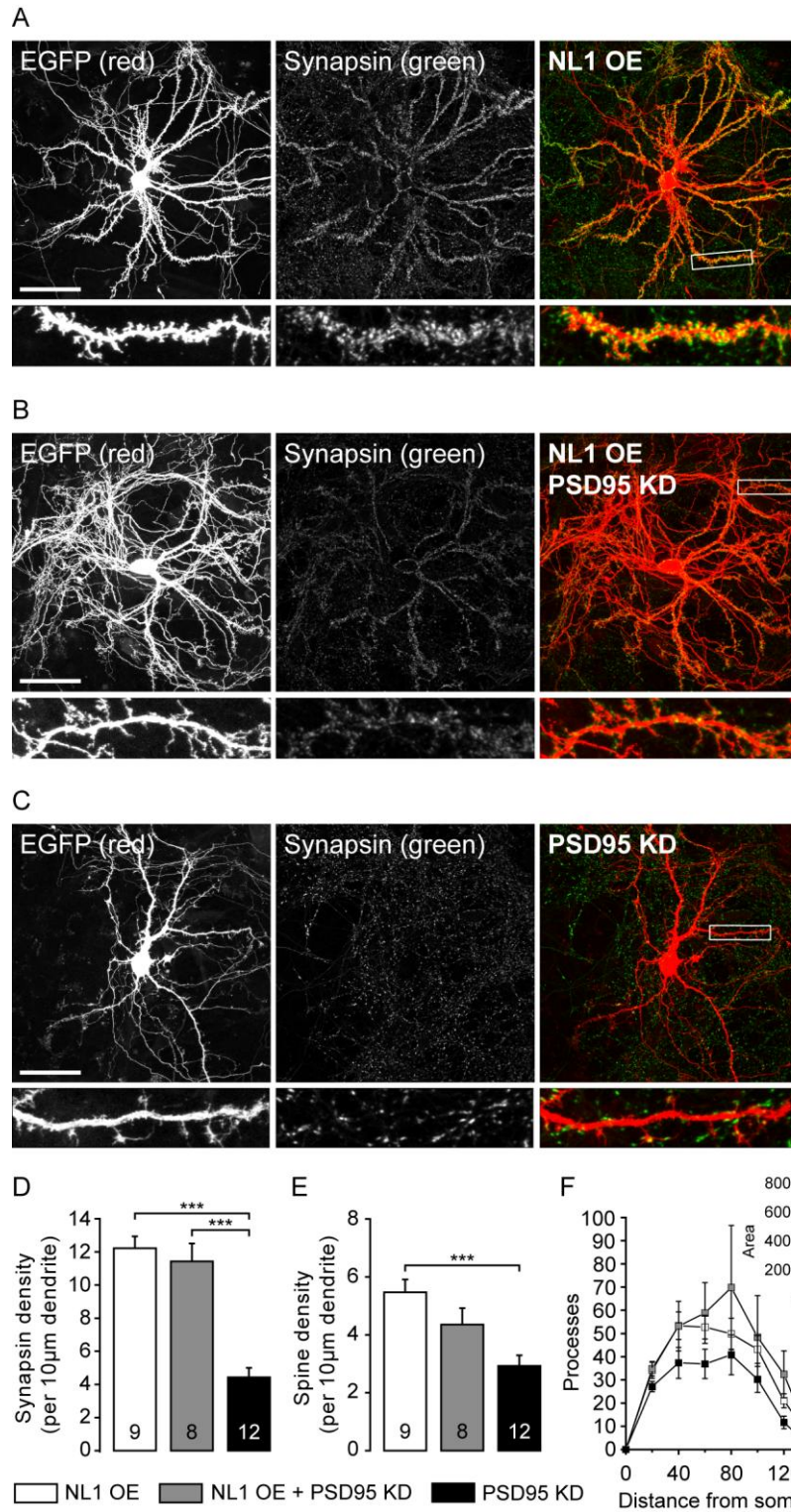
Figure 11: High overexpression of NL1 in hippocampal neurons induces presynaptic differentiation independent of PSD95 expression levels

Dissociated neurons were transfected with plasmids expressing (A) HA:NL1, (B) HA:NL1 with shPSD95, or (C) shPSD95 together with GFP at DIV9-10 and fixed at DIV12-13 for synapsin immunostaining. (D)

RNAi knockdown of PSD95 did not preclude NL1-mediated gains in synapsin puncta densities but (E) did moderate NL1-induced spine morphogenesis. (F) Sholl analysis revealed no significant difference in dendritic arbor complexities among all conditions (inset: area under Sholl curves). Rightmost figures show merge of individual channels displayed on left. Boxed regions of interest (50μm long) defined in merged images are enlarged in insets. Scale bars: 50μm. Objective: 60X. Digital zoom: 1X. Resolution: 2048x2048. Confocal step size: 0.5μm. ***$p < 0.001$, ANOVA, Tukey post-hoc test.

3.3 INVESTIGATION OF COMBINED NEUROLIGIN-1 AND SYNCAM1 SIGNALING

3.3.1 Perturbation of SynCAM1 expression levels in primary hippocampal neurons does not alter synapse densities

Previous investigations have revealed no effect of SC1 overexpression on synapse densities (Sara et al., 2005; Chubykin et al., 2007; Fogel et al., 2007). Data from recent examination of transgenic and knockout mice, however, have been interpreted to suggest that SC1 is primarily involved in morphological synapse formation. Acute knockdown of SC1 expression in mammalian neurons has thus far not been reported and, in conjunction with replication of SC1 overexpression experiments, may help to resolve the impact SC1 has on regulating synapse densities.

Thus, to achieve specific and acute reduction of SC1 expression, a short hairpin RNA sequence was designed to target SC1 transcripts for RNAi-mediated post-transcriptional silencing, in accordance with published design criteria (Reynolds et al., 2004). DNA oligonucleotides encoding the designed short hairpin were annealed and subcloned downstream of the U6 promoter of the LL3.7 vector, generating "LL3.7/shSC1". Lack of commercially-available SC1 antibodies precluded validation of shSC1 efficacy in dissociated neuronal cultures. Thus, to evaluate the designed hairpin, HEK293 cells were cotransfected with an epitope-tagged murine SC1 expression construct (Fogel et al., 2007) and either the empty LL3.7 vector, the LL3.7/shSC1 vector, or the LL3.7 vector expressing a control hairpin not matching any endogenous mammalian transcript in BLAST searches (data not shown). Immunoblotting for

heterologous FLAG:SC1 and actin as a loading control revealed shSC1 mediates strong knockdown of SC1 (Figure 12). Moreover, independent immunoblots demonstrated shSC1 had no effect on heterologous SC2 expression (data not shown), as expected from target sequence differences. Thus, expression of shSC1 confers specific and strong knockdown of SC1 expression.
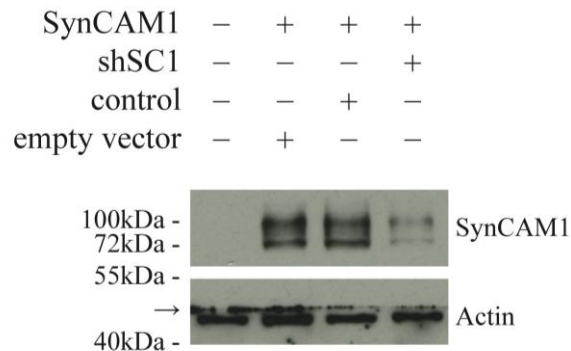
Figure 12: Validation of shSC1 efficacy in mediating RNAi knockdown of heterologous SC1 expression in HEK293 cells

HEK293 cells were cotransfected with pCAGGS-FLAG:SC1 and either the empty LL3.7 vector expressing GFP alone, LL3.7 containing the shSC1 hairpin targeting SC1 for RNAi-mediated knockdown, or a control hairpin sequence not targeting any mammalian transcripts. Whole-cell lysates were collected two days post-transfection and equal amounts loaded into separate lanes. Nontransfected HEK293 protein sample was loaded into the first lane as a negative control, and actin was used as a loading control. Immunoblotting for the FLAG epitope revealed strong RNAi-mediated reduction of SC1 expression by shSC1. Arrow: artifact from membrane edge.

Neither SC1 overexpression nor knockdown in dissociated hippocampal neurons had any noticeable effect on synapsin clustering or spine morphogenesis (Figure 13). In particular, compared to the robust effects of NL1, processes of SC1-overexpressing neurons were not outlined in suprathreshold synapsin puncta (Figure 13A). Quantification of synapsin puncta and spine densities indeed revealed no significant differences from GFP control levels (Figure 13D and E). These results strongly agree

with previous overexpression experiments (Sara et al., 2005; Fogel et al., 2007; Chubykin et al., 2007). Moreover, in agreement with lack of an effect of SC1 knockdown here, expression of the dominant negative SCΔIg mutant did not alter spontaneous miniature event frequency or amplitude in prior reports (Biederer et al., 2002; Sara et al., 2005). These results suggest that the minimal synaptic density changes observed in transgenic SC1 overexpression and knockdown mouse strains may reflect compensatory network alterations and/or indirect effects of synapse maintenance, rather than the proposed direct role in morphological synapse formation.
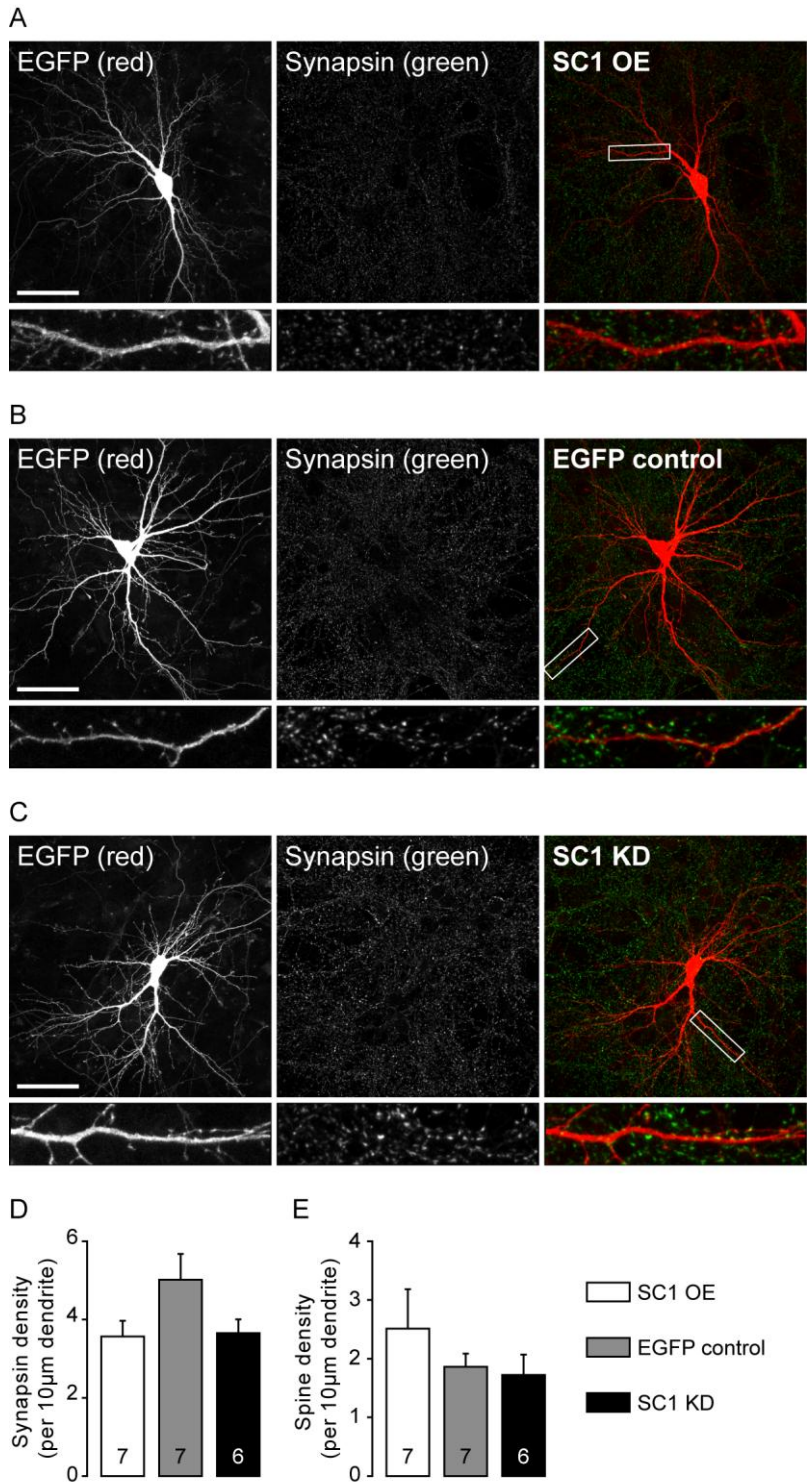
Figure 13: Perturbation of SC1 levels in hippocampal neurons does not affect synapsin recruitment or spine formation

Dissociated neurons were transfected with plasmids expressing (A) SC1:FLAG and GFP, (B) GFP, or (C) shSC1 and GFP at DIV9-10 and fixed at DIV12-13 for synapsin immunostaining. Overexpression or RNAi knockdown of SC1 did not significantly alter (D) synapsin puncta densities or (E) dendritic spine densities.

Rightmost figures show merge of individual channels displayed on left. Boxed regions of interest (50μm long) defined in merged images are enlarged in insets. Scale bars: 50μm. Objective: 60X. Digital zoom: 1X. Resolution: 2048x2048. Confocal step size: 0.5μm.

3.3.2 Neuroligin-1 is significantly more potent in the mixed-culture assay than SynCAM1

The ability of heterologous SC1 to induce functional presynaptic differentiation in contacting axons (but not dendrites) of cocultured neurons is well established (Biederer et al., 2002; Sara et al., 2005; Nam and Chen, 2005; Fogel et al., 2007; Fogel et al., 2010). Such a synaptogenic potential is at odds with *in vitro* overexpression and knockdown results, however, which showed no change in synapse densities with acute SC1 perturbation (Figure 13; Sara et al., 2005; Fogel et al., 2007; Chubykin et al., 2007). Importantly, identical experimental methodologies were able to show a potent effect of acute NL1 perturbation (Figure 3). To clarify this discrepancy, the potency of NL1 and SC1 in recruiting synapsin in the mixed-culture assay was directly compared. Again, the experimental methods employed were previously able to clearly resolve a potent synapse-inducing ability of NL1 (Figure 7; Figure 9).

As before, heterologous expression of NL1 in HEK293 cells induced clear accumulation of synapsin in contacting processes of cocultured neurons, despite slightly lower neuronal culture densities (Figure 14A). Under these conditions, SC1 demonstrated far less synapsin recruitment (Figure 14B). Quantification of the total suprathreshold synapsin area normalized to the total HEK293 cell area revealed significantly greater synaptogenic potential of NL1 in the mixed-culture assay than SC1 (Figure 14C). These results agree well with the greater potency observed with NL1 overexpression in neurons, and likely reflect a general function of NL1 and not SC1 in synapse formation.
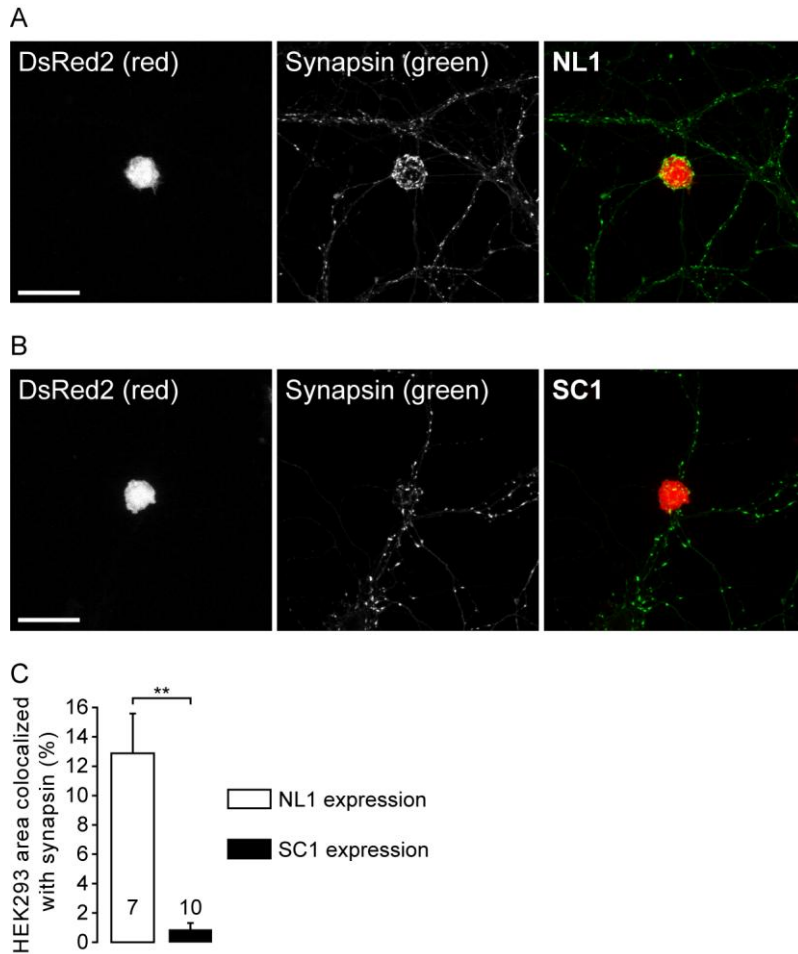
Figure 14: NL1 is more potent than SC1 in the mixed-culture assay

HEK293 cells expressing (A) HA:NL1 or (B) FLAG:SC1 together with transfection marker DsRed2 were cocultured with DIV10 dissociated hippocampal neurons for two days before fixation and immunostaining for synapsin. (C) Heterologous expression of NL1 recruited significantly greater levels of synapsin than expression of SC1. Rightmost figures show merge of individual channels displayed on left. Scale bars: 25μm. Objective: 60X. Digital zoom: 2X. Resolution: 1024x1024. Confocal step size: 0.5μm. **$p<0.01$ t-test.

3.3.3   Coordinate overexpression of neuroligin-1 with SynCAM1 precipitates NMDAR-dependent neurodegeneration

SC1 gain-of-function perturbations primarily promote increased spontaneous miniature event frequencies (Biederer et al., 2002; Sara et al., 2005; Fogel et al., 2007; Robbins

73

et al., 2010), while NL1 gain-of-function consistently promotes increased synapse densities (Figure 3; Prange et al., 2004; Levinson et al., 2005; Sara et al., 2005; Chih et al., 2005). These potentially complementary roles have led to the theory that SC1 may function to activate nascent NL1-induced immature synaptic contacts (Sara et al., 2005). To test this hypothesis and begin to consider interactions of multiple adhesion systems within a single synapse, NL1 and SC1 were coordinately overexpressed in dissociated hippocampal neurons. Strikingly, all neurons examined overexpressing both NL1 and SC1 revealed pronounced degeneration within 1-2 days post-transfection, with segmented processes and thick swellings and varicosities along intact processes (Figure 15B). This was not due to a general defect of the cultures, as transfections from the same preparations in which only NL1 was overexpressed revealed the typical complex dendritic arborization characteristic of NL1 gain-of-function (Figure 15A). Thus, coordinate NL1 and SC1 overexpression specifically induced pronounced neurodegeneration.

At least two mechanisms may drive the NL1/SC1 degeneration. One, SC1 may indeed be maturing a large proportion of the new synaptic contacts initiated by NL1 overexpression and thereby precipitating excitotoxicity; and two, the intense perisomatic dendritic branching induced by NL1 overexpression may enable extensive homophilic adhesion between surface-expressed SC1, yielding large dendritic aggregations and intense recurrent autaptic excitation, also precipitating excitotoxicity. Thus, the two proposed mechanisms are not mutually exclusive and together may be tested using a single experimental modification. Chronic NMDAR blockade from the time of transfection should prevent a degree of the complex yet spatially-restricted dendritic arborization, as observed previously (Figure 6) and preclude excitotoxic signaling through Ca^{2+}-permeable NMDAR.

Remarkably, chronic AP5 application from the time of transfection indeed prevented any noticeable neurodegeneration in a majority of the transfected neurons coordinately overexpressing NL1 with SC1 (Figure 15D). This experimental modification thus enabled further evaluation of the combined effects of NL1 and SC1 on synapse formation and function. Coordinate overexpression of SC1 with NL1 had no effect on synapse densities compared with overexpression of NL1 alone (Figure 15E), as

expected from previous experiments demonstrating minimal synapse gains with SC1 gain-of-function. Moreover, NL1 overexpression was again shown to mediate robust recruitment of synapsin-positive terminals independent of NMDAR-mediated activity (Figure 15C), establishing this as a consistent and robust finding. Coordinate overexpression of SC1 with NL1 further did not significantly alter dendritic spine densities (Figure 15F), though this is likely an effect of chronic NMDAR blockade, as both NL1- and NL1/SC1-overexpression conditions yielded low spine densities matching those previously observed with chronic AP5 application (Figure 6). Sholl analysis was not performed for similar reasons.

Unfortunately, the combination of high NL1 overexpression and chronic AP5 application reduced spontaneous synaptic activity to negligible levels, thereby preventing physiological evaluation of combined NL1/SC1 overexpression. Following chronic NMDAR blockade, both NL1- and NL1/SC1-overexpressing neurons displayed exceedingly few spontaneous events (data not shown).
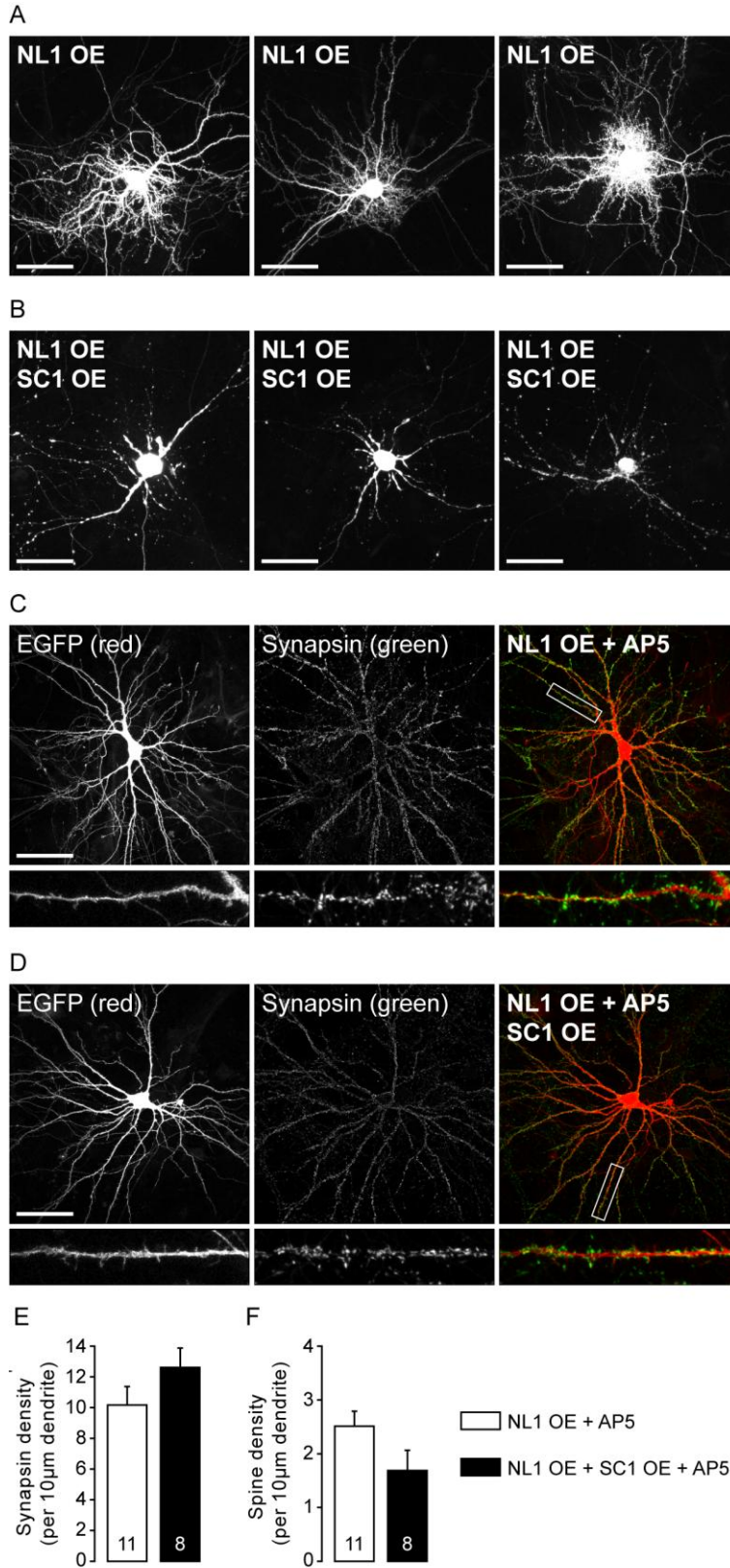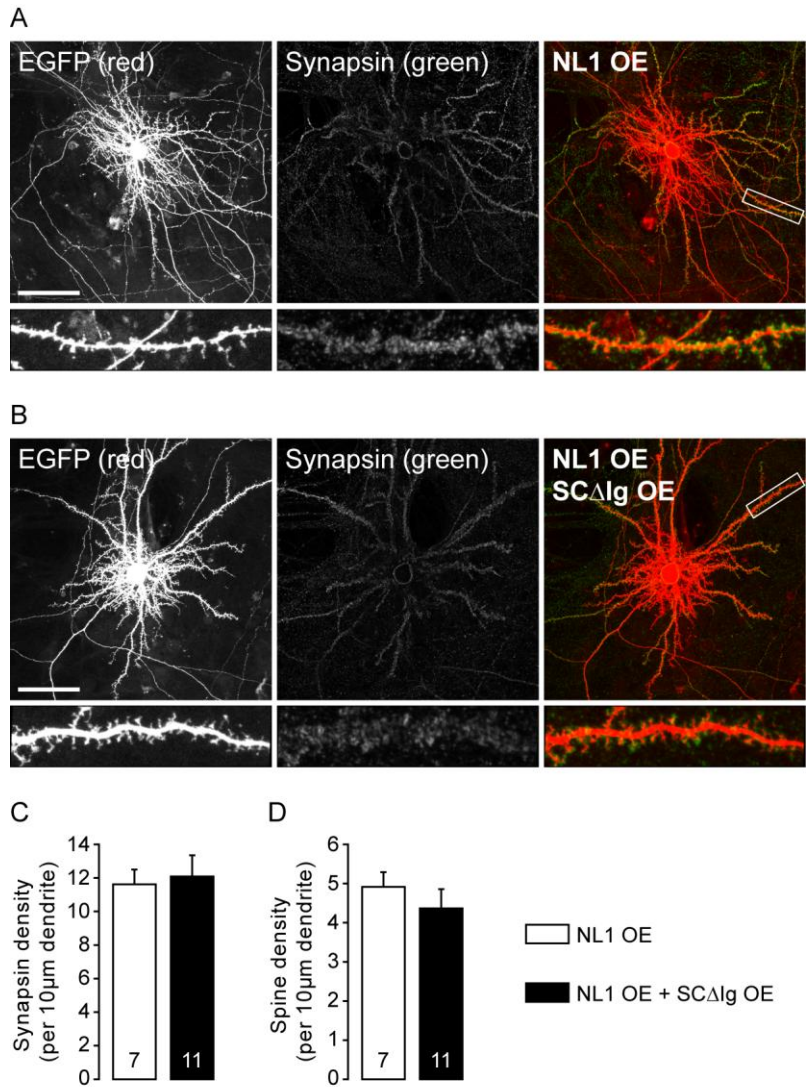
Figure 15: Coordinate overexpression of NL1 and SC1 in hippocampal neurons precipitates NMDAR-dependent degeneration without increasing synapsin densities

Dissociated neurons were transfected with plasmids expressing (A,C) HA:NL1 or (B,D) HA:NL1 and SC1:FLAG together with GFP at DIV9-10 and (A,B) cultured normally or (C,D) under chronic 100µM AP5 treatment from the time of transfection. (A) Neurons overexpressing NL1 developed prototypically (extensive spine morphogenesis and dendritic arborization) while (B) neurons transfected to overexpress SC1 with NL1 consistently exhibited hallmarks of degeneration, including fragmented processes with numerous swellings and blebs; three representative neurons shown for each case. All neurons examined from the coordinate NL1/SC1 overexpression condition (n>10) displayed clear degeneration. (D) Chronic NMDAR blockade with AP5 precluded NL1/SC1-mediated degeneration. (E) Immunostaining for synapsin revealed no significant effect of SC1 coexpression on normal NL1-mediated gains in synapsin puncta densities. (F) Spine densities were also unaltered from normal NL1 levels (in AP5) by SC1 coexpression. Rightmost figures of C and D show merge of individual channels displayed on left. Boxed regions of interest (50µm long) defined in merged images are enlarged in insets. Scale bars: 50µm. Objective: 60X. Digital zoom: 1X. Resolution: 2048x2048. Confocal step size: 0.5µm.

To confirm that the these morphological results are a specific reflection of coordinate NL1 and SC1 signaling, the experiment was repeated with the extracellular dominant negative mutant SCΔIg. Exogenous expression of SCΔIg in neurons overexpressing NL1 indeed had no effect on synapse or spine densities, and importantly did not precipitate any signs of the neurodegeneration previously observed (Figure 16).

Figure 16: NMDAR-dependent neurodegeneration induced by coordinate NL1 and SC1 overexpression specifically requires extracellular SC1 signaling

Dissociated neurons were transfected with plasmids expressing (A) HA:NL1 or (B) HA:NL1 and SCΔIg together with GFP at DIV9-10 and fixed at DIV12-13 for synapsin immunostaining. Coexpression of extracellular dominant mutant SCΔIg with NL1 did not precipitate neurodegeneration, as observed with coordinate overexpression of SC1 with NL1. Coexpression of SCΔIg additionally did not affect NL1-mediated gains in (C) synapsin puncta density or (D) spine morphogenesis. Rightmost figures show merge of individual channels displayed on left. Boxed regions of interest (50μm long) defined in merged images are enlarged in insets. Scale bars: 50μm. Objective: 60X. Digital zoom: 1X. Resolution: 2048x2048. Confocal step size: 0.5μm.

3.4 ENGINEERING MODELS OF THE POSTSYNAPSE

3.4.1 Generating a stable HEK293 cell line expressing neuroligin-1

Since the inception of the mixed-culture assay to demonstrate the capacity of isolated NL1 to induce full presynaptic differentiation in contacting axons of cocultured neurons (Scheiffele et al., 2000), the mixed-culture assay has been repeatedly employed as a standard assay of synaptogenicity (Biederer and Scheiffele, 2007). Moreover, coexpression of glutamatergic or GABAergic receptors has enabled functional reconstitution of neurotransmission at these artificial synaptic sites (Biederer et al., 2002; Fu et al., 2003; Sara et al., 2005; Dong et al., 2007; Fu and Vicini, 2009). Further, postsynaptic scaffolding molecules have been heterologously coexpressed with NLs to generate increasingly complex models of the postsynapse (Fu et al., 2003; Lee et al., 2010). Lastly, the mixed-culture assay has recently been used to probe more subtle aspects of synapse formation and function, including synapse stabilization (Ripley et al., 2011), recruitment rates (Lee et al., 2010), and presynaptic maturation (Wittenmayer et al., 2009).

The mixed-culture assay thus affords tremendous potential as a delimited, controllable model of complex synaptic mechanisms. A current limiting factor of the mixed-culture assay, however, is reliance on standard transient transfection methods. Not only can transfection lead to variable expression levels between cells of a single culture, but cotransfection and coexpression efficiencies decrease with increasing numbers of plasmids. Moreover, confirming simultaneous coexpression of multiple cotransfected constructs is limited by the number of available non-overlapping fluorescent channels, protein distribution patterns, and selectable drug resistances.

A potential solution to these limitations is to genetically engineer clonal nonneuronal cell lines using lentiviral transduction. Recombinant lentiviruses are capable of integrating into the host genome and stably and heritably expressing a chosen transgene (Lois et al, 2002). By employing sequential rounds of transduction and confirmation of expression, it could be possible to generate exceedingly complex yet fully defined biological models of the postsynaptic compartment.

As an initial proof of this concept, a stable clonal HEK293 cell line expressing HA:NL1 was generated as follows. To prepare a lentiviral vector expressing HA:NL1, the HA:NL1 coding sequence was first amplified from the pCAGGS-HA:NL1 vector using a polymerase chain reaction (PCR) and endowed with directional flanking restriction sites. The GFP coding sequence of the LL3.7 lentiviral vector (Rubinson et al., 2003) was then excised and replaced with a custom multi-cloning site, yielding LL3.7ΔGFP. The amplified HA:NL1 coding sequence and LL3.7ΔGFP vector were then appropriately digested, purified, ligated, transformed into bacteria, amplified, and confirmed through restriction digest and sequencing, yielding LL3.7ΔGFP-HA:NL1. Expression of HA:NL1 from this vector was then confirmed by transfection of HEK293 cells and immunostaining and -blotting for the HA epitope, which is not normally expressed in HEK293 cells (data not shown). Having thus confirmed successful creation of a lentiviral vector capable of expressing HA:NL1, a separate set of HEK293 cultures were transiently transfected with VSVg, Δ8.9, and LL3.7ΔGFP-HA:NL1 to produce recombinant lentiviral particles capable of expressing HA:NL1. Transduction and expression were confirmed as before via immunostaining and -blotting (data not shown). A separate culture of HEK293 cells was then transduced with concentrated LL3.7ΔGFP-HA:NL1 viral particles, passaged a day later, and seeded at extremely sparse densities amenable to growth of single isolated cells, which was confirmed visually. After 1-2weeks in culture, single cells had expanded into small adherent clonal colonies. Several dozen colonies were individually removed, dissociated, re-plated into two separate wells each, and grown to confluency. Whole-cell protein was collected from one well of each clonal line and immunoblotted for HA:NL1 expression (data not shown). Success rates by these methods were rather low, but multiple clonal HA:NL1-expressing lines were nevertheless recovered.

3.4.2   Verification of neuroligin-1 expression in HEK-NL1 cells

Two transduced clonal HA:NL1-expressing HEK293 cell lines (HEK-NL1 clone A and B lines) were selected for further characterization. After multiple passages and freeze/thaw cycles to ensure stable, heritable HA:NL1 expression, protein was collected

from HEK-NL1 clone A and B lines, as well as from standard, non-transduced HEK293 cells transiently transfected two days prior with the pCAGGS-HA:NL1 vector. Immunoblotting against the HA epitope revealed stable NL1 expression in both clonal cell lines. HEK-NL1 clone A demonstrated ~25% of the total NL1 expression observed in transfected HEK293 cells, while HEK-NL1 clone B demonstrated ~50% (Figure 17). All subsequent experiments focused on HEK-NL1 clone B line.
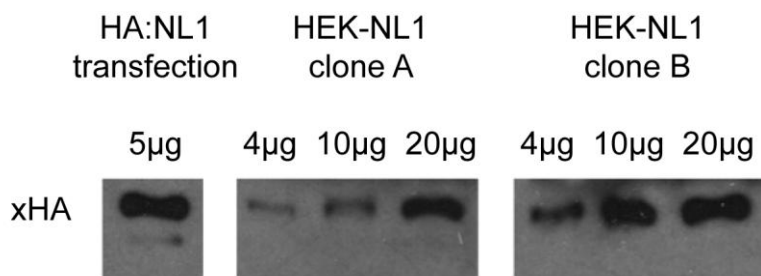
Figure 17: Comparison of total NL1 protein levels in transfected HEK293 cells and transduced HEK-NL1 clone A and B cell lines

HEK293 cell lines engineered to constitutively and stably express HA:NL1 via lentiviral transduction and clonal selection were lysed after several passages and whole-cell protein was collected. Three different masses of cell lysates were immunoblotted for the HA epitope to demonstrate HEK-NL1 clone A and B cell line expression levels. Protein collected from HEK293 cells transiently transfected to express HA:NL1 served as both a positive control and basis for comparison. Based on lysate masses loaded and resulting HA:NL1 bands, NL1 expression in HEK-NL1 clone "A" cells was approximately 25% that of standard transfection levels, while expression in HEK-NL1 clone "B" cells was approximately 50%. Whole-cell lysates from standard HEK293 cells prior to transfection or transduction do not express any detectable HA (data not shown).

To facilitate cell visualization, the HEK-NL1 clone B line underwent a second round of transduction and clonal selection with LL3.7 lentiviral particles to generate a clonal cell line stably expressing both HA:NL1 and GFP. Successful generation of this line (here on referred to as "HEK-NL1") directly evinces the possibility of using

successive lentiviral transduction and clonal selection to create increasingly complex mammalian cell lines.

To confirm proper membrane delivery and surface expression of HA:NL1, HEK-NL1 cells were grown at low density for two days, fixed, and immunostained for the HA epitope without permeabilization. HEK293 cells transiently transfected with pCAGGS-HA:NL1 and LL3.7 plasmids were again considered as a positive control and basis for comparison. HEK-NL1 cells exhibited both marked GFP expression and successful membrane delivery and surface expression of HA:NL1 (Figure 18A). As expected, intensity of the HA:NL1 signal was significantly higher in transiently transfected HEK293 cells (Figure 18B), requiring adjustment of photomultiplier tube sensitivities to accurately visualize surface expression profiles without extensive signal saturation in transfected cells. Curiously, HA:NL1 expression appeared punctate in HEK-NL1 cells, while transfected HEK293 cells consistently demonstrated a continuous lawn of HA:NL1 expression (Figure 18), similar to previous reports (Chubykin et al., 2005). The punctate HA:NL1 expression is potentially a consequence of lower expression levels, particularly following trypsinization and passaging, and/or aggregation of expressed HA:NL1 over several passages of expression. Collectively, results from both immunoblotting and immunocytochemistry verify successful creation of a clonal HEK293 cell line capable of stable coordinate HA:NL1 and GFP expression.
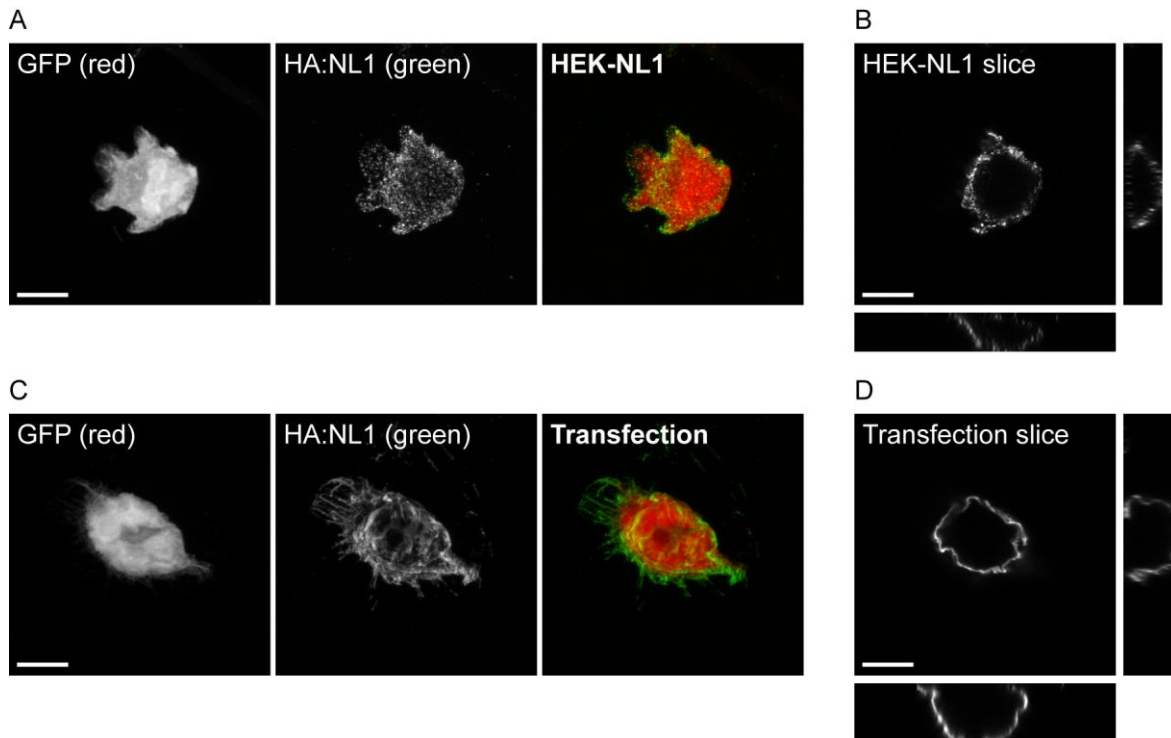
Figure 18: Comparison of surface NL1 expression in transfected HEK293 cells and the HEK-NL1 cell line

HEK293 cells either constitutively expressing HA:NL1 and GFP as a stable, genetically-engineered cell line (A,B) or via standard transient transfection (C,D) were immunostained for the HA epitope two days after trypsinization and passaging. Cells were not permeabilized, enabling staining of surface HA:NL1. Intensity of HA:NL1 immunoreactivity in HEK-NL1 cells was markedly lower than in transfected HEK293 cells, as expected. Photomultiplier tube sensitivities were thus adjusted to enable full visualization of HA:NL1 surface expression in the cell line. To collect the representative images shown, detection sensitivities were approximately doubled between transfection and cell line slides. In (B) and (D) each main image displays the fluorescent signal halfway through the height of the HEK293 cell, as determined using confocal z-stacks, while vertical and horizontal images display midline side views throughout the entire cell depth. HEK-NL1 cells exhibited punctate surface expression of HA:NL1 in both maximum-intensity projections (A) and in single confocal slices and cross-sections (B). In contrast, transfected HEK293 cells exhibited more continuous HA:NL1 surface expression in both maximum-intensity projections (C) and in single confocal slices (D). Rightmost figures of A and C show merge of individual channels displayed on left. Scale bars: 10μm. Objective: 60X. Digital zoom: 4X. Resolution: 2048x2048. Confocal step size: 0.5μm.

3.4.3 Testing HEK-NL1 cells in the mixed-culture assay

The clonal HEK-NL1 cell line was then tested in a preliminary mixed-culture assay, with a GFP-expressing cell line ("HEK-GFP") serving as a negative control and all other experimental conditions unchanged from previous mixed-culture experiments utilizing transient transfection. Surprisingly, HEK-NL1 cells failed to recruit significantly more synapsin or axonal marker Tau-1 than GFP-expressing control cells (Figure 19). Consideration of the ratio of recruited synapsin to Tau-1 as a metric of axonal synapsin densities further revealed no significant difference between HEK-NL1 and HEK-GFP cells.
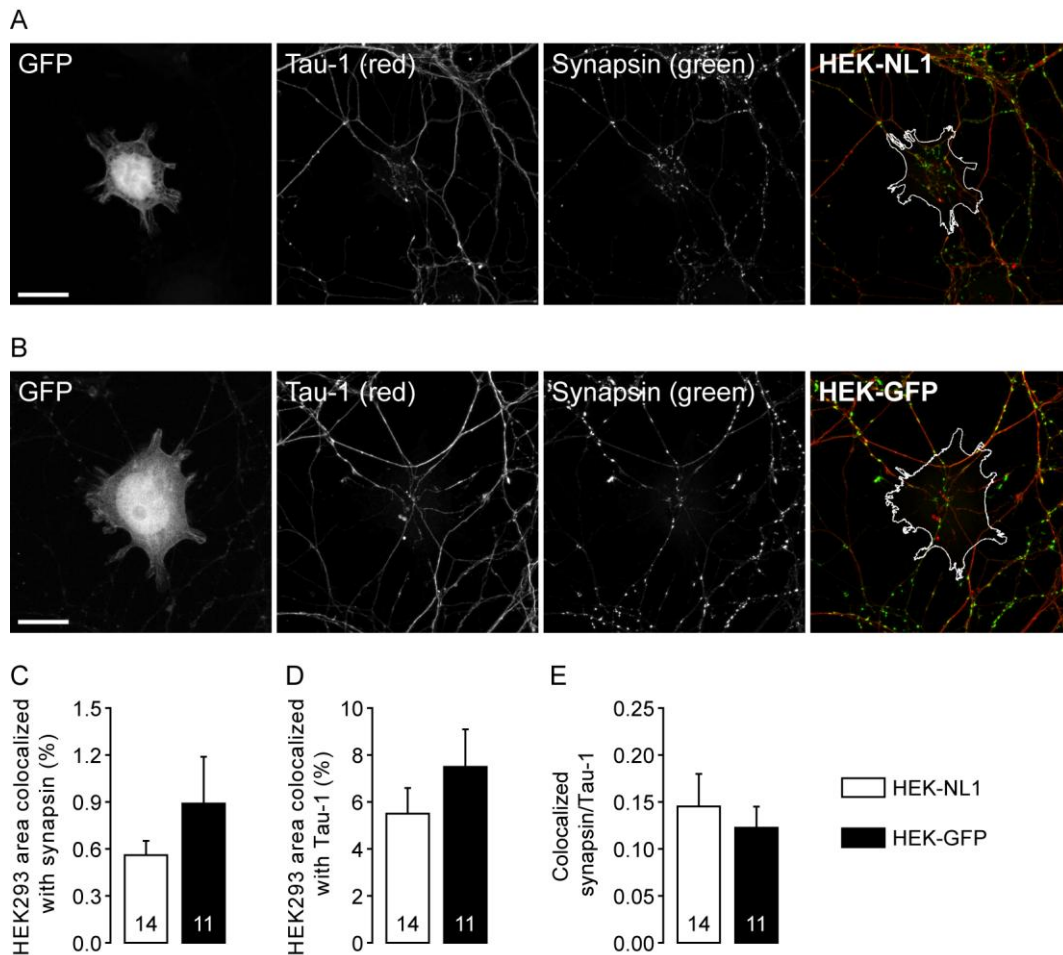

Figure 19: Mixed-culture of dissociated hippocampal neurons and HEK-NL1 or HEK-GFP cells

Nonneuronal HEK293 cell lines stably and constitutively expressing (A) HA:NL1 with GFP ("HEK-NL1") or (B) GFP alone ("HEK-GFP") were cocultured with DIV9-10 dissociated hippocampal neurons for two days before fixation and immunostaining for synapsin and axonal marker Tau-1. (C-E) HEK-GFP and HEK-NL1 did not significantly differ in recruitment of synapsin, Tau-1, or the ratio of synapsin recruitment to Tau-1 recruitment, reflecting axonal synapsin densities. Rightmost figures show merge of Tau-1 (red) and synapsin (green) channels displayed on left, with cell outlines defined from soluble GFP signals drawn in white. Scale bars: 20µm. Objective: 60X. Digital zoom: 2X. Resolution: 2048x2048. Confocal step size: 0.5µm.

Failure of the HEK-NL1 cell line to demonstrate significant synaptogenic potential in the mixed-culture assay is surprising, given successful confirmation of HA:NL1 expression (Figure 17) and membrane insertion (Figure 18), and suggests that HA:NL1 expression between HEK-NL1 and transfected HEK293 cells is somehow fundamentally different. As only one mixed-culture assay was attempted due to time restrictions, however, these negative results are likely only a reflection of the initial stages of this experiment and not a shortcoming of the general strategy. Several parameters, including replacing trypsinization with mechanical dissociation of HEK-NL1 cells prior to coculturing and the duration of coculture remain to be optimized for the lower expression rates observed in the clonal cell line. Indeed, adjustment of both of these factors could feasibly alter the punctate appearance of surface HA:NL1 expression and thereby enable greater NL-NRX interaction in the mixed-culture assay. Thus, this general approach still bears potential in generating complex multi-molecular postsynaptic models.

4.0   DISCUSSION

Capitalizing on the capacity of high NL overexpression to disrupt clustering of multiple postsynaptic components (Graf et al., 2004), I have shown that NL1 can robustly increase the density of immature synaptic connections independent of proper postsynaptic differentiation (Figure 3). Four measures were used to identify the level of exogenous NL1 expression as "high overexpression". First, exogenous NL1 was found in both clustered and diffuse pools along dendritic membranes and spine heads, as previously reported (Prange et al., 2004; Levinson et al., 2005; Barrow et al., 2009), but also diffusely throughout all dendritic compartments (Figure 2). Second, exogenous NL1 mislocalized to axonal processes (Figure 2), which has not previously been reported. Third, the described "high overexpression" protocol yielded significantly greater exogenous NL1 signal intensities and synapsin densities than two other overexpression protocols within titration experiments (Figure 5). Fourth, overexpression of wild-type NL1 tended to reduce spontaneous synaptic activity below control levels, similar to expression of the dominant negative NLswap construct (Figure 3), likely through disruption of basal formation of active synapses. While thus beyond physiological expression levels, these initial high NL1 overexpression experiments nevertheless present key evidence that isolated NL1 signaling in a neuronal setting is sufficient to induce presynaptic differentiation in contacting axons.

Similar results have been obtained in the mixed-culture assay (Figure 7) as well as with exogenous expression of the intracellular mutant NL1ΔC (Chih et al., 2005). In the latter experiment, however, NMDAR were still found to cluster with NLΔC at synaptic sites (Chih et al., 2005), consistent with both trafficking of NRTPs to synapses independent of NL1-PSD95 linkage (Washbourne et al., 2002) and the hypothesis that NL1 mediates synaptic gains via NMDAR activity-dependent synapse validation (Chubykin et al., 2007). In perhaps the most significant finding of this body of work,

however, high NL1 overexpression repeatedly induced pronounced recruitment of synapsin-positive terminals independent of NMDAR activity (Figure 6; Figure 15). This evidence strongly contests previous claims that NL1 functions exclusively to validate pre-existent synapses in an NMDAR activity-dependent manner (Chubykin et al., 2007).

As a caveat, critical examination of the current results may suggest that lack of a significant decrease in synapsin densities with chronic AP5 application may stem from the strong potency of NL1 imposing a ceiling effect on synapsin recruitment. Arguing against this, however, high NL1 overexpression also robustly increased the density of dendritic spines (Figure 3), which are generally associated with glutamatergic synapses. It is reasonable to expect then that any ceiling effect in synapse densities would also extend to spine densities, but chronic NMDAR blockade was able to significantly reduce NL1-mediated spine gains to baseline levels (Figure 6). Moreover, other results indirectly support activity-independent synapse initiation by NL1. The strong trend towards decreased spontaneous event frequencies observed (Figure 3) suggests that the high overexpression protocol has already disrupted proper postsynaptic development, including NMDAR recruitment, at the majority of synaptic sites. Any dependence of NL1-mediated synapse initiation on NMDAR activity should thus also manifest as equal or reduced synapsin recruitment across 100-200 ng and 500 ng transfection levels in the titration experiment (Figure 5), but this is not observed. The current results thus strongly support a capacity of NL1 to robustly recruit synapsin-positive terminals independent of postsynaptic differentiation and NMDAR activity.

Within the context of previous NL1 research, the most likely account of this current data is that NL1 contributes to multiple synaptic processes, including both activity-independent synapse initiation and activity-dependent synapse maturation and maintenance. In direct support of this proposal, NL1 is recruited within seconds to nascent axodendritic contact sites (Barrow et al., 2009), preceding timeframes of NRTP, PSD95, and AMPAR recruitment (Friedman et al., 2000; Bresler et al., 2001; Washbourne et al., 2002; Gerrow et al., 2006; Barrow et al, 2009) and postsynaptic-driven synaptic vesicle recruitment (Gerrow et al., 2006). Further, NL1 is able to recruit active zone scaffolding (Wittenmayer et al., 2009) and synapsin-positive terminals (Figure 6; Figure 15) and maintain dendritic filopodia (Chen et al., 2010) independent of

chronic NMDAR blockade, but requires NMDAR activity to mature presynaptic terminals (Wittenmayer et al., 2009) and stabilize dendritic filopodia (Chen et al., 2010). Finally, both chronic and acute *in vivo* perturbation of NL1 is inexorably linked to alteration in NMDAR activity and NMDAR-dependent plasticity (Chubykin et al., 2007; Kim et al., 2008; Blundell et al., 2010; Dahlhaus et al., 2010). The sum of this evidence thus clearly argues for a critical role of NL1 across multiple synaptic mechanisms.

What evidence argues against NL1 function in both activity-independent synapse initiation and activity-dependent synapse maturation and maintenance? Südhof and colleagues have previously reported that chronic NMDAR blockade precludes NL1-mediated gains in synapse densities (Chubykin et al., 2007). This study employed a calcium-phosphate transfection method, however, and likely achieved markedly lower levels of NL1 overexpression than utilized in the current study. Indeed, this lower overexpression induced only a two fold gain in synapsin puncta densities (Chubykin et al., 2007), while the higher overexpression levels attained in this study triggered a three to four fold gain (Figure 3). Ultimately, these lower overexpression levels likely did not disrupt clustering of postsynaptic components, enabling exogenous NL1 to contribute to activity-dependent synapse maturation, as reflected by increased EPSC amplitudes with low NL1 overexpression (Chubykin et al., 2007). Under these conditions, synapse densities should thus reflect both activity-independent and -dependent NL1-mediated effects, and chronic NMDAR blockade should mitigate (but not abolish) total effects of NL1 overexpression. Indeed, synapse densities on NL1-overexpressing neurons were reduced by chronic NMDAR blockade but still appeared greater than densities on control neurons under chronic NMDAR blockade (Chubykin et al., 2007). In contrast, the current study employed high overexpression to isolate transsynaptic NL1 signaling from proper postsynaptic differentiation, including synaptic activity. Under these conditions, synapse densities should largely reflect the role of NL1 in activity-independent synapse initiation, and indeed chronic NMDAR blockade had no effect on synapsin puncta densities (Figure 6). The prior results from Südhof and colleagues thus do not discount roles of NL1 in both activity-independent synapse initiation and activity-dependent synapse maturation and maintenance.

Lack of a pronounced loss of synapse densities in NL and NRX knockout mouse strains may suggest that NL is strictly involved in synapse function and not formation. Such direct interpretation of knockout results is problematical, however. Ablation of NL or α-NRX expression throughout all of development precipitates complex compensatory changes that must be considered. Triple α-NRX knockout engenders decreased whole-brain protein levels of CASK, β-NRXs, dystroglycan, axonal protein GAP43, and Mint1, while triple NL knockout decreases protein levels of several presynaptic terminal molecules, NMDAR subunits, and the potassium-chloride cotransporter KCC2, which is responsible for the crucial developmental switch in chloride reversal potential (Missler et al., 2003; Varoqueaux et al., 2006). Moreover, as synaptic activity is clearly altered in knockout animals, activity-dependent homeostatic shifts are also expected. Notably Gibson et al. reported that while GABAergic transmission is impaired between fast-spiking interneurons and principal neurons in barrel cortex of NL2 knockout mice, reciprocal glutamatergic transmission was potently augmented (Gibson et al., 2009). Lastly, the greater degree of redundancy in transsynaptic adhesion complexes at excitatory synapses, including NLs-NRXs, SCs, leucine-rich repeat transmembrane proteins (LRRTMs)-NRXs, EphB2s-EphrinBs, and netrin-G-ligands (Dalva et al., 2007; Linhoff et al., 2009; de Wit et al., 2009; Ko et al., 2009b; Siddiqui et al., 2010) must also be considered. Remarkably, the only known transsynaptic adhesion complex regulating GABAergic synapses throughout the brain is NL2-NRX (Varoqueaux et al., 2004; Graf et al., 2004; Chih et al., 2005; Levinson et al., 2005; Patrizi et al., 2008; Poulopoulos et al., 2009). Perturbation of NL2 *in vivo* thus naturally precipitates greater phenotypic changes than perturbation of NL1, and must accordingly be considered to more accurately reflect the endogenous role of NL-NRX signaling. Indeed, in agreement with *in vitro* studies, triple NL knockout most prominently disrupts inhibitory synapse formation and function, while NL2 deletion mirrors these deficits and transgenic NL2 gain-of-function promotes synapse formation. Moreover, neither GABAergic synaptic activity nor scaffolding molecule gephyrin proved necessary for proper synaptic localization of NL2. Collectively, results of *in vivo* NL and NRX perturbation thus also support a role for NL-NRX signaling in both synapse function and formation.

Importantly, this work further presents the first direct account of NL1 contribution to dendritic morphogenesis in mammalian neurons. High overexpression of NL1 in dissociated mouse hippocampal neurons engendered significantly greater total arbor complexities compared to GFP controls (Figure 3) that was independent of chronic NMDAR blockade (Figure 6). Strikingly, a subset of NL1-overexpressing neurons also exhibited unique morphologies with intense perisomatic dendritic branching (Figure 4) that could not be accurately quantified using two-dimensional Sholl analysis of maximum intensity projections. Of great interest, development of this unique morphology was blocked by chronic AP5 application. These results strongly parallel recent findings from Haas and colleagues examining contributions of NL1 to dendritic morphogenesis in the intact *Xenopus* system (Chen et al., 2010) and are further congruent with the rapid recruitment of NL1 to stabilize nascent axodendritic contact sites (Barrow et al., 2009). Observation of stunted dendrites in double α-NRX knockout mice (Dudanova et al., 2007) provides additional evidence that NRXs mediate NL1 intercellular morphogenetic signaling (Chen et al., 2010). While the current evidence is only preliminary in nature given the limited quantifications completed, a marked morphogenetic potential of NL1 was nevertheless robustly observed across numerous trials and experiments (for instance, see Figure 3, Figure 4, Figure 6, Figure 15, and Figure 16). This morphogenetic potential of NL1 signaling was likely not previously observed due to the comparatively high overexpression conditions employed in this study. Whether the subset of neurons exhibiting intense perisomatic dendritic branching corresponds to a specific neuron subtype will be of great interest to future investigations. Alternatively, this apparent subset may represent the extreme end of a continuum of NL1-mediated morphogenesis. Future experiments using transfected slice cultures and/or time-lapse imaging should enable greater elucidation of this phenomenon.

Considerable evidence suggests that PSD95 significantly contributes to both excitatory specification of NL-mediated synapses (Prange et al., 2004; Graf et al., 2004; Levinson et al., 2005) and maturation of NL-recruited presynaptic terminals (Futai et al., 2007), but less is known regarding NL-PSD95 interactions during synapse initiation. El-Husseini and colleagues previously observed that coordinate overexpression of PSD95

with NL1 in dissociated hippocampal neurons restricted NL1-mediated gains in synapse densities (Prange et al., 2004). Results from the mixed-culture assay, however, reveal that interaction of PSD95 alone with NL1 does not restrict initial recruitment of synapsin-positive terminals by NL1 (Figure 9). This suggests that PSD95 restricts NL1-mediated synapse densities downstream of initial terminal recruitment. Further, knockdown of endogenous PSD95 expression (coupled with the postsynaptic disruption incurred with high NL1 overexpression) did not preclude the robust recruitment of synapsin-positive terminals by NL1 overexpression (Figure 11). This experiment extends prior electrophysiological work utilizing the same perturbation (Futai et al., 2007) to morphological settings, thereby differentiating PSD95-independent NL1-mediated synapse initiation from interdependent NL1/PSD95 regulation of presynaptic release probability at established synapses.

Lastly, preliminary investigations of combined NL1/SC1 perturbations in dissociated hippocampal cultures provide tentative evidence for SC1-mediated activation of immature NL1-initiated synaptic contacts (Figure 15). Specifically, driving both NL1 and SC1 overexpression led to NMDAR-dependent neurodegeneration. Replication of this experiment at lower overexpression levels with titration of AP5 application should provide more conclusive results as to whether combined NL1/SC1 synapses are functionally mature. Regardless of limitations in the current experimental approach, however, the clear inability of coordinate SC1 overexpression in NL1-overexpressing neurons to enhance synapsin recruitment strongly complements the results from SC1 knockdown and mixed-culture experiments (Figure 13 and Figure 14) to conclusively show that SC1 does not initiate synapses *in vitro*, in clear contrast to the potent capacity of NL1 to recruit synapsin-positive terminals. These results collectively evince a role for NL1 in synapse initiation independent of postsynaptic differentiation, NMDAR activity, PSD95 interactions, and SC1 contributions. Building from this fundamental conclusion, future investigation of how other adhesion complexes coordinate with NL-NRX *in vitro* and compensate for NL/NRX mutations *in vivo* will significantly abet our understanding of specific NL/NRX contributions and general synaptic contributions to normal and aberrant neural development.

BIBLIOGRAPHY

Abrahams BS, Geschwind DH (2008) Advances in autism genetics: on the threshold of a new neurobiology. Nat Neurosci 9:341-355.

Aiga M, Levinson JN, Bamji SX (2011) N-cadherin and neuroligins cooperate to regulate synapse formation in hippocampal cultures. J Biol Chem 286:851-858.

Banovic D, Khorramshahi O, Owald D, Wichmann C, Riedt T, Fouquet W, Tian R, Sigrist SJ, Aberle H (2010) Drosophila neuroligin 1 promotes growth and postsynaptic differentiation at glutamatergic neuromuscular junctions. Neuron 66:724-738.

Barrow SL, Constable JRL, Clark E, El-Sabeawy F, McAllister AK, Washbourne P (2009) Neuroligin I: a cell adhesion molecule that recruits PSD-95 and NMDA receptors by distinct mechanisms during synaptogenesis. Neural Development 4:17.

Béïque JC, Andrade R (2003) PSD-95 regulates synaptic transmission and plasticity in rat cerebral cortex. J Physiol (Lond) 546:859-867.

Béïque JC, Lin DT, Kang MG, Aizawa H, Takamiya K, Huganir RL (2006) Synapse-specific regulation of AMPA receptor function by PSD-95. Proc Natl Acad Sci USA 103:19535-19540.

Biederer T, Südhof TC (2000) Mints as adaptors; direct binding to neurexins and recruitment of munc18. J Biol Chem 275:39803-39806.

Biederer T, Sara Y, Mozhayeva M, Atasoy D, Liu X, Kavalali ET, Südhof TC (2002) SynCAM, a synaptic adhesion molecule that drives synapse assembly. Science 297:1525-1531.

Biederer T (2006) Bioinformatic characterization of the SynCAM family of immunoglobulin-like domain-containing adhesion molecules. Genomics 87:139-150.

Biederer T, Scheiffele P (2007) Mixed-culture assays for analyzing neuronal synapse formation. Nat Protoc 2:670-676.

Blundell J, Tabuchi K, Bolliger MF, Blaiss CA, Brose N, Liu X, Südhof TC, Powell CM (2009). Increased anxiety-like behavior in mice lacking the inhibitory synapse cell adhesion molecule neuroligin 2. Genes Brain Behav 8:114-126.

Blundell J, Blaiss CA, Etherton MR, Espinosa F, Tabuchi K, Walz C, Bolliger MF, Südhof TC, Powell CM (2010) Neuroligin-1 deletion results in impaired spatial memory and increased repetitive behavior. J Neurosci 30:2115-2129.

Bolliger MF, Frei K, Winterhalter KH, Gloor SM (2001) Identification of a novel neuroligin in humans which binds to PSD-95 and has a widespread expression. Biochem J 356:581-588.

Bolliger MF, Pei J, Maxeiner S, Boucard AA, Grishin NV, Südhof TC (2008) Unusually rapid evolution of neuroligin-4 in mice. Proc Natl Acad Sci USA 105:6421-6426.

Boucard AA, Chubykin AA, Comoletti D, Taylor P, Südhof TC (2005) A splice code for trans-synaptic cell adhesion mediated by binding of neuroligin 1 to alpha- and beta-neurexins. Neuron 48:229-236.

Bresler T, Ramati Y, Zamorano PL, Zhai R, Garner CC, Ziv NE (2001) The dynamics of SAP90/PSD-95 recruitment to new synaptic junctions. Mol Cell Neurosci 18:149-167.

Budreck EC, Scheiffele P (2007) Neuroligin-3 is a neuronal adhesion protein at GABAergic and glutamatergic synapses. Eur J Neurosci 26:1738-1748.

Chadman KK, Gong S, Scattoni ML, Boltuck SE, Gandhy SU, Heintz N, Crawley JN (2008) Minimal aberrant behavioral phenotypes of neuroligin-3 R451C knockin mice. Autism Res 1:147-158.

Chen L, Chetkovich DM, Petralia RS, Sweeney NT, Kawasaki Y, Wenthold RJ, Bredt DS, Nicoll RA (2000) Stargazin regulates synaptic targeting of AMPA receptors by two distinct mechanisms. Nature 408:936-943.

Chen SX, Tari PK, She K, Haas K (2010) Neurexin-neuroligin cell adhesion complexes contribute to synaptotropic dendritogenesis via growth stabilization mechanisms in vivo. Neuron 67:967-983.

Chih B, Afridi SK, Clark L, Scheiffele P (2004) Disorder-associated mutations lead to functional inactivation of neuroligins. Hum Mol Genet 13:1471-1477.

Chih B, Engelman H, Scheiffele P (2005) Control of excitatory and inhibitory synapse formation by neuroligins. Science 307:1324-1328.

Chih B, Gollan L, Scheiffele P (2006) Alternative splicing controls selective trans-synaptic interactions of the neuroligin-neurexin complex. Neuron 51:171-178.

Cho KO, Hunt CA, Kennedy MB (1992) The rat brain postsynaptic density fraction contains a homolog of the Drosophila discs-large tumor suppressor protein. Neuron 9:929-942.

Chubykin AA, Liu X, Comoletti D, Tsigelny I, Taylor P, Südhof TC (2005) Dissection of synapse induction by neuroligins: effect of a neuroligin mutation associated with autism. J Biol Chem 280:22365-22374.

Chubykin AA, Atasoy D, Etherton MR, Brose N, Kavalali ET, Gibson JR, Südhof TC (2007) Activity-dependent validation of excitatory versus inhibitory synapses by neuroligin-1 versus neuroligin-2. Neuron 54:919-931.

Comoletti D, De Jaco A, Jennings LL, Flynn RE, Gaietta G, Tsigelny I, Ellisman MH, Taylor P (2004) The Arg451Cys-neuroligin-3 mutation associated with autism reveals a defect in protein processing. J Neurosci 24:4889-4893.

Dahlhaus R, Hines RM, Eadie BD, Kannangara TS, Hines DJ, Brown CE, Christie BR, El-Husseini A (2010) Overexpression of the cell adhesion protein neuroligin-1 induces learning deficits and impairs synaptic plasticity by altering the ratio of excitation to inhibition in the hippocampus. Hippocampus 20:305-322.

Dalva MB, McClelland AC, Kayser MS (2007) Cell adhesion molecules: signaling functions as the synapse. Nat Rev Neurosci 8:206-220.

Davletov BA, Krasnoperov V, Hata Y, Petrenko AG, Südhof TC (1995) High affinity binding of α-latrotoxin to recombinant neurexin Iα. J Biol Chem 270:23903-23905.

de Wit J, Sylwestrak E, O'Sullivan ML, Otto S, Tiglio K, Savas JN, Yates JR 3rd, Comoletti D, Taylor P, Ghosh A (2009) LRRTM2 interacts with Neurexin1 and regulates excitatory synapse formation. Neuron 64:799-806.

Dean C, Scholl FG, Choih J, DeMaria S, Berger J, Isacoff E, Scheiffele P (2003) Neurexin mediates the assembly of presynaptic terminals. Nat Neurosci 6:708-716.

Dobrunz LE, Stevens CF (1997) Heterogeneity of release probability, facilitation, and depletion at central synapses. Neuron 18:995-1008.

Dong N, Qi J, Chen G (2007) Molecular reconstitution of functional GABAergic synapses with expression of neuroligin-2 and $GABA_A$ receptors. Mol Cell Neurosci 35:14-23.

Dresbach T, Neeb A, Meyer G, Gundelfinger ED, Brose N (2004) Synaptic targeting of neuroligin is independent of neurexin and SAP90/PSD95 binding. Mol Cell Neurosci 27:227-235.

Dudanova I, Tabuchi K, Rohlmann A, Südhof TC, Missler M (2007) Deletion of α-neurexins does not cause a major impairment of axonal pathfinding or synapse formation. J Comp Neurol 502:261-274.

Durand GM, Kovalchuk Y, Konnerth A (1996) Long-term potentiation and functional synapse induction in developing hippocampus. Nature 381:71-75.

El-Husseini A, Schnell E, Chetkovich DM, Nicoll RA, Bredt DS (2000) PSD-95 involvement in maturation of excitatory synapses. Science 290:1364-1368.

Etherton MR, Blaiss CA, Powell CM, Südhof TC (2009) Mouse neurexin-1alpha deletion causes correlated electrophysiological and behavioral changes consistent with cognitive impairments. Proc Natl Acad Sci USA 106:17998-18003.

Fiala JC, Feinberg M, Popov V, Harris KM (1998) Synaptogenesis via dendritic filopodia in developing hippocampal area CA1. J Neurosci 18:8900-8911.

Fletcher TL, De Camilli P, Banker G (1994) Synaptogenesis in hippocampal cultures: evidence indicating that axons and dendrites become competent to form synapses at different stages of neuronal development. J Neurosci 14:6695-6706.

Fogel AI, Akins MR, Krupp AJ, Stagi M, Stein V, Biederer T (2007) SynCAMs organize synapses through heterophilic adhesion. J Neurosci 27:12516-12530.

Fogel AI, Li Y, Giza J, Wang Q, Lam TT, Modis Y, Biederer T (2010) N-glycosylation at the SynCAM (synaptic cell adhesion molecule) immunoglobulin interface modulates synaptic adhesion. J Biol Chem 285:34864-34874.

Friedman HV, Bresler T, Garner CC, Ziv NE (2000) Assembly of new individual excitatory synapses: time course and temporal order of synaptic molecule recruitment. Neuron 27:57-69.

Fu Z, Washbourne P, Ortinski P, Vicini S (2003) Functional excitatory synapses in HEK293 cells expressing neuroligin and glutamate receptors. J Neurophysiol 90:3950-3957.

Fu Z, Vicini S (2009) Neuroligin-2 accelerates GABAergic synapse maturation in cerebellar granule cells. Mol Cell Neurosci 42:45-55.

Futai K, Kim MJ, Hashikawa T, Scheiffele P, Sheng M, Hayashi Y (2007) Retrograde modulation of presynaptic release probability through signaling mediated by PSD-95-neuroligin. Nat Neurosci 10:186-195.

Galuska SP, Rollenhagen M, Kaup M, Eggers K, Oltmann-Norden I, Schiff M, Hartmann M, Weinhold B, Hildebrandt H, Geyer R, Mühlenhoff M, Geyer H (2010) Synaptic cell adhesion molecule SynCAM 1 is a target for polysialylation in postnatal mouse brain. Proc Natl Acad Sci USA 107:10250-10255.

Gerrow K, Romorini S, Nabi SM, Colicos MA, Sala C, El-Husseini A (2006) A preformed complex of postsynaptic proteins is involved in excitatory synapse development. Neuron 49:547-562.

Gibson JR, Huber KM, Südhof TC (2009) Neuroligin-2 deletion selectively decreases inhibitory synaptic transmission originating from fast-spiking but not from somatostatin-positive interneurons. J Neurosci 29:13883-13897.

Glynn MW, McAllister AK (2006) Immunocytochemistry and quantification of protein colocalization in cultured neurons. Nat Protoc 1:1287-1296.

Graf ER, Zhang X, Jin SX, Linhoff MW, Craig AM (2004) Neurexins induce differentiation of GABA and glutamate postsynaptic specializations via neuroligins. Cell 119:1013-1026.

Graf ER, Kang Y, Hauner AM, Craig AM (2006) Structure function and splice site analysis of the synaptogenic activity of the neurexin-1beta LNS domain. J Neurosci 26:4256-4265.

Harris KM, Jensen FE, Tsao B (1992) Three-dimensional structure of dendritic spines and synapses in rat hippocampus (CA1) at postnatal day 15 and adult ages: implications for the maturation of synaptic physiology and long-term potentiation. J Neurosci 12:2685-2705.

Hata Y, Davletov B, Petrenko AG, Jahn R, Südhof TC (1993) Interaction of synaptotagmin with the cytoplasmic domains of neurexins. Neuron 10:307-315.

Hata Y, Butz S, Südhof TC (1996) CASK: a novel dlg/PSD95 homolog with an N-terminal calmodulin-dependent protein kinase domain identified by interaction with neurexins. J Neurosci 16:2488-2494.

Hines RM, Wu L, Hines DJ, Steenland H, Mansour S, Dahlhaus R, Singaraja RR, Cao X, Sammler E, Hormuzdi SG, Zhuo M, El-Husseini A (2008) Synaptic imbalance, sterotypies, and impaired social interactions in mice with altered neuroligin 2 expression. J Neurosci 28:6055-6067.

Hunt CA, Schenker LJ, Kennedy MB (1996) PSD-95 is associated with the postsynaptic density and not with the presynaptic membrane at forebrain synapses. J Neurosci 16:1380-1388.

Ichtchenko K, Hata Y, Nguyen T, Ullrich B, Missler M, Moomaw C, Südhof TC (1995) Neuroligin 1: a splice site-specific ligand for beta-neurexins. Cell 81:435-443.

Ichtchenko K, Nguyen T, Südhof TC (1996) Structures, alternative splicing, and neurexin binding of multiple neuroligins. J Biol Chem 271:2676-2682.

Irie M, Hata Y, Takeuchi M, Ichtchenko K, Toyoda A, Hirao K, Takai Y, Rosahl TW, Südhof TC (1997) Binding of neuroligins to PSD-95. Science 277:1511-1515.

Isaac JTR, Crair MC, Nicoll RA, Malenka RC (1997) Silent synapses during development of thalamocortical inputs. Neuron 18:269-280.

Jamain S, Quach H, Betancur C, Råstam M, Colineaux C, Gillberg IC, Soderstrom H, Giros B, Leboyer M, Gillberg C, Bourgeron T (2003) Mutations of the X-linked genes encoding neuroligins NLGN3 and NLGN4 are associated with autism. Nat Genet 34:27-29.

Jamain S, Radyushkin K, Hammerschmidt K, Granon S, Boretius S, Varoqueaux F, Ramanantsoa N, Gallego J, Ronnenberg A, Winter D, Frahm J, Fischer J, Bourgeron T, Ehrenreich H, Brose N (2008). Reduced social interaction and ultrasonic communication in a mouse model of monogenic heritable autism. Proc Natl Acad Sci USA 105:1710-1715.

Kang Y, Zhang X, Dobie F, Wu H, Craig AM (2008) Induction of GABAergic postsynaptic differentiation by alpha-neurexins. J Biol Chem 283:2323-2334.

Kattenstroth G, Tantalaki E, Südhof TC, Gottmann K, Missler M (2004) Postsynaptic N-methyl-D-aspartate receptor function requires α-neurexins. Proc Natl Acad Sci USA 101:2607-2612.

Kim E, Niethammer M, Rothschild A, Jan YN, Sheng M (1995) Clustering of Shaker-type K^+ channels by interaction with a family of membrane-associated guanylate kinases. Nature 378:85-88.

Kim E, Sheng M (2004) PDZ domain proteins of synapses. Nat Rev Neurosci 5:771-781.

Kim J, Jung SY, Lee YK, Park S, Choi JS, Lee CJ, Kim HS, Choi YB, Scheiffele P, Bailey CH, Kandel ER, Kim JH (2008) Neuroligin-1 is required for normal expression of LTP and associated fear memory in the amygdala of adult animals. Proc Natl Acad Sci USA 105:9087-9092.

Ko J, Zhang C, Arac D, Boucard AA, Brunger AT, Südhof TC (2009a) Neuroligin-1 performs neurexin-dependent and neurexin-independent functions in synapse validation. EMBO J 28:3244-55.

Ko J, Fuccillo MV, Malenka RC, Südhof TC (2009b) LRRTM2 functions as a neurexin ligand in promoting excitatory synapse formation. Neuron 64:791-798.

Kornau HC, Schenker LT, Kennedy MB, Seeburg PH (1995) Domain interaction between NMDA receptor subunits and the postsynaptic density protein PSD-95. Science 269:1737-1740.

Laumonnier F, Bonnet-Brilhault F, Gomot M, Blanc R, David A, Moizard MP, Raynaud M, Ronce N, Lemonnier E, Calvas P, Laudier B, Chelly J, Fryns JP, Ropers HH, Hamel BC, Andres C, Barthélémy C, Moraine C, Briault S (2004) X-linked mental

retardation and autism are associated with a mutation in the NLGN4 gene, a member of the neuroligin family. Am J Hum Genet 74:552-557.

Lee H, Dean C, Isacoff E (2010) Alternative splicing of neuroligin regulates the rate of presynaptic differentiation. J Neurosci 30:11435-11446.

Levinson JN, Chery N, Huang K, Wong TP, Gerrow K, Kang R, Prange O, Wang YT, El-Husseini A (2005) Neuroligins mediate excitatory and inhibitory synapse formation: involvement of PSD-95 and neurexin-1β in neuroligin-induced synaptic specificity. J Biol Chem 280:17312-17319.

Levinson JN, Li R, Kang R, Moukhles H, El-Husseini A, Bamji SX (2010) Postsynaptic scaffolding molecules modulate the localization of neuroligins. Neurosci 165:782-793.

Li J, Ashley J, Budnik V, Bhat MA (2007) Crucial role of Drosophila neurexin in proper active zone apposition to postsynaptic densities, synaptic growth, and synaptic transmission. Neuron 55:741-755.

Liao D, Zhang X, O'Brien R, Ehlers MD, Huganir RL (1999) Regulation of morphological postsynaptic silent synapses in developing hippocampal neurons. Nat Neurosci 2:37-43.

Linhoff MW, Laurén J, Cassidy RM, Dobie FA, Takahashi H, Nygaard HB, Airaksinen MS, Strittmatter SM, Craig AM (2009) An unbiased expression screen for synaptogenic proteins identifies the LRRTM protein family as synaptic organizers. Neuron 61:734-49.

Lois C, Hong EJ, Pease S, Brown EJ, Baltimore D (2002) Germline transmission and tissue-specific expression of transgenes delivered by lentiviral vectors. Science 295:868-872.

Losi G, Prybylowski K, Fu Z, Luo J, Wenthold RJ, Vicini S (2003) PSD-95 regulates NMDA receptors in developing cerebellar granule neurons of the rat. J Physiol (Lond) 548:21-29.

Matteoli M, Takei K, Perin MS, Südhof TC, De Camilli P (1992) Exo-endocytotic recycling of synaptic vesicles in developing processes of cultured hippocampal neurons. J Cell Biol 117:849-861.

Micheva KD, Beaulieu C (1996) Quantitative aspects of synaptogenesis in the rat barrel field cortex with special reference to GABA circuitry. J Comp Neurol 373:340-354.

Migaud M, Charlesworth P, Dempster M, Webster LC, Watabe AM, Makhinson M, He Y, Ramsay MF, Morris RG, Morrison JH, O'Dell TJ, Grant SGN (1998) Enhanced long-term potentiation and impaired learning in mice with mutant postsynaptic density-95 protein. Nature 396:433-439.

Missler M, Zhang W, Rohlmann A, Kattenstroth G, Hammer RE, Gottmann K, Südhof TC (2003) α-Neurexins couple Ca^{2+} channels to synaptic vesicle exocytosis. Nature 423:939-948.

Moss S, Smart T (2001) Constructing inhibitory synapses. Nat Rev Neurosci 2:240-250.

Nam CI, Chen L (2005) Postsynaptic assembly induced by neurexin-neuroligin interaction and neurotransmitter. Proc Natl Acad Sci USA 102:6137-6142.

Papadopoulos T, Korte M, Eulenburg V, Kubota H, Retiounskaia M, Harvey RJ, Harvey K, O'Sullivan GA, Laube B, Hülsmann S, Geiger JRP, Betz H (2007) Impaired GABAergic transmission and altered hippocampal synaptic plasticity in collybistin-deficient mice. EMBO J 26:3888-3899.

Papadopoulos T, Eulenburg V, Reddy-Alla S, Mansuy IM, Betz H (2008) Collybistin is required for both the formation and maintenance of GABAergic postsynapses in the hippocampus. Mol Cell Neurosci 39:161-169.

Patrizi A, Scelfo B, Viltono L, Briatore F, Fukaya M, Watanabe M, Strata P, Varoqueaux F, Brose N, Fritschy JM, Sassoè-Pognetto M (2008) Synapse formation and clustering of neuroligin-2 in the absence of GABA$_A$ receptors. Proc Natl Acad Sci USA 105:13151-13156.

Peng J, Kim MJ, Cheng D, Duong DM, Gygi SP, Sheng M (2004) Semiquantitative proteomic analysis of rat forebrain postsynaptic density fractions by mass spectrometry. J Biol Chem 279:21003-21011.

Petrenko AG, Lazaryeva VD, Geppert M, Tarasyuk TA, Moomaw C, Khokhlatchev AV, Ushkaryov YA, Slaughter C, Nasimov IV, Südhof TC (1993) Polypeptide composition of the α-latrotoxin receptor; high affinity binding protein consists of a family of related high molecular weight polypeptides complexed to a low molecular weight protein. J Biol Chem 268:1860-1867.

Poulopoulos A, Aramuni G, Meyer G, Soykan T, Hoon M, Papadopoulos T, Zhang M, Paarmann I, Fuchs C, Harvey K, Jedlicka P, Schwarzacher SW, Betz H, Harvey RJ, Brose N, Zhang W, Varoqueaux F (2009) Neuroligin 2 drives postsynaptic assembly at perisomatic inhibitory synapses through gephyrin and collybistin. Neuron 63:628-642.

Prange O, Wong TP, Gerrow K, Wang YT, El-Husseini A (2004) A balance between excitatory and inhibitory synapses is controlled by PSD-95 and neuroligin. Proc Natl Acad Sci USA 101:13915-13920.

Radyushkin K, Hammerschmidt K, Boretius S, Varoqueaux F, El-Kordi A, Ronnenberg A, Winter D, Frahm J, Fischer J, Brose N, Ehrenreich H (2009) Neuroligin-3-deficient mice: model of a monogenic heritable form of autism with an olfactory deficit. Genes Brain Behav 8:416-425.

Rao A, Kim E, Sheng M, Craig AM (1998) Heterogeneity in the molecular composition of excitatory postsynaptic sites during development of hippocampal neurons in culture. J Neurosci 18:1217-1229.

Reynolds A, Leake D, Boese Q, Scaringe S, Marshall WS, Khvorova A (2004) Rational siRNA design for RNA interference. Nat Biotechnol 22:326-330.

Ripley B, Otto S, Tiglio K, Williams ME, Ghosh A (2011) Regulation of synaptic stability by AMPA receptor reverse signaling. Proc Natl Acad USA 108:367-372.

Robbins EM, Krupp AJ, Perez de Arce K, Ghosh AK, Fogel AI, Boucard A, Südhof TC, Stein V, Biederer T (2010) SynCAM 1 adhesion dynamically regulates synapse number and impacts plasticity and learning. Neuron 68:894-906.

Rosales CR, Osborne KD, Zuccarino GV, Scheiffele P, Silverman MA (2005) A cytoplasmic motif targets neuroligin-1 exclusively to dendrites of cultured hippocampal neurons. Eur J Neurosci 22:2381-2386.

Rubinson DA, Dillon CP, Kwiatkowski AV, Sievers C, Yang L, Kopinja J, Rooney DL, Zhang M, Ihrig MM, McManus MT, Gertler FB, Scott ML, Van Parijs L (2003) A lentivirus-based system to functionally silence genes in primary mammalian cells, stem cells and transgenic mice by RNA interference. Nat Genet 33:401-406.

Rumpel S, Hatt H, Gottmann K (1998) Silent synapses in the developing rat visual cortex: evidence for postsynaptic expression of synaptic plasticity. J Neurosci 18:8863-8874.

Sara Y, Biederer T, Atasoy D, Chubykin A, Mozhayeva MG, Südhof TC, Kavalali ET (2005) Selective capability of SynCAM and neuroligin for functional synapse assembly. J Neurosci 25:260-270.

Schapitz IU, Behrend B, Pechmann Y, Lappe-Siefke C, Kneussel SJ, Wallace KE, Stempel AV, Buck F, Grant SGN, Schweizer M, Schmitz D, Schwarz JR, Holzbaur ELF, Kneussel M (2010) Neuroligin 1 is dynamically exchanged at postsynaptic sites. J Neurosci 30:12733-12744.

Scheiffele P, Fan J, Choih J, Fetter R, Serafini T (2000) Neuroligin expressed in nonneuronal cells triggers presynaptic development in contacting axons. Cell 101:657-669.

Schnell E, Sizemore M, Karimzadegan S, Chen L, Bredt DS, Nicoll RA (2002) Direct interactions between PSD-95 and stargazin control synaptic AMPA receptor number. Proc Natl Acad Sci USA 99:13902-13907.

Siddiqui TJ, Pancaroglu R, Kang Y, Rooyakkers A, Craig AM (2010) LRRTMs and neuroligins bind neurexins with a differential code to cooperate in glutamate synapse development. J Neurosci 30:7495-7506.

Song Jy, Ichtchenko K, Südhof TC, Brose N (1999) Neuroligin 1 is a postsynaptic cell-adhesion molecule of excitatory synapses. Proc Natl Acad Sci USA 96:1100-1105.

Stan A, Pielarski KN, Brigadski T, Wittenmayer N, Fedorchenko O, Gohla A, Lessmann V, Dresbach T, Gottmann K (2010) Essential cooperation of N-cadherin and neuroligin-1 in the transsynaptic control of vesicle accumulation. Proc Natl Acad Sci USA 107:11116-11121.

Stein V, House DRC, Bredt DS, Nicoll RA (2003) Postsynaptic density-95 mimics and occludes hippocampal long-term potentiation and enhances long-term depression. J Neurosci 23:5503-5506.

Südhof TC (2008) Neuroligins and neurexins link synaptic function to cognitive disease. Nature 455:903-911.

Sugita S, Khvotchev M, Südhof TC (1999) Neurexins are functional α-latrotoxin receptors. Neuron 22:489-496.

Tabuchi K, Blundell J, Etherton MR, Hammer RE, Liu X, Powell CM, Südhof TC (2007) A neuroligin-3 mutation implicated in autism increases inhibitory synaptic transmission in mice. Science 318:71-76.

Taniguchi H, Gollan L, Scholl FG, Mahadomrongkul V, Dobler E, Limthong N, Peck M, Aoki C, Scheiffele P (2007) Silencing of neuroligin function by postsynaptic neurexins. J Neurosci 27:2815-2824.

Thomas LA, Akins MR, Biederer T (2008) Expression and adhesion profiles of SynCAM molecules indicate distinct neuronal functions. J Comp Neurol 510:47-67.

Thyagarajan A, Ting AY (2010) Imaging activity-dependent regulation of neurexin-neuroligin interactions using trans-synaptic enzymatic biotinylation. Cell 143:456-469.

Ullrich B, Ushkaryov YA, Südhof TC (1995) Cartography of neurexins: more than 1000 isoforms generated by alternative splicing and expressed in distinct subsets of neurons. Neuron 14:497-507.

Ushkaryov YA, Petrenko AG, Geppert M, Südhof TC (1992) Neurexins: synaptic cell surface proteins related to the alpha-latrotoxin receptor and laminin. Science 257:50-56.

Ushkaryov YA, Südhof TC (1993) Neurexin IIIα: extensive alternative splicing generates membrane-bound and soluble forms. Proc Natl Acad Sci USA 90:6410-6414.

Ushkaryov YA, Hata Y, Ichtchenko K, Moomaw C, Afendi S, Slaughter CA, Südhof TC (1994) Conserved domain structure of beta-neurexins. Unusual cleaved signal

sequences in receptor-like neuronal cell-surface proteins. J Biol Chem 269:11987-11992.

Varoqueaux F, Jamain S, Brose N (2004) Neuroligin 2 is exclusively localized to inhibitory synapses. Eur J Cell Biol 83:449-456.

Varoqueaux F, Aramuni G, Rawson RL, Morhmann R, Missler M, Gottmann K, Zhang W, Südhof TC, Brose N (2006) Neuroligins determine synapse maturation and function. Neuron 51:741-754.

Washbourne P, Bennet JE, McAllister AK (2002) Rapid recruitment of NMDA receptor transport packets to nascent synapses. Nat Neurosci 5:751-759.

Wittenmayer N, Körber C, Liu H, Kremer T, Varoqueaux F, Chapman ER, Brose N, Kuner T, Dresbach T (2009) Postsynaptic Nueroligin1 regulates presynaptic maturation. Proc Natl Acad Sci USA 106:13564-13569.

Wu G-Y, Malinow R, Cline HT (1996) Maturation of a central glutamatergic synapse. Science 274:972-976.

Zeng X, Sun M, Liu L, Chen F, Wei L, Xie W (2007) Neurexin-1 is required for synapse formation and larvae associative learning in Drosophila. FEBS Lett 581:2509-2516.

Zhai RG, Friedman HV, Cases-Langhoff C, Becker B, Gundelfinger ED, Ziv NE, Garner CC (2001). Assembling the presynaptic active zone: a characterization of an active zone precursor vesicle. Neuron 29:131-143.

Zhang W, Benson DL (2001) Stages of synapse development defined by dependence on F-actin. J Neurosci 21:5169-5181.

Zhang W, Rohlmann A, Sargsyan V, Aramuni G, Hammer RE, Südhof TC, Missler M (2005). Extracellular domains of α-neurexins participate in regulating synaptic transmission by selectively affecting N- and P/Q-type Ca^{2+} channels. J Neurosci 25:4330-4342.

Ziv NE, Garner CC (2001) Principles of glutamatergic synapse formation: seeing the forest for the trees. Curr Opin Neurobiol. 11:536-543.

Ziv NE, Garner CC (2004) Cellular and molecular mechanisms of presynaptic assembly. Nat Rev Neurosci 5:385-399.

Zoghbi HY (2003) Postnatal neurodevelopmental disorders: meeting at the synapse? Science 302:826-830.